Growing Up POMC: Pro-opiomelanocortin in the Developing Brain

Stephanie Louise Padilla

Submitted in partial fulfillment of the requirements for the degree of Doctor of Philosophy
under the Executive Committee of the Graduate School of Arts and Sciences

COLUMBIA UNIVERSITY

2011

ABSTRACT

Growing Up POMC: Pro-opiomelanocortin in the Developing Brain

Stephanie Louise Padilla

Neurons in the arcuate nucleus of the hypothalamus (ARH) play a central role in the regulation of body weight and energy homeostasis. ARH neurons directly sense nutrient and hormonal signals of energy availability from the periphery and relay this information to secondary nuclei targets, where signals of energy status are integrated to regulate behaviors related to food intake and energy expenditure. Transduction of signals related to energy status by Pro-opiomelanocortin (POMC) and neuropeptide-Y/agouti-related protein (NPY/AgRP) neurons in the ARH exert opposing influences on secondary neurons in central circuits regulating energy balance. My thesis research focused on the developmental events regulating the differentiation and specification of cell fates in the ARH.

My first project was designed to characterize the ontogeny of *Pomc*- and *Npy*-expressing neurons in the developing mediobasal hypothalamus (Chapter 2). These experiments led to the unexpected finding that during mid-gestation, *Pomc* is broadly expressed in the majority of newly-born ARH neurons, but is subsequently down-regulated during later stages of development as cells acquire a terminal cell identity. Moreover, these studies demonstrated that most immature *Pomc*-expressing progenitors subsequently differentiate into non-POMC neurons, including a subset of functionally distinct NPY/AgRP neurons.

The second aspect of my work focused on characterizing *Pomc*-expressing progenitors throughout the brain (Chapter 3). Similar to findings in Chapter 2, *Pomc* was broadly expressed in many aspects of the developing brain and subsequently down-regulated as cells further differentiated into non-*Pomc* terminal identities. In the CNS, the percentage of POMC neurons derived from *Pomc*-expressing progenitors are marginal. These findings are of general importance to the field of energy homeostasis research, because many genetically targeted

functional manipulations of POMC cells have been induced during early development, a time in which *Pomc* is expressed in many cells that will not persist into a POMC terminal identity. The off target consequences of these manipulations have yet to be considered. Our work will provide the foundational evidence for potential confounds of targeted genetic POMC manipulations and may help to explain some of the unexpected phenotypes that have arisin using a BAC transgenic *Pomc-Cre* reagent.

My current research efforts are focused on elucidating the molecular mechanism regulating differentiation and cell fate specification in the ARH during gestation and the early postnatal period (Chapter 4). Consistent with the identification of *Pomc* transcriptional activity during embryogenesis, functional POMC-processing products (β-endorphin and α-melanocyte-stimulating hormone) are also detected in embryonic hypothalamic extracts (at embryonic day (E) 13.5 and E15.5, respectively). The presence of POMC-derived peptides in the embryo, prior to the establishment of circuits regulating food intake, may be involved in the local differentiation events. Preliminary loss-of-function studies are underway to determine the role of POMC-derived peptides in differentiation of hypothalamic terminal fates. Early results from this work indicate that both β-endorphin and α-melanocyte-stimulating hormone are critical to the differentiation of the *Pomc* lineage. The goal of this work is to define the developmental origins of critical components of neuronal circuits that determine body weight. Evidence in the literature supports that maternal signals influence these events, our studies may provide a means to the design of effective strategies to reduce transmission of signals that increase susceptibility to obesity in offspring.

TABLE OF CONTENTS

CHAPTER 1: BACKGROUND OVERVIEW

Body Weight Homeostasis and the Sensation of Hunger

Thermodynamics of living systems must accommodate the constant exchange of mass and energy from the environment. While open systems cannot achieve flat-line equilibrium, they instead fluctuate about threshold levels of dynamic equilibrium referred to as homeostasis. One example of homeostatic regulation occurs in the cellular supply of energy. The specific energy charge of most cells is maintained at a ratio of ATP:ADP equaling 10:1 (Hardie and Hawley, 2001). This relationship is used as a sensor of the cell's energy availability; in cases when the ratio is low, catabolic oxidation pathways are activated to replenish levels of ATP. Conversely, when the ratio is high, excess ATP can either be utilized for mechanical work or stored via anabolic metabolism. This process of homeostasis, the fluctuation around a "set-point" or "threshold", is a means of regulation for biologically open systems. In mammals, homeostatic regulation maintains cellular energy charge, blood glucose levels, the insulin:glucagon ratio, bone density, body weight, temperature, pH, etc. Biological systems utilize sensor molecules (relative to each unique homeostatic system) to initiate perpetual feedback regulation about each threshold.

Human body weight, over the course of one year, is relatively constant (Leibel et al., 1995). The sensor system involved in maintaining body weight is complex and the details remain somewhat unresolved. Homeostasis of body weight or a certain percent body fat is constantly adjusted by alterations in food intake and energy expenditure. If the percent body fat of a subject is relatively low, increasing food intake relative to energy expenditure will replenish stores. Conversely, decreasing energy consumption relatively to energy expenditure serves as a means to restore body weight homeostasis when fat stores are ample. Hunger, satiety and energy expenditure are the output measures that determine body weight, but critically important

to this flux are the input signals that coordinate this response according to energy availability, thus beginning the early investigations into the sensations of hunger.

At the turn of the twentieth century Babinski-Frohlich syndrome was first described in children with rare tumors found at the base of the brain just anterior to the brain stem who presented with hyperphagia, were obese and had retarded puberty (Bruch, 1993). Based on such cases, it was hypothesized that this area of the brain (in and around the hypothalamus) may be responsible for body weight regulation and feeding behavior. At the time, researchers lacked the tools needed to thoroughly investigate this observation.

At University College London, Horsley and Clark invented a stereotactic apparatus, an instrument used to three dimensionally map and target precise regions of the brain. This device, assembled on the head of an animal model, provided a novel tool to test hypotheses related to physiology of the brain. Using this technology, the first hypothalamic lesion experiments were performed to investigate the role of the hypothalamus in the sensation of hunger. Data from numerous labs in the 40s and 50s found that bilateral lesions administered to the mediobasal hypothalamus of rats resulted in hyperphagia induced obesity (Anand BK, 1951; Hervey, 1959; Hetherington AW, 1940). Lesioned animals became “voracious,” eating approximately 30 percent more kcal/day compared to controls (Hervey, 1959). This work established the importance of central hypothalamic signaling in the determination of body weight and opened the field to explore the afferent signaling factors underlying this specific motor output.

G.R. Hervey, a scientist at Cambridge, proposed that blood born substances were the source of hypothalamic input responsible for determining satiety. He predicted that circulating satiety signals would increase in hypothalamic-lesioned obese animals, and that their consequent weight gain was the result of damaged sensing cells in the hypothalamus. Using parabiosis technology – in which animals were surgically fastened together (parabiosed), sharing a plasma volume exchange of ~0.3 to 2.1 percent per minute with the conjoined animal

– Hervey investigated circulating blood factors in hypothalamic-lesioned animals. Upon parabiosis of two wild-type animals, one was subjected to a bilateral hypothalamic lesion, while the other not. Of these lesioned/non-lesioned parabiosed pairs, the lesioned animals became obese, while the non-lesioned animals became “listless, inactive, thin and presented a starved appearance.” Upon sacrifice (30 days following lesioning), the non-lesioned animals weighed approximately 25 percent less than littermate controls (Hervey, 1959). These experiments supported Hervey’s hypothesis that blood born satiety signals were one source of afferent inputs to the hypothalamus responsible for mediating bodyweight.

These early lesion experiments left the field eager to discover the responsible circulating satiety signal/s. In the 1950’s Gordon Kennedy proposed that because adipose levels varied among lesioned animals, that the adipose tissue was the source of the elusive satiety signal (Kennedy, 1953). However, beyond this idea, Kennedy did not perform experiments to test his hypothesis.

In the 1960s, Doug Coleman performed a seminal set of experiments which provided the foundation for the ultimate discovery and cloning of leptin, 30 years later. Coleman was very interested in two strains of monogenetic mutant “obese” mice that had emerged from Jackson Laboratory, and sought to discover the genes underlying the obese phenotype of these mutants, coined: *db (diabetes)* and *ob (obesity)*. Using a similar approach to Hervey, Coleman performed parabiosis experiments and found that wild-type animals paired with *db/db* animals suffered from lethal aphagia. Furthermore, he found that *ob/ob* animals also became lethally anorexic when paired with *db/db*s. This work provided the tantalizing evidence that *db/db* mice harbored excessive amounts of a yet undefined circulating satiety factor, and also that both the *db* and *ob* genes were involved in a common pathway (Coleman, 1973).

Today, both the *db* and *ob* genes have been mapped and cloned, and we now know that the *ob* gene encodes the polypeptide hormone leptin, while *db* gene encodes the leptin receptor

protein (Tartaglia et al., 1995; Zhang et al., 1994). As originally hypothesized by Kennedy, it has been demonstrated that leptin is an adipokine produced by adipocytes in proportion to their triglyceride content (reviewed in: (Myers et al., 2010)). Furthermore, many cells within hypothalamic nuclei express a brain specific splice variant of the leptin receptor (ObRb), which is localized with particular density in the mediobasal hypothalamus (MBH) (Elmquist et al., 1998; Lee et al., 1996; Scott et al., 2009). Recombinant leptin protein administered directly into the brain (via intracerebroventricular (ICV) injection) of *ob/ob* animals largely rescued the body weight phenotype (Campfield et al., 1995). Based on this work, contemporary belief is that leptin is expressed peripherally and then relayed to hypothalamic circuits via systemic circulation, acting to determine food intake and energy expenditure in response to peripheral levels of adiposity. It is also thought that because *ob/ob* and *db/db* mutants are lacking hypothalamic leptin signaling, they are in a paradoxical state of starvation, and that hyperphagia in these animals is the consequence of a failure to detect feedback leptin signaling from the adipose.

The Hypothalamic-Adipose Axis

The above findings represent the foundational evidence toward defining the molecular details of body weight homeostasis. Research vested in furthering such efforts are of critical importance to contemporary society as obesity at large has reached pandemic proportions in the developed world and constitutes a considerable burden to the health and wellbeing of affected individuals (Bjorntorp, 1992; Flegal et al., 2010; Popkin). Obesity – characterized by excessive fat storage and indicated a body mass index of greater than 30 kg/m^2 – is implicated in the dysregulation of many homeostatic processes that lead to the life threatening complications of diabetes, hypertension, and dyslipidemia. The prevalence of obesity over the past 40 years has increased dramatically, in trends that are not accompanied significant alterations in dietary conditions, and surely too rapid to be explained by evolutionary adaptations (Ogden et al., 2010).

It is well established that individuals regulate and defend threshold levels (set-points) of body fat, such that body weight over the course of a year is remarkably stable – a paradigm that holds true for both lean and obese subjects (reviewed in: (Leibel, 2008). In a weight-reduced state ≤ 10 percent of baseline, humans display reductions in energy expenditure and increased hunger (referred to as metabolic adaptation) that drives a rebound to original adiposity levels (Leibel and Hirsch, 1984; MacLean et al., 2004). Both obese and non-obese models exemplify this same metabolic paradigm; however, in the case of obesity the threshold of regulation is set to maintain much higher adipose levels.

Upon cloning of leptin, the field largely anticipated its potential as a cure for human obesity. However, surprisingly, most obese patients have high levels of circulating leptin, and the rate of monogenetic mutations in either the *ob* or *db* genes are exceedingly rare (Clement et al., 1998; Farooqi et al., 2007; Montague et al., 1997). The majority of obesity among humans is instead characterized as a polygenic disorder accompanied by leptin resistance – leptin levels that are proportionally higher than expected when normalized to fat mass – in which recombinant leptin therapy is ineffective (Bluher and Mantzoros, 2009; Frederich et al., 1995).

Hypothalamic Determinants of Body Weight: Melanocortin System

To circumvent leptin resistance, much work has gone into determining downstream targets of leptin action in the brain. Exciting work towards this end has come from the identification of the central melanocortin (MC) system. Using a mouse model of monogenetic obesity, agouti viable yellow A^{vy}, researchers have defined a class of leptin induced satiety signals which mediate their action through stimulation of the melanocortin receptor, MC4R. ICV injections of an MC4R/melanocyte agonist, MTII, acutely reduce hyperphagia in the *ob/ob* animals similar to that of leptin (Fan et al., 1997).

Similar to Coleman's early studies an alternative model of monogenetic obesity, Agouti viable yellow A^{vy}, was used to elucidate many properties of central MC signaling. Agouti viable

yellow $A^{vy/vy}$ homozygous mutant mice are obese, have a distinctive yellow coat coloring, are slightly longer than controls and are prone to tumors (Wolff, 1963). Initially, the A^{vy} mutation was genetically mapped to the *Agouti* gene locus, and found to cause aberrant, ectopic expression of *Agouti* (Bultman et al., 1992; Yen et al., 1994). Canonical agouti expression and signaling was first described in melanocytes of the skin, where its inhibitory action on the melanocortin receptor, MC1R, prevented synthesis of eumelanin, a protein responsible for black/brown pigmentation of hair follicles (Lu et al., 1994; Wolff, 1963). The yellow coat color phenotype of $A^{vy/vy}$ mutants was attributed to the inhibition of MC1R by AGOUTI protein, preventing binding of the endogenous ligand alpha-melanocyte stimulatin hormone (α-MSH) and the subsequent synthesis of eumelanin. Along with the elucidation of this mechanism, it was further discovered that melanocortin receptors had multiple isoforms and were expressed in a tissue specific manner. Currently, 5 MCR isoforms have been identified (MC1R-5R), two of which (-3R, -4R) are expressed in the brain (Gantz et al., 1993a; Gantz et al., 1993b; Mountjoy et al., 1994; Roselli-Rehfuss et al., 1993).

Based on evidence presented previously, leptin signaling in the brain was believed to orchestrate a large part of energy homeostasis. Given this, Cone and colleagues hypothesized that the action of Agouti signaling on MC3R and MC4R in the brain was responsible for the body weight phenotype of $A^{vy/vy}$ animals. To test this, Cone et al. (1997) performed ICV injections of an α-MSH analogue, MT-II (Ac-Nle-c[Asp-His-D-phe-Arg-Trp-Lys]-NH_2), and found it to induce satiety (Al-Obeidi et al., 1989; Chhajlani and Wikberg, 1992; Roselli-Rehfuss et al., 1993). To further prove that AGOUTI protein inhibited MCR signaling in the brain, Cone went on to develop an agouti specific mimetic called SHU9119, finding that the effects of MT-II were blunted by the corresponding ICV administration of SHU9119 (Fan et al., 1997). In *ob/ob* animals, ICV administration of MTII recapitulated feeding suppression similar to that found with

ICV leptin, suggesting that the effects of melanocortin signaling were downstream of leptin's action in the brain (Campfield et al., 1995).

These seminal findings prompted a response among the research community to further elucidate the properties of MC3R and MC4R, and the mechanisms by which they mediate satiety. Loss-of-function mutations targeted to neural MCRs can have dramatic effects on adiposity levels similar to those of *ob/ob* and *db/db* models. Specifically, genetic ablation of *mc4r-/-*, resulted in maturity onset obesity with noted sexual dimorphism: female adiposity compared to controls was approximately 50 percent more than that of males (Huszar et al., 1997). *Mc3r*$^{-/-}$ loss-of-function mutants did not present an overt adiposity phenotype, but the animals were more prone to obesity when challenged on a high fat diet and were shorter in length compared to controls (Chen et al., 2000). Altogether, this work supported that the influence of central MC signaling on body weight determination was predominantly mediated by MC4R, while MC3R appeared to play a minor role.

Generally, MC3R and 4R are thought to localize to mutually exclusive neuronal populations. Transgenic *mc4r* reporter analysis indicated the presence of MC4R in both neurons and astrocytes of the: cortex, thalamus, hypothalamus, parabrachial (PB), brainstem, spinal cord and hippocampus; with notable density in the paraventricular nucleus of the hypothalamus (PVH) and also in the dorsal motor nucleus of the vagus nerve (DMX) in the brainstem (Gantz et al., 1993b; Liu et al., 2003). In the brain, *mc3r* expression was more limited, identified mainly in the arcuate nucleus of the hypothalamus (ARH) with low levels of expression detected in the thalamus and brainstem. *Mc3r* expression was also identified in some peripheral tissues including: placenta, heart, kidney, stomach, adipose tissue, skeletal muscle, duodenum, and pancreas (Chhajlani, 1996; Gantz et al., 1993a).

To further understand the physiologic role of central MC signaling in energy homeostasis, researchers went on to define the endogenous ligands of the system. As discussed previously,

the endogenous melanocyte agonist, α-MSH was known to mediate MC1R dependent hair follicle pigmentation. α-MSH is a cleavage product of the pro-peptide POMC. Post-translation modifications of the pro-peptide, POMC, has been demonstrated to occur in a tissue specific manner, resulting in a multitude of functional POMC derived peptides. In the hypothalamus processing of POMC occurs according to the diagram below (depicted in a recent review by Dr. Sharon Wardlaw, Figure 1.1 (Wardlaw, 2011)). The processing enzymes pro-hormone convertase (PC) isoforms PC1/3 and PC2 are expressed in the hypothalamus along with carboxypeptidase E (CPE). Upon translation, POMC is targeted and trafficked to the golgi where the functional products are then processed and packaged into secretory granules. POMC is initially cleaved into two main functional derivatives; adrenocorticotropic hormone (ACTH) and beta-lipotropin (β-LPH). In the hypothalamus these products are further processed by the action of PC2 and CPE which converts ACTH into an amidated form of deacetyl-α-MSH (1-13) and CLIP, while β-LPH is further processed into β-endorphin (β-EP) and β-MSH (Emeson and Eipper, 1986). In the mature brain *Pomc* is expressed throughout the medialbasal hypothalamus in regions of the retrochiasmatic area, ARH and mammillary nucleus (Knigge et al., 1981). Extra-hypothalamic sites of *Pomc* expression in the mature brain include the retina, spinal cord, commissural nucleus of the solitary tract (cNTS) and area postrema (AP) (Bronstein et al., 1992; Gallagher et al., 2010; Lein et al., 2007; Watson et al., 1978). To date POMC derived MSH variants are the only known endogenous ligand agonists of MCRs.

Figure 1.1

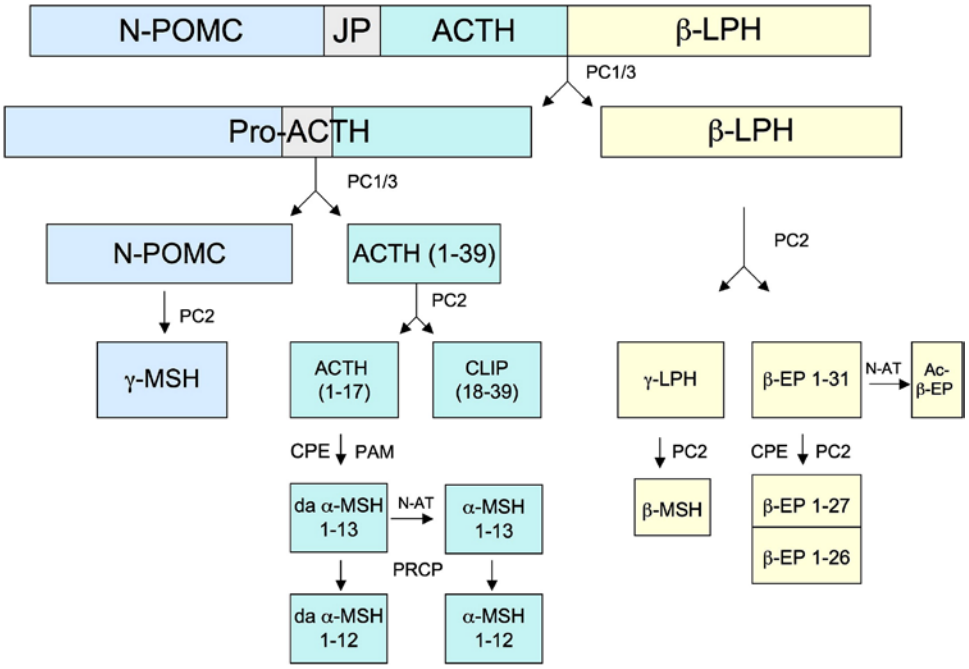

Fig. 1.1. "POMC processing. Schematic diagram of the POMC precursor molecule and the major peptide products that are derived from this precursor by endoproteolytic cleavage. JP = Joining peptide; LPH = Lipotropin; EP = Endorphin; CLIP = Corticotropin-like-intermediate lobe peptide; da-α-MSH = desacetyl α-MSH; PC1/3 and PC2 = Prohormone convertases 1/3 and 2; CPE = Carboxypeptidase E; N-AT = N-acetyltransferase; PAM = Peptidyl α-amidating monooxygenase; PRCP = Prolylcarboxypeptidase." (Wardlaw, 2011)

Targeted genetic ablation of the *Pomc* gene resulted in a phenotype that trended toward *mc4r*$^{-/-}$null characteristics, including maturity onset obesity and an increase in body length (Yaswen et al., 1999). However, the phenotype of these two models differed in final body weight; adult *Pomc*$^{-/-}$ nulls weighed ~20 percent less than *mc4r*$^{-/-}$nulls. One explanation for this discrepancy: unlike *Mc4r*-expressing cells, *Pomc*-expressing cells are not restricted to the brain and in particular are present in corticotrophs of the anterior pituitary. To resolve this issue, Low et al. (2006) generated animals in which pituitary *Pomc* expression was rescued on a *Pomc*$^{-/-}$ background. Surprisingly, the obesity phenotype of these *Pomc*$^{-/-}$*tg*$^{+}$ animals was exacerbated, achieving adiposity levels comparable to that of the *mc4r*$^{-/-}$ (Smart et al., 2006). Importantly, POMC in the pituitary is processed to Adrenocorticotropic Hormone (ACTH) and communicated

to the adrenal gland via the pituitary/adrenal axis. In the adrenal, ACTH stimulates the release of corticosterone, a peripherally circulating orexigen. Hence, *Pomc*$^{-/-}$*tg*$^{+}$ animals weigh more than global *Pomc*$^{-/-}$ nulls due to corticosterone signaling in the periphery.

Further work identified an endogenously expressed Agouti isoform in the brain. Agouti-related protein (AgRP) expression was identified in neurons of the medial aspect the ARH and also in the adrenal gland (Broberger et al., 1998). Using an *in-vitro* culture system, Barsh et al. (1997) used kinetic binding assays to investigate AgRPs action on distinct MCR isoforms. These studies showed that AgRP specifically prevented α-MSH-induced cAMP in both MC3R and MC4R isoforms, but did not disrupt this activity in other MCR variants (Ollmann et al., 1997). In this same study the Barsh lab also generated an *in vivo* model of AgRP overexpression, by engineering an *Agrp* transgene under the control of the β-actin promoter, *Tg-Agrp*. This gain-of-function model resulted in animals that were obese and longer in naso-anal length compared to controls. Compared to *mc4r*$^{-/-}$, *Tg-Agrp* overexpression achieved ~70 percent of the body weight phenotype (Ollmann et al., 1997).

Similar to central leptin signaling, MC circuits in the brain can dramatically influence body weight homeostasis. Because ICV injections of the melanocyte agonist MTII, had similar effects to ICV leptin in *ob/ob* animals, it was anticipated that targeting this downstream circuit would bypass leptin resistance in many common forms of obesity. Diet induced obese (DIO) animals have a form of heritable susceptibility to obesity which is induced by a Western-type diet (Levin et al., 1997). In these animals, leptin levels are high in proportion to fat mass, however they are resistant to its effects in the brain. Unfortunately, administration of pharmacologic MTII into the brains of DIO animals had marginal effects body weight and adiposity, indicating that central leptin resistance may lie at the level of MC circuits (Banno et al., 2007). A search for an effective pharmacologic treatment for obesity remains elusive.

Hypothalamic Determinants of Body Weight: NPY/AgRP

Prior to the discovery of AgRP (1998), an alternative neuropeptide circuit, stimulated by the endogenous ligand neuropeptide Y (NPY), was determined to elicit orexigenic effects. NPY is the most abundant neuropeptide in the brain and numerous physiologic functions are attributed to NPY signaling including: food intake, blood pressure and circadian rhythms (Allen et al., 1983; Balasubramaniam, 1997). NPY is a member of homologous proteins including: pancreatic polypeptide and polypeptide YY, peptide YY and seminalplasmin, all characterized by a 36 amino acid sequence and a structural signature that includes a hairpin-like loop referred to has a PP-fold (Fuhlendorff et al., 1990; Tatemoto, 1982; Tatemoto et al., 1982). Central ICV injections of NPY stimulate consummatory behavior; injected animals eat more frequently and overall consume more calories (Clark et al., 1984; Levine and Morley, 1984).

The orexigenic effects of NPY are predominantly determined by the ligands interaction with NPY receptor-expressing neurons in the paraventricular nucleus of the hypothalamus (PVH). Compared to ICV injections, direct injections of NPY into the PVH induced a fourfold greater effect on stimulated caloric intake (Stanley and Leibowitz, 1985). Diurnal analyses of NPY protein concentration in the PVH revealed that levels of NPY released into the PVH change dynamically in relation to prandial state. Levels of NPY in the PVH were highest in the fasted state and lowest postprandial (Kalra et al., 1991). Together, these data support that NPY is released into the PVH in response to fluctuating feeding patterns and that the action of NPY in the PVH can stimulate feeding.

In the 80s it was assumed that alpha-adrenergic receptors in the PVH were mediating the effects of NPY via the autonomic nervous system. However, administration of phentolamine, an alpha-adrenergic receptor antagonist, prior to direct NPY injections did not attenuate stimulated food intake (Stanley and Leibowitz, 1985). Since these studies, five NPY receptor isoforms, NPYR 1-5 (YR1-YR5), have been defined. YRs are stereotypical class A, G protein coupled,

rhodopsin-like receptors, which exclusively bind NPY family ligands. In vitro kinetic studies have shown that, of NPY family proteins, NPY has the most affinity for YR1, YR2 and YR5. Pharmacologic agonist and antagonists against these receptor subtypes have shown that NPY mediates its effects on orexigenic behavior predominantly through YR5 receptors (Gerald et al., 1996). YR5 is expressed in many areas of the brain, including a dense population of cells in the hippocampus and cortex with moderate expression levels in the thalamus, amygdala, dorsal raphe and the hypothalamus (including the PVH, LHA, SON and ARH) (Gerald et al., 1996).

In 1998, numerous studies determined that *Npy* transcript was co-localized with *Agrp*, indicating that ≥ 95 percent of NPY neurons in the ARH were AgRP+ (Hahn et al., 1998; Shutter et al., 1997). Because *Agrp* expression is restricted to the ARH (Broberger et al., 1998), it can be used to distinguish NPY/AgRP neurons in the ARH from 'other' NPY+ neurons in alternative regions of the CNS.

Given these findings, a series of *in vivo* loss-of-function genetic mutants were engineered to further understand the physiology of the NPY/AgRP system. Initially, the Palmiter laboratory generated a genetically null $Npy^{-/-}$ mouse model, and surprisingly found that $Npy^{-/-}$ mice did not exhibit a body weight phenotype and responded normally when fast challenged (Erickson et al., 1996). Furthermore, genetically null $Agrp^{-/-}$ mutants, along with double null $Npy^{-/-}/Agrp^{-/-}$, did not present a phenotype related to energy homeostasis (Qian et al., 2002). Next, based on the pharmacologic data implicating Y5Rs in NPY stimulated food intake, Palmiter et al. (1998) generated a genetically null Y5R mouse model. As with the NPY null animals these mice did not have an overt body weight phenotype (Marsh et al., 1998). Despite considerable evidence that NPY, AgRP and Y5R play a central role in stimulating appetite, genetic ablation of these genes had little impact on energy homeostasis outcomes. At the time, Palmiter hypothesized that these genetic manipulations altered the developmental establishment of the hypothalamus leading to compensatory modifications. To avoid these potential confounds, the Palmiter group

(2005), along with others, went on to ablate NPY/AgRP neurons in a temporally controlled manner (Gropp et al., 2005; Luquet et al., 2005). Specifically, Palmiter et al (2005) generated transgenic animals in which the regulatory elements of *Agrp* were used to drive expression of a diphtheria toxin receptor (DTR) transgene, AgRP:*dtr*$^{+/+}$. Upon administration of diphtheria (DT), *Agrp* expressing cells were targeted for complete cellular ablation. These studies revealed that ablation of AgRP neurons in the mature brain results in lethal anorexia; the mice became aphagic and rapidly died of starvation (Luquet et al., 2005). Interestingly, if DT was administered early, during the perinatal period, the animals survived, had a lean phenotype and were resistant to diet-induced obesity.

To narrow down some of the compensatory signals Palmiter and colleagues crossed AgRP:*dtr*$^{+/+}$ transgenics to genetically null *Npy*$^{-/-}$/*Agrp*$^{-/-}$ animals. Administration of DT to these animals surprisingly induced acute lethal anorexia. The compensation found in double null *Npy*$^{-/-}$/*Agrp*$^{-/-}$ mutants was diminished by later ablation of these cell bodies, consistent with the idea that a potent compensatory orexigenic signal resided in AgRP neurons (Phillips and Palmiter, 2008). Because AgRP was thought to largely act through antagonism of MC3 and 4R, Palmiter et al. (2008) next crossed AgRP:*dtr*$^{+/+}$ transgenics to the agouti viable yellow strain, *A*$^{vy/vy}$ and found that administration of DT in mature animals also induced lethal anorexia (Wu et al., 2008). Because ectopic AGOUTI, of the *A*$^{vy/vy}$ mutant strain should inhibit MCRs, it was surprising that such a manipulation, in the absence on anorexigenic melanocortin signaling, induced hypophagia. This model is consistent with the idea that central melanocortin circuits are not paramount to the anorexigenic response.

At the time it was known that gamma-aminobutyric acid (GABA) receptor agonists stimulated feeding (Cooper and Higgs, 2005; Ebenezer and Surujbally, 2007), and also that NPY/AgRP neurons co-expressed GABA (Cowley et al., 2001; Horvath et al., 1997). To test whether the neurotransmitter, GABA, was the elusive compensatory orexigenic signal, Palmiter

et al. (2009) infused a GABA agonist via subcutaneous minipump to AgRP:*dtr*$^{+/+}$ mutants, finding it sufficient to rescue the lethal anorexia phenotype upon DT administration. The lab went on to define the PB as the critical secondary target, which, in the absence of GABA inhibition, elicits potent anorexigenic affects (Wu et al., 2009). It should be noted that genetic inactivation of GABA signaling in AgRP neurons – achieved by conditional inactivation of the vesicular GABA transporter gene (*Vgat*), AgRP:*Vgat*$^{fl/fl}$ – phenotypically resembled the mild phenotype observed after ablation of AgRP in neonatal mice. AgRP:*Vgat*$^{fl/fl}$ were lean and resistant to diet-induced obesity, suggesting that, as with AgRP ablation, compensation can occur when GABA production in AgRP neurons is compromised during early development (Tong et al., 2008). All together, these studies suggest that plasticity during development can overcome early insults to central feeding circuits, and are particularly adept to compensate for orexigenic signals which assure the health and survival of the organism.

In the recent literature many labs have designed inducible genetic reagents, which can be activated in the mature system, avoiding developmental compensation. For example the Lowell laboratory has engineered designer receptors exclusively activated by designer drugs (DREADD) technology into AgRP neurons, AGRP:*Dreadd*$^{+/+}$, to provide specific and reversible regulation of neuronal activity. In the mature state, a DREADD agonist was administered, inducing AgRP-specific depolarization, and induced an acute stimulation of food intake (3-fold induction following a single injection) and decreased energy expenditure (1.3-fold). Upon multiple dosages of the DREADD agonist, the mice gained a substantial amount of weight in the form of adiposity, which was acutely reversed upon withdrawal of treatment (Krashes et al., 2011). Similarly, investigators of the Sternson laboratory have engineered a channelrhodopsin-2 channel into AgPR neurons; *AgRP:Chr2*$^{+/+}$, to provide a means for conditional photostimulation. In the mature state, light was used to selectively stimulate AgRP-specific depolarization, and

similar to the DREADD agonist, induced an acute stimulation of food intake, which diminished upon decreasing stimulus frequency (Aponte et al., 2011).

POMC and NPY Neurons: Response to the Environment

The current dogma of energy homeostasis is that autonomic and neuroendocrine effects on feeding behavior and energy expenditure are primarily elicited by the anorexigenic POMC and orexigenic AgRP neurons in the ARH. Electrophysiological recording studies have shown that POMC and AgRP neuronal activity is influenced by peripheral energy status namely: leptin, insulin and glucose (reviewed in: (Morton et al., 2006)). Because the ARH is positioned adjacent to the median eminence, a uniquely fenestrated area of the blood brain barrier, it is believed that these signals in the peripheral circulation are transmitted into the internal milieu of the ARH to regulate food intake and energy expenditure.

Leptin: Leptin-sensing in proportion to adiposity stores and has been shown to play a critical role in hypothalamic determination of food intake. Via modulation of the downstream transcription factor STAT3, leptin transduction induces expression of *Pomc* while inhibiting that of Agrp (Kitamura et al., 2006; Korner et al., 2001; Morrison et al., 2005). Consistent with this, electrophysiological recordings indicate that leptin depolarizes a subset of POMC neurons, while conversely hyperpolorizing NPY/AgRP neurons (Claret et al., 2007; Cowley et al., 2001; Plum et al., 2006; Williams et al., 2010). Given this, it was anticipated that *in vivo* loss-of-function leptin receptor mutations ($Lepr^{fl/fl}$) targeted to POMC and AgRP neurons would induce an obesity phenotype comparable to that of global leptin mutants (approximately 2.6-fold increase). Surprisingly, targeted genetic ablation of $Lepr^{fl/fl}$ using conditional *Agrp-Cre* and *Pomc-Cre* had a marginal effect compared to the global leptin mutants. POMC:$Lepr^{fl/fl}$ animals were relatively eumetabolic, with a body weight phenotype accounting for a modest 15 percent of that incurred in global leptin mutants (Balthasar et al., 2004). AgRP: $Lepr^{fl/fl}$ mutants likewise presented a mild obesity phenotype attributed to transient hyperphagia and reduced energy

expenditure in young male mice (van de Wall et al., 2008). AGRP+POMC:*Lepr*$^{fl/fl}$ double knock-outs were expected to exacerbate the body weight phenotype, but instead presented marginal increases in body weight, accruing only 18 percent of the body weight phenotype of global mutants, along with decreased core temperature and locomotor activity.

Insulin: Insulin, a hormone released in response to elevated blood glucose levels, circulates as an indicator of peripheral glucose supply. Like leptin, insulin has been shown to influence central circuits involved in feeding behavior and energy expenditure, albeit with much lesser effects. Neuronal specific ablation of the insulin receptor (*Ir*$^{fl/fl}$) using the *Nestin-Cre driver* (NIRKO) resulted in mild, sex-specific phenotypes including: insulin resistance, body weight and adiposity (achieving roughly 20 percent of global leptin mutants) (Bruning et al., 2000). Via modulation of the downstream transcription factor FOXO1, insulin transduction acts to activate *Pomc* transcription while inhibiting *Agrp* (Belgardt et al., 2008; Kitamura et al., 2006). Furthermore, ICV administration of insulin up-regulates *Pomc* and down-regulates *Npy* expression levels (Schwartz et al., 1992; Sipols et al., 1995). While the transcriptional influence of insulin on *Pomc* and *Agrp* corresponds with that of leptin, electrophysiological recordings yield a paradoxical response. Insulin inhibits a subset a subset of POMC neurons while activating AgRP neurons (Claret et al., 2007; Konner et al., 2007; Plum et al., 2006; Williams et al., 2010). Because NIRKO mice did not yield a striking phenotype, in vivo loss-of-function studies targeting AgRP and POMC neurons were not anticipated to yield dramatic body weight phenotypes. Both AgRP:*Ir*$^{fl/fl}$ and POMC:*Ir*$^{fl/fl}$ present normal body weight and energy homeostasis, even when challenged on a high fat diet (Konner et al., 2007; Lin et al., 2010).

Glucose: Glucose is an essential fuel for cells in the CNS, but can also act as a signaling molecule influencing membrane potential in disparate “glucose-sensing” neurons. It is estimated that 10 to 30 percent of neurons in the hypothalamus are glucose-sensing, characterized by the action and expression of two gating intermediates – 5' adenosine monophosphate-activated

protein kinase alpha 2 (AMPKα2) and an ATP-activated potassium channel (K_{ATP}) – which influence membrane potential in response to glucose (Levin et al., 2004; Minokoshi et al., 2004). Measured by electrophysiological recording a subset of POMC neurons (approximately 50 percent) are glucose-excited, while AgRP neurons can exhibit either glucose stimulated depolarization or hyperpolarization in mutually exclusive subsets (Claret et al., 2007; Fioramonti et al., 2007; Ibrahim et al., 2003; Murphy et al., 2009; Parton et al., 2007). It has been argued that the concentration of glucose in the internal milieu of the brain is much less than that found in the blood, calling to question the physiological relevance of the doses of glucose used in many of the afore mentioned recording studies (de Vries et al., 2003; Routh, 2002). In the literature *in vivo* loss-of-function studies find inconsistent results with respect to the glucose-sensing hypothalamic response. AgRP:*ampkα2$^{fl/fl}$* are eumetabolic with respect to glucose homeostasis, metabolic rate, feeding behavior, physical activity and percent adiposity, but present a mild lean mass phenotype (Claret et al., 2007). POMC: *ampkα2$^{fl/fl}$* demonstrate significantly increased in food intake, body weight and percent adiposity, accompanied by a decrease in resting metabolic rate and brown adipose tissue UCP1 (Claret et al., 2007). On the other hand, POMC:$K_{ATP}^{-/-}$ mutants do not exhibit alterations relative to body weight, adiposity or metabolic rate, but instead exhibit increased glucose excursion upon glucose tolerance testing (Parton et al., 2007). In summary, the parameters used to study glucose-sensing neurons have been either out of the physiologic range or did not yield consistent *in vivo* results, leading the field to largely dismiss the relevance of glucose-sensing neurons in the hypothalamus (reviewed in: (Levin, 2007)).

To date, conditionally targeted *in vivo* functional manipulations using *Argp-Cre* or *Pomc-Cre* driver lines have produced mild phenotypes with respect to energy homeostasis. It is clear from electrophysiological recordings that discrete subpopulations of POMC and AgRP neurons respond uniquely to leptin, insulin and glucose, thus targeting the entire heterogenous

population may result in confounding outcomes. In the future, the elucidation of genetic reagents for distinct POMC and AgRP homogenous subpopulations will be paramount to defining the physiologic relevance of these subsets. Also, as illustrated by genetic knock-out models of *Npy*$^{-/-}$ and *Agrp*$^{-/-}$, the developing brain is highly plastic, and early genetic manipulations can influence the function of germ cells leading to compensatory alterations. It is important to keep in mind that the onset of both *Agrp-Cre* (postnatal day 9) and *Pomc-Cre* (embryonic day 10.5) expression occur during development when cells of the mediobasal are undergoing differentiation. It is possible that targeted genetic manipulations using these drivers may induce compensatory changes in the developing system, resulting in diminished outcomes.

Development of the ARH

To better understand plasticity, it is important to understand the ontogeny of cells in the ARH. The presumptive ARH derives from the ventral diencephalon (an aspect of the developing forebrain that gives rise to the thalamus and hypothalamus). Naïve progenitor cells in this region of anterior neuroectoderm are steered toward a ventral forebrain fate by the influence of WNT and NODAL signals that diffuse from the axial mesoderm during gastrulation (reviewed in: (Wilson and Houart, 2004)). In subsequent stages of development, sonic hedgehog (SHH) plays a role in defining ventral cell identity along the rostral-caudal extent of the neural tube (Ericson et al., 1995). Recent reports find that the SHH derived from ventral forebrain neuroepithelium is the primary inducer in of cell fates of the anterior and tuberal hypothalamus, including the ARH (Shimogori et al., 2010). Exogenous hedgehog signaling in the hypothalamus induces the expression of the transcription factor NKX2.1 – activated as early as embryonic day 8 in the mouse – a principle intrinsic factor common to most cells of the ventral subpallium and hypothalamus (Price et al., 1992; Shimamura and Rubenstein, 1997; Sussel et al., 1999).

Transcription factors direct genetic programs involved in the specification of distinct cell identities. NKX2.1 is a member of mammalian NKX family of homeobox-containing genes, found

(among other regions) in the proliferative zone of the hypothalamus, including the presumptive ARH (Shimamura et al., 1995). Lineage tracing studies have shown that most cells of the mature ARH derive from *Nkx2.1*-expressing precursors (Ring and Zeltser; Xu et al., 2008). More specifically, most ARH cells destined toward a neuronal fate are derived from *Mash1*-expressing progenitors. MASH1 is a pro-neural transcription factor that promotes neurogenesis via activation of the Neurogenin (NGN) transcription factor family (Horton et al., 1999). Both MASH1 and NGN family transcription factors contain stereotypic basic helix-loop-helix (bHLH) structures. In the developing hypothalamus, MASH1 activation of NGN2 is thought to determine the neurogenic potential of both the ARH and VMH (Parras et al., 2002). *Mash1*$^{-/-}$ null mice display an underdeveloped ventral hypothalamus including a loss of neuroendocrine type cell types in the ARH and VMH (McNay et al., 2006).

Birthdating studies have shown that the majority of neurons in the ARH are born – exit mitotic division – between E11.5 and E12.5 in the developing mouse (Altman and Bayer, 1978; Padilla et al., 2010). Of the entire population of cells in the ARH, POMC and NPY/AgRP neurons comprise only a minority, with others including: tyrosine hydroxylase (TH), growth hormone related hormone (GHRH), gonadotropin-releasing hormone (GnRH), somatostatin (SS), kisspeptin (KISS), galenin (GAL) and pro-dynorphin (pDNY). The function of neurons that reside in the ARH is not limited to energy homeostasis, but also includes outputs involving: somatic growth, reproduction, sexual behavior and analgesics. While the specific programs involved in the differentiation of POMC and AgRP terminal fates are unknown, recent data investigating the role of NGN3 provides some clues as to the differentiation of the *Pomc* lineage. In an *Ngn3*$^{-/-}$ mouse model, Ang et al. (2010) find a diminished number of POMC neurons accompanied by a counterbalance expansion of both NPY and TH+ cells in the MBH (Pelling et al., 2010). This data supports that *Ngn3* is involved in the specification of a lineage including

NPY, TH and POMC terminal fates, and provides rudimentary evidence toward understanding the patterning of neurons in the ARH.

Programming of Body Weight Outcomes

During development, pluripotent progenitor cells differentiate to acquire a terminal cell fate, precise projection pattern and appropriate physical location. In the murine model, the timing of terminal cell fate decisions occurs during embryogenesis, while axonal extension occurs during the perinatal period (Altman and Bayer, 1978; Bouret et al., 2004; Padilla et al., 2010). During such processes of cellular definition, the developing organism is highly plastic and vulnerable to alterations. For example, experiments performed in the 1960's demonstrated that male sex steroids administered to female animals during development could permanently impact the female reproductive axis. Specifically, Gorski and Barraclough (1963) found that a single bolus injection of testosterone administered 5 days after birth (P5) was sufficient to permanently stunt the reproductive outcome in females. Exposed females became sterile and lacked an estrus cycle in later life (Gorski and Barraclough, 1963). Alternatively, in classical studies of ocular dominance, Hubel and Wiesel (1963) first demonstrated that retinal exposure to the specific sensory input of light and patterns are critical to proper development of neural projections that determine visual sensations. In seminal studies, they sewed the eye of a cat shut and found that if deprived of patterned visual inputs during a critical period of perinatal development, the animal experienced a permanent loss of cortical responsiveness in the manipulated eye (Wiesel and Hubel, 1963).

Findings of this sort, led David Barker to hypothesize that the maternal nutrient and hormonal environment can impart lasting effects on the developing offspring. He argued that because exposure to environmental toxins during specific susceptible periods of development – for example testosterone exposure at P5 or the absence of visual input perinatally – can bias the establishment of the future reproductive axis and visual axis, then it was possible that

maternal nutrient and hormonal environment could impart lasting effects of the developing offspring. These ideas lead to a new field of research vested in defining the fetal-origins of adult disease.

Today, a large body of epidemiologic data in humans and studies of animal models supports that maternal nutrition during gestation can impart permanent changes on the metabolic outcome of the developing fetus. Studies of both over- and under-nutrition during gestation have shown an increased risk for the offspring to develop obesity in adulthood (reviewed in: (Grattan, 2008)). Along with this, long-term prospective, longitudinal clinical studies investigating the effects of gestational diabetes have found that a diabetic intrauterine environment increased the relative risk for the offspring to develop obesity and Type 2 diabetes (Dabelea et al., 2000; Silverman et al., 1998). Furthermore, retrospective data following humans after bariatric surgery induced weight loss have found that siblings gestated in a lean maternal environment were ~50 percent less likely to become obese than those of an obese maternal environment (Kral et al., 2006). Together, this data supports Barker's hypothesis that the intrauterine nutrient and hormonal environment has effects on offspring that extend well beyond the neonatal period, and can program metabolic outcomes in developing offspring.

To date, little is known regarding the mechanisms underlying maternal programing of metabolic outcomes, however a growing body of evidence supports that feeding related signals generated in the hypothalamus can be programmed and may play a role in body weight outcomes in offspring. Since the early 1990s Plagemann et al. have established numerous models of gestational over- and under-nutrition to study the detailed effects of the gestational environment in exposed offspring. In this work they have provided seminal data to suggest hypothalamic nuclei and feeding related signals are compromised in obesity-prone offspring from these models (reviewed in: (Plagemann, 2005)). Towards this same end, others have found that base-line levels of hypothalamic signals that regulate food intake and energy

expenditure, including *Npy/Agrp* and *Pomc* transcripts, are altered in obesity-prone/gestationally exposed offspring (Chen et al., 2008; Leibowitz et al., 2007). Together, these findings correlate alterations of energy-related signals from the ARH in response to the maternal nutrient and hormonal environment. To further investigate this effect at the single cell level, Simerly et al. (2008) have investigated the outcome of neurons in the hypothalamus using a model of maternal obesity previously established to impart a propensity toward obesity in exposed offspring. In this model, they found approximately 24 percent fewer leptin-responsive neurons (PSTAT3 +) in the ARH of exposed animals, suggesting that the gestational nutrient and hormonal can influence the establishment of functional populations in the ARH (Bouret et al., 2008). In studies unrelated to energy expenditure, Spitzer et al. (2008) have found that cell-type neurotransmitter identity in motorneurons can be biased by acute exposure to excitatory, glutamate or inhibitory GABA signals during sensitive periods of differentiation (Root et al., 2008). Based on this evidence we hypothesize that exogenous nutrient and hormonal factors during gestation can act on differentiating neurons in the hypothalamus during sensitive periods of development to bias the cell-type identities of these neurons. For example, the obese microenvironment includes elevated circulating levels of: insulin, leptin, triglyceride and cortisol, all of which may serve as exogenous signals influencing cell fate decisions in the ARH, potentially resulting in Simerly et al's finding of reduced leptin-sensing neurons in exposed offspring. In conclusion, these studies raise the possibility that developmental events can influence cell fate decisions in the developing hypothalamus, and provide a target to further investigate epidemiologic data that maternal obesity confers risk for obesity in offspring.

Hypothalamic Projections Related to Feeding

The ontogeny of neurite outgrowth from the ARH has been mapped. Using Di-I crystal labeling, Simerly et al. (2004) find that the majority axonal extension from the ARH occurs during the second week of postnatal development reaching mature projection patterns by

postnatal day 18 (P18) (Bouret et al., 2004). Mature projection patterns from the ARH largely terminate within the hypothalamus with a minority of projections terminating in other regions of the brain. Inter-hypothalamic targets from the ARH include: the PVH, preoptic area (POA), anteroventral periventricular nucleus (AVPV), dorsal medial hypothalamic nucleus (DMH), ventral medial hypothalamic nucleus (VMH), lateral hypothalamic area (LHA) and interneurons within the ARH (Bouret et al., 2004; Cowley et al., 2001). Extra-hypothalamic targets from the ARH include: the AP, *bed nucleus of the* stria terminalis (BNST), DMX, intermediolateral cell column (IML), lateral septal nucleus (LS), median eminence (ME), nucleus of the solitary tract (NTS), PB and periaqueductal gray (PAG) (Broberger et al., 1998; Elias et al., 1998a; Risold et al., 1997; Shin et al., 2008; Wu et al., 2009; Zhang et al., 2011). The ARH is not the only nucleus within the hypothalamus that mediates energy homeostasis, others include: the PVH, DMH, VMH, LHA, POA and *suprachiasmatic nucleus (*SCH), hereafter referred to as the "feeding centers" (Morton et al., 2006). Aside from mediating bodyweight, overall hypothalamic function is attributed to: hydration, growth, reproduction, thermoregulation, circadian rhythm, defense, arousal, motivated behavior and the onset of puberty (Swanson, 2000). In an evolutionary sense, the fitness of an organism depends on ample energy supply and therefore the efficiency of energy homeostasis to meet cellular work demands will establish the baseline for the ancillary hypothalamic functions listed above. For example, reproduction and somatic growth require positive energy balance; these processes are blunted in starving organisms (Rosenbaum and Leibel, 1999). As mentioned earlier, because *ob/ob* and *db/db* animals lack leptin signaling, they represent an insatiably starved system, and are also infertile.

Hypothalamic body weight regulation is ultimately determined by efferent signaling circuits which originate in the feeding centers and terminate in areas of the brain responsible for mediating all aspects of motor output, including: visceromotor, secretomotor and somatomotor (Fig 1.1). For example, circuits traced from the ARH, VMH, PVH and DMH terminate in the IML

(Elias et al., 1998a; Risold et al., 1997; Zhang et al., 2011). The IML is the primary autonomic nervous system hub, sending signals to sympathetic ganglia which induce visceromotor function; and in this case, influence autonomic basal metabolic rate via sympathetic nervous system (SNS) tone (Saper, 2002). In addition, some neurons in the ARH and PVH terminate in the median eminence, at the base of the hypothalamic-pituitary portal. Central signals released in the hypothalamic-pituitary portal are then communicated to the pituitary, defining neuroendocrine secretomotor output, which among other things can directly influence caloric intake and energy expenditure. Finally, non-homeostatic, cognitive and hedonic aspects of feeding behavior are determined by somatomotor output from the hypothalamus to regions of the midbrain including the PAG, PB and ventral tegmental area (VTA). Retrograde labeling from these areas has identified sources of efferent input in the ARH and LHA (Harris et al., 2005).

Sensory, cortical and behavioral afferent projections, along with endogenous hormones that influence the "feeding centers," act in concert to determine body weight in response to the energy supply and work demand. The PVH receives input from the hippocampus, medial amygdala, subiculum, ARH, DMH, pre-optic area (POA) and NTS. The VMH receives input from the ILA, BNST and ARH. The DMH receives input from the ARH and POA. The ARH receives input from POA, VMN, SCH and NTS. The LHA receives input from the ARH (Bouret et al., 2004; Elias et al., 1998b; Sternson et al., 2005; Swanson, 2000; Swanson and Kuypers, 1980; Zhang et al., 2011). Along with the influence of signals from these afferent circuits, the "feeding centers" are also influenced by endogenous signals in peripheral circulation; such afferents include: the pancreatic hormone insulin, and the adipose derived adipokine leptin, along with meal related signals from the gut: PYY, GLP-1, CCK and ghrelin, act on primary hypothalamic neurons to influence energy homeostasis, reproduction and somatic growth (Flier, 2004).

The diagram below illustrates the central circuits involved in mediating body weight [please note, this diagram does NOT represent all hypothalamic circuits, but includes what is known about those relevant to energy homeostasis] (Figure 1.1).

Figure 1.2

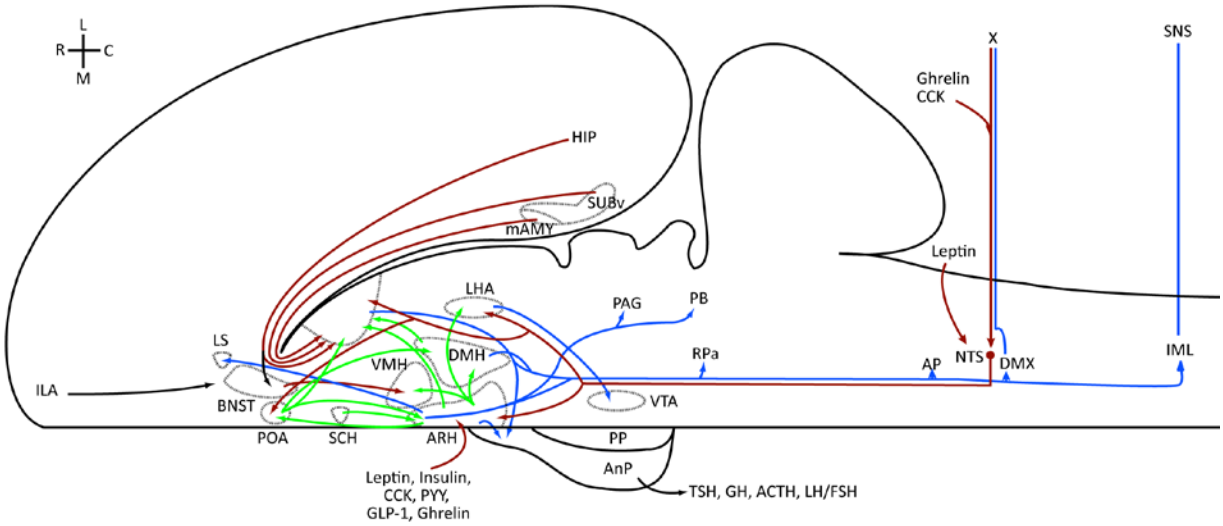

Fig. 1.2 Hypothalamic circuits involved in body weight homeostasis, depicted in a hemi-horizontal plane from the ventral surface. Arrows denote axonal projections: **green**, inter-hypothalamic; **red**, hypothalamic input; **blue**, hypothalamic output; black, extra-hypothalamic relays. (literature summary: (Bouret et al., 2004; Broberger et al., 1998; Elias et al., 1998b; Shin et al., 2008; Sternson et al., 2005; Swanson, 2000; Swanson and Kuypers, 1980; Wu et al., 2009; Zhang et al., 2011)).

Projection patterns of neurons of POMC and AgRP neurons have also been characterized. Many AgRP+ fibers terminate locally within the hypothalamus, in aspects of the PVH, VMH, DMH and inter-ARH. Some AgRP fibers project outside of the hypothalamus terminating in the lateral septal nucleus, *bed nucleus of the* stria terminalis, periaqueductal gray, parabrachial, AP, NTS, DMX and IML (Broberger et al., 1998; Shin et al., 2008; Wu et al., 2009). Considering that AgRP acts in an inhibitory fashion to MC signaling, most AgRP and αMSH+ fibers terminate in similar regions of the brain (Elmquist et al., 1998; Elmquist et al., 1999; Zheng et al., 2010).

Concluding Remarks

Obesity is implicated in the dysregulation of many homeostatic processes that lead to the life threatening complications of diabetes, hypertension, and dyslipidemia (Bjorntorp, 1992).

Despite concerted efforts toward dietary intervention, the prevalence of obesity over the past 40 years has increased dramatically (Leibel et al., 1995; Ogden et al., 2010). A large body of epidemiologic data in humans and studies of animal models supports that maternal nutrition during gestation can impart permanent changes on the metabolic outcome of the developing fetus, and (among other things) can program a propensity for obesity in offspring, such that exposure to a high-fat diet can induce permanent body weight increases. It is possible that susceptibility of obesity is instilled during gestational development, and considering high-fat diets are available at little to no energetic cost in the developed world, may explain the rapid emergence of this disorder in these societies. Relatively little is known regarding the molecular determinants of maternally programmed obesity susceptibility; however some early findings indicate that hypothalamic output and composition are altered in maternally programmed, obesity-prone offspring. In the following studies we will begin to establish the ontogeny of energy-related signals in the hypothalamus. If these events are susceptible to environmental insult during gestation, then it is possible that targeted intervention of early hypothalamic differentiation decisions may prove an effective target towards combating obesity.

References

Al-Obeidi, F., Castrucci, A.M., Hadley, M.E., and Hruby, V.J. (1989). Potent and prolonged acting cyclic lactam analogues of alpha-melanotropin: design based on molecular dynamics. J Med Chem *32*, 2555-2561.

Allen, Y.S., Adrian, T.E., Allen, J.M., Tatemoto, K., Crow, T.J., Bloom, S.R., and Polak, J.M. (1983). Neuropeptide Y distribution in the rat brain. Science *221*, 877-879.

Altman, J., and Bayer, S.A. (1978). Development of the diencephalon in the rat. I. Autoradiographic study of the time of origin and settling patterns of neurons of the hypothalamus. J Comp Neurol *182*, 945-971.

Anand BK, B.J. (1951). Localization of a feeding center in the hypothalamus of the rat. Proc Soc Exp Biol Med *77*, 323-324.

Aponte, Y., Atasoy, D., and Sternson, S.M. (2011). AGRP neurons are sufficient to orchestrate feeding behavior rapidly and without training. Nat Neurosci *14*, 351-355.

Balasubramaniam, A.A. (1997). Neuropeptide Y family of hormones: receptor subtypes and antagonists. Peptides *18*, 445-457.

Balthasar, N., Coppari, R., McMinn, J., Liu, S.M., Lee, C.E., Tang, V., Kenny, C.D., McGovern, R.A., Chua, S.C., Jr., Elmquist, J.K.*, et al.* (2004). Leptin receptor signaling in POMC neurons is required for normal body weight homeostasis. Neuron *42*, 983-991.

Banno, R., Arima, H., Hayashi, M., Goto, M., Watanabe, M., Sato, I., Ozaki, N., Nagasaki, H., and Oiso, Y. (2007). Central administration of melanocortin agonist increased insulin sensitivity in diet-induced obese rats. FEBS Lett *581*, 1131-1136.

Belgardt, B.F., Husch, A., Rother, E., Ernst, M.B., Wunderlich, F.T., Hampel, B., Klockener, T., Alessi, D., Kloppenburg, P., and Bruning, J.C. (2008). PDK1 deficiency in POMC-expressing cells reveals FOXO1-dependent and -independent pathways in control of energy homeostasis and stress response. Cell Metab *7*, 291-301.

Bjorntorp, P. (1992). Abdominal obesity and the metabolic syndrome. Ann Med *24*, 465-468.

Bluher, S., and Mantzoros, C.S. (2009). Leptin in humans: lessons from translational research. Am J Clin Nutr *89*, 991S-997S.

Bouret, S.G., Draper, S.J., and Simerly, R.B. (2004). Formation of projection pathways from the arcuate nucleus of the hypothalamus to hypothalamic regions implicated in the neural control of feeding behavior in mice. J Neurosci *24*, 2797-2805.

Bouret, S.G., Gorski, J.N., Patterson, C.M., Chen, S., Levin, B.E., and Simerly, R.B. (2008). Hypothalamic neural projections are permanently disrupted in diet-induced obese rats. Cell Metab *7*, 179-185.

Broberger, C., Johansen, J., Johansson, C., Schalling, M., and Hokfelt, T. (1998). The neuropeptide Y/agouti gene-related protein (AGRP) brain circuitry in normal, anorectic, and monosodium glutamate-treated mice. Proc Natl Acad Sci U S A *95*, 15043-15048.

Bronstein, D.M., Schafer, M.K., Watson, S.J., and Akil, H. (1992). Evidence that beta-endorphin is synthesized in cells in the nucleus tractus solitarius: detection of POMC mRNA. Brain Res *587*, 269-275.

Bruch, H. (1993). The Frohlich syndrome: report of the original case. 1939. Obes Res *1*, 329-331.

Bruning, J.C., Gautam, D., Burks, D.J., Gillette, J., Schubert, M., Orban, P.C., Klein, R., Krone, W., Muller-Wieland, D., and Kahn, C.R. (2000). Role of brain insulin receptor in control of body weight and reproduction. Science *289*, 2122-2125.

Bultman, S.J., Michaud, E.J., and Woychik, R.P. (1992). Molecular characterization of the mouse agouti locus. Cell *71*, 1195-1204.

Campfield, L.A., Smith, F.J., Guisez, Y., Devos, R., and Burn, P. (1995). Recombinant mouse OB protein: evidence for a peripheral signal linking adiposity and central neural networks. Science *269*, 546-549.

Chen, A.S., Marsh, D.J., Trumbauer, M.E., Frazier, E.G., Guan, X.M., Yu, H., Rosenblum, C.I., Vongs, A., Feng, Y., Cao, L.*, et al.* (2000). Inactivation of the mouse melanocortin-3 receptor results in increased fat mass and reduced lean body mass. Nat Genet *26*, 97-102.

Chen, H., Simar, D., Lambert, K., Mercier, J., and Morris, M.J. (2008). Maternal and postnatal overnutrition differentially impact appetite regulators and fuel metabolism. Endocrinology.

Chhajlani, V. (1996). Distribution of cDNA for melanocortin receptor subtypes in human tissues. Biochem Mol Biol Int *38*, 73-80.

Chhajlani, V., and Wikberg, J.E. (1992). Molecular cloning and expression of the human melanocyte stimulating hormone receptor cDNA. FEBS Lett *309*, 417-420.

Claret, M., Smith, M.A., Batterham, R.L., Selman, C., Choudhury, A.I., Fryer, L.G., Clements, M., Al-Qassab, H., Heffron, H., Xu, A.W.*, et al.* (2007). AMPK is essential for energy homeostasis regulation and glucose sensing by POMC and AgRP neurons. The Journal of clinical investigation *117*, 2325-2336.

Clark, J.T., Kalra, P.S., Crowley, W.R., and Kalra, S.P. (1984). Neuropeptide Y and human pancreatic polypeptide stimulate feeding behavior in rats. Endocrinology *115*, 427-429.

Clement, K., Vaisse, C., Lahlou, N., Cabrol, S., Pelloux, V., Cassuto, D., Gourmelen, M., Dina, C., Chambaz, J., Lacorte, J.M.*, et al.* (1998). A mutation in the human leptin receptor gene causes obesity and pituitary dysfunction. Nature *392*, 398-401.

Coleman, D.L. (1973). Effects of parabiosis of obese with diabetes and normal mice. Diabetologia *9*, 294-298.

Cooper, S.J., and Higgs, S. (2005). Benzodiazepine effects on licking responses for sodium chloride solutions in water-deprived male rats. Physiol Behav *85*, 252-258.

Cowley, M.A., Smart, J.L., Rubinstein, M., Cerdan, M.G., Diano, S., Horvath, T.L., Cone, R.D., and Low, M.J. (2001). Leptin activates anorexigenic POMC neurons through a neural network in the arcuate nucleus. Nature *411*, 480-484.

Dabelea, D., Knowler, W.C., and Pettitt, D.J. (2000). Effect of diabetes in pregnancy on offspring: follow-up research in the Pima Indians. J Matern Fetal Med *9*, 83-88.

de Vries, M.G., Arseneau, L.M., Lawson, M.E., and Beverly, J.L. (2003). Extracellular glucose in rat ventromedial hypothalamus during acute and recurrent hypoglycemia. Diabetes *52*, 2767-2773.

Ebenezer, I.S., and Surujbally, A. (2007). The effects of 8-hydroxy-2-(di-n-propylamino)-tetralin (8-OH-DPAT) on food intake in non-deprived C57BL6 mice. Eur J Pharmacol *559*, 184-188.

Elias, C.F., Lee, C., Kelly, J., Aschkenasi, C., Ahima, R.S., Couceyro, P.R., Kuhar, M.J., Saper, C.B., and Elmquist, J.K. (1998a). Leptin activates hypothalamic CART neurons projecting to the spinal cord. Neuron *21*, 1375-1385.

Elias, C.F., Saper, C.B., Maratos-Flier, E., Tritos, N.A., Lee, C., Kelly, J., Tatro, J.B., Hoffman, G.E., Ollmann, M.M., Barsh, G.S.*, et al.* (1998b). Chemically defined projections linking the mediobasal hypothalamus and the lateral hypothalamic area. J Comp Neurol *402*, 442-459.

Elmquist, J.K., Bjorbaek, C., Ahima, R.S., Flier, J.S., and Saper, C.B. (1998). Distributions of leptin receptor mRNA isoforms in the rat brain. J Comp Neurol *395*, 535-547.

Elmquist, J.K., Elias, C.F., and Saper, C.B. (1999). From lesions to leptin: hypothalamic control of food intake and body weight. Neuron *22*, 221-232.

Emeson, R.B., and Eipper, B.A. (1986). Characterization of pro-ACTH/endorphin-derived peptides in rat hypothalamus. J Neurosci *6*, 837-849.

Erickson, J.C., Clegg, K.E., and Palmiter, R.D. (1996). Sensitivity to leptin and susceptibility to seizures of mice lacking neuropeptide Y. Nature *381*, 415-421.

Ericson, J., Muhr, J., Placzek, M., Lints, T., Jessell, T.M., and Edlund, T. (1995). Sonic hedgehog induces the differentiation of ventral forebrain neurons: a common signal for ventral patterning within the neural tube. Cell *81*, 747-756.

Fan, W., Boston, B.A., Kesterson, R.A., Hruby, V.J., and Cone, R.D. (1997). Role of melanocortinergic neurons in feeding and the agouti obesity syndrome. Nature *385*, 165-168.

Farooqi, I.S., Wangensteen, T., Collins, S., Kimber, W., Matarese, G., Keogh, J.M., Lank, E., Bottomley, B., Lopez-Fernandez, J., Ferraz-Amaro, I.*, et al.* (2007). Clinical and molecular genetic spectrum of congenital deficiency of the leptin receptor. N Engl J Med *356*, 237-247.

Fioramonti, X., Contie, S., Song, Z., Routh, V.H., Lorsignol, A., and Penicaud, L. (2007). Characterization of glucosensing neuron subpopulations in the arcuate nucleus: integration in neuropeptide Y and pro-opio melanocortin networks? Diabetes *56*, 1219-1227.

Flegal, K.M., Carroll, M.D., Ogden, C.L., and Curtin, L.R. (2010). Prevalence and trends in obesity among US adults, 1999-2008. Jama *303*, 235-241.

Flier, J.S. (2004). Obesity wars: molecular progress confronts an expanding epidemic. Cell *116*, 337-350.

Frederich, R.C., Hamann, A., Anderson, S., Lollmann, B., Lowell, B.B., and Flier, J.S. (1995). Leptin levels reflect body lipid content in mice: evidence for diet-induced resistance to leptin action. Nat Med *1*, 1311-1314.

Fuhlendorff, J., Johansen, N.L., Melberg, S.G., Thogersen, H., and Schwartz, T.W. (1990). The antiparallel pancreatic polypeptide fold in the binding of neuropeptide Y to Y1 and Y2 receptors. J Biol Chem *265*, 11706-11712.

Gallagher, S.K., Witkovsky, P., Roux, M.J., Low, M.J., Otero-Corchon, V., Hentges, S.T., and Vigh, J. (2010). beta-Endorphin expression in the mouse retina. J Comp Neurol *518*, 3130-3148.

Gantz, I., Konda, Y., Tashiro, T., Shimoto, Y., Miwa, H., Munzert, G., Watson, S.J., DelValle, J., and Yamada, T. (1993a). Molecular cloning of a novel melanocortin receptor. J Biol Chem *268*, 8246-8250.

Gantz, I., Miwa, H., Konda, Y., Shimoto, Y., Tashiro, T., Watson, S.J., DelValle, J., and Yamada, T. (1993b). Molecular cloning, expression, and gene localization of a fourth melanocortin receptor. J Biol Chem *268*, 15174-15179.

Gerald, C., Walker, M.W., Criscione, L., Gustafson, E.L., Batzl-Hartmann, C., Smith, K.E., Vaysse, P., Durkin, M.M., Laz, T.M., Linemeyer, D.L.*, et al.* (1996). A receptor subtype involved in neuropeptide-Y-induced food intake. Nature *382*, 168-171.

Gorski, R.A., and Barraclough, C.A. (1963). Effects of Low Dosages of Androgen on the Differentiation of Hypothalamic Regulatory Control of Ovulation in the Rat. Endocrinology *73*, 210-216.

Grattan, D.R. (2008). Fetal programming from maternal obesity: eating too much for two? Endocrinology *149*, 5345-5347.

Gropp, E., Shanabrough, M., Borok, E., Xu, A.W., Janoschek, R., Buch, T., Plum, L., Balthasar, N., Hampel, B., Waisman, A.*, et al.* (2005). Agouti-related peptide-expressing neurons are mandatory for feeding. Nat Neurosci *8*, 1289-1291.

Hahn, T.M., Breininger, J.F., Baskin, D.G., and Schwartz, M.W. (1998). Coexpression of Agrp and NPY in fasting-activated hypothalamic neurons. Nat Neurosci *1*, 271-272.

Hardie, D.G., and Hawley, S.A. (2001). AMP-activated protein kinase: the energy charge hypothesis revisited. Bioessays *23*, 1112-1119.

Harris, G.C., Wimmer, M., and Aston-Jones, G. (2005). A role for lateral hypothalamic orexin neurons in reward seeking. Nature *437*, 556-559.

Hervey, G.R. (1959). The effects of lesions in the hypothalamus in parabiotic rats. J Physiol *145*, 336-352.

Hetherington AW, R.S. (1940). Hypothalamic lesions and adiposity in the rat. The Anatomical record *78*.

Horton, S., Meredith, A., Richardson, J.A., and Johnson, J.E. (1999). Correct coordination of neuronal differentiation events in ventral forebrain requires the bHLH factor MASH1. Mol Cell Neurosci *14*, 355-369.

Horvath, T.L., Bechmann, I., Naftolin, F., Kalra, S.P., and Leranth, C. (1997). Heterogeneity in the neuropeptide Y-containing neurons of the rat arcuate nucleus: GABAergic and non-GABAergic subpopulations. Brain Res *756*, 283-286.

Huszar, D., Lynch, C.A., Fairchild-Huntress, V., Dunmore, J.H., Fang, Q., Berkemeier, L.R., Gu, W., Kesterson, R.A., Boston, B.A., Cone, R.D.*, et al.* (1997). Targeted disruption of the melanocortin-4 receptor results in obesity in mice. Cell *88*, 131-141.

Ibrahim, N., Bosch, M.A., Smart, J.L., Qiu, J., Rubinstein, M., Ronnekleiv, O.K., Low, M.J., and Kelly, M.J. (2003). Hypothalamic proopiomelanocortin neurons are glucose responsive and express K(ATP) channels. Endocrinology *144*, 1331-1340.

Kalra, S.P., Dube, M.G., Sahu, A., Phelps, C.P., and Kalra, P.S. (1991). Neuropeptide Y secretion increases in the paraventricular nucleus in association with increased appetite for food. Proc Natl Acad Sci U S A *88*, 10931-10935.

Kennedy, G.C. (1953). The role of depot fat in the hypothalamic control of food intake in the rat. Proc R Soc Lond B Biol Sci *140*, 578-596.

Kitamura, T., Feng, Y., Kitamura, Y.I., Chua, S.C., Jr., Xu, A.W., Barsh, G.S., Rossetti, L., and Accili, D. (2006). Forkhead protein FoxO1 mediates Agrp-dependent effects of leptin on food intake. Nat Med *12*, 534-540.

Knigge, K.M., Joseph, S.A., and Nocton, J. (1981). Topography of the ACTH-immunoreactive neurons in the basal hypothalamus of the rat brain. Brain Res *216*, 333-341.

Konner, A.C., Janoschek, R., Plum, L., Jordan, S.D., Rother, E., Ma, X., Xu, C., Enriori, P., Hampel, B., Barsh, G.S*., et al.* (2007). Insulin Action in AgRP-Expressing Neurons Is Required for Suppression of Hepatic Glucose Production. Cell Metab *5*, 438-449.

Korner, J., Savontaus, E., Chua, S.C., Jr., Leibel, R.L., and Wardlaw, S.L. (2001). Leptin regulation of Agrp and Npy mRNA in the rat hypothalamus. J Neuroendocrinol *13*, 959-966.

Kral, J.G., Biron, S., Simard, S., Hould, F.S., Lebel, S., Marceau, S., and Marceau, P. (2006). Large maternal weight loss from obesity surgery prevents transmission of obesity to children who were followed for 2 to 18 years. Pediatrics *118*, e1644-1649.

Krashes, M.J., Koda, S., Ye, C., Rogan, S.C., Adams, A.C., Cusher, D.S., Maratos-Flier, E., Roth, B.L., and Lowell, B.B. (2011). Rapid, reversible activation of AgRP neurons drives feeding behavior in mice. The Journal of clinical investigation.

Lee, G.H., Proenca, R., Montez, J.M., Carroll, K.M., Darvishzadeh, J.G., Lee, J.I., and Friedman, J.M. (1996). Abnormal splicing of the leptin receptor in diabetic mice. Nature *379*, 632-635.

Leibel, R.L. (2008). Molecular physiology of weight regulation in mice and humans. Int J Obes (Lond) *32 Suppl 7*, S98-108.

Leibel, R.L., and Hirsch, J. (1984). Diminished energy requirements in reduced-obese patients. Metabolism\ *33*\, 164-170\.

Leibel, R.L., Rosenbaum, M., and Hirsch, J. (1995). Changes in energy expenditure resulting from altered body weight. N Engl J Med *332*, 621-628.

Leibowitz, K.L., Chang, G.Q., Pamy, P.S., Hill, J.O., Gayles, E.C., and Leibowitz, S.F. (2007). Weight gain model in prepubertal rats: prediction and phenotyping of obesity-prone animals at normal body weight. Int J Obes (Lond) *31*, 1210-1221.

Lein, E.S., Hawrylycz, M.J., Ao, N., Ayres, M., Bensinger, A., Bernard, A., Boe, A.F., Boguski, M.S., Brockway, K.S., Byrnes, E.J.*, et al.* (2007). Genome-wide atlas of gene expression in the adult mouse brain. Nature *445*, 168-176.

Levin, B.E. (2007). Neuronal glucose sensing: still a physiological orphan? Cell Metab *6*, 252-254.

Levin, B.E., Dunn-Meynell, A.A., Balkan, B., and Keesey, R.E. (1997). Selective breeding for diet-induced obesity and resistance in Sprague-Dawley rats. Am J Physiol *273*, R725-730.

Levin, B.E., Routh, V.H., Kang, L., Sanders, N.M., and Dunn-Meynell, A.A. (2004). Neuronal glucosensing: what do we know after 50 years? Diabetes *53*, 2521-2528.

Levine, A.S., and Morley, J.E. (1984). Neuropeptide Y: a potent inducer of consummatory behavior in rats. Peptides *5*, 1025-1029.

Lin, H.V., Plum, L., Ono, H., Gutierrez-Juarez, R., Shanabrough, M., Borok, E., Horvath, T.L., Rossetti, L., and Accili, D. (2010). Divergent regulation of energy expenditure and hepatic glucose production by insulin receptor in agouti-related protein and POMC neurons. Diabetes *59*, 337-346.

Liu, H., Kishi, T., Roseberry, A.G., Cai, X., Lee, C.E., Montez, J.M., Friedman, J.M., and Elmquist, J.K. (2003). Transgenic mice expressing green fluorescent protein under the control of the melanocortin-4 receptor promoter. J Neurosci *23*, 7143-7154.

Lu, D., Willard, D., Patel, I.R., Kadwell, S., Overton, L., Kost, T., Luther, M., Chen, W., Woychik, R.P., Wilkison, W.O.*, et al.* (1994). Agouti protein is an antagonist of the melanocyte-stimulating-hormone receptor. Nature *371*, 799-802.

Luquet, S., Perez, F.A., Hnasko, T.S., and Palmiter, R.D. (2005). NPY/AgRP neurons are essential for feeding in adult mice but can be ablated in neonates. Science *310*, 683-685.

MacLean, P.S., Higgins, J.A., Johnson, G.C., Fleming-Elder, B.K., Donahoo, W.T., Melanson, E.L., and Hill, J.O. (2004). Enhanced metabolic efficiency contributes to weight regain after weight loss in obesity-prone rats. Am J Physiol Regul Integr Comp Physiol *287*, R1306-1315.

Marsh, D.J., Hollopeter, G., Kafer, K.E., and Palmiter, R.D. (1998). Role of the Y5 neuropeptide Y receptor in feeding and obesity. Nat Med *4*, 718-721.

McNay, D.E., Pelling, M., Claxton, S., Guillemot, F., and Ang, S.L. (2006). Mash1 is required for generic and subtype differentiation of hypothalamic neuroendocrine cells. Mol Endocrinol *20*, 1623-1632.

Minokoshi, Y., Alquier, T., Furukawa, N., Kim, Y.B., Lee, A., Xue, B., Mu, J., Foufelle, F., Ferre, P., Birnbaum, M.J.*, et al.* (2004). AMP-kinase regulates food intake by responding to hormonal and nutrient signals in the hypothalamus. Nature *428*, 569-574.

Montague, C.T., Farooqi, I.S., Whitehead, J.P., Soos, M.A., Rau, H., Wareham, N.J., Sewter, C.P., Digby, J.E., Mohammed, S.N., Hurst, J.A.*, et al.* (1997). Congenital leptin deficiency is associated with severe early-onset obesity in humans. Nature *387*, 903-908.

Morrison, C.D., Morton, G.J., Niswender, K.D., Gelling, R.W., and Schwartz, M.W. (2005). Leptin inhibits hypothalamic Npy and Agrp gene expression via a mechanism that requires phosphatidylinositol 3-OH-kinase signaling. Am J Physiol Endocrinol Metab *289*, E1051-1057.

Morton, G.J., Cummings, D.E., Baskin, D.G., Barsh, G.S., and Schwartz, M.W. (2006). Central nervous system control of food intake and body weight. Nature *443*, 289-295.

Mountjoy, K.G., Mortrud, M.T., Low, M.J., Simerly, R.B., and Cone, R.D. (1994). Localization of the melanocortin-4 receptor (MC4-R) in neuroendocrine and autonomic control circuits in the brain. Mol Endocrinol *8*, 1298-1308.

Murphy, B.A., Fioramonti, X., Jochnowitz, N., Fakira, K., Gagen, K., Contie, S., Lorsignol, A., Penicaud, L., Martin, W.J., and Routh, V.H. (2009). Fasting enhances the response of arcuate neuropeptide Y-glucose-inhibited neurons to decreased extracellular glucose. Am J Physiol Cell Physiol *296*, C746-756.

Myers, M.G., Jr., Leibel, R.L., Seeley, R.J., and Schwartz, M.W. (2010). Obesity and leptin resistance: distinguishing cause from effect. Trends Endocrinol Metab.

Ogden, C.L., Carroll, M.D., Curtin, L.R., Lamb, M.M., and Flegal, K.M. (2010). Prevalence of high body mass index in US children and adolescents, 2007-2008. Jama *303*, 242-249.

Ollmann, M.M., Wilson, B.D., Yang, Y.K., Kerns, J.A., Chen, Y., Gantz, I., and Barsh, G.S. (1997). Antagonism of central melanocortin receptors in vitro and in vivo by agouti-related protein. Science *278*, 135-138.

Padilla, S.L., Carmody, J.S., and Zeltser, L.M. (2010). Pomc-expressing progenitors give rise to antagonistic neuronal populations in hypothalamic feeding circuits. Nat Med *16*, 403-405.

Parras, C.M., Schuurmans, C., Scardigli, R., Kim, J., Anderson, D.J., and Guillemot, F. (2002). Divergent functions of the proneural genes Mash1 and Ngn2 in the specification of neuronal subtype identity. Genes Dev *16*, 324-338.

Parton, L.E., Ye, C.P., Coppari, R., Enriori, P.J., Choi, B., Zhang, C.Y., Xu, C., Vianna, C.R., Balthasar, N., Lee, C.E.*, et al.* (2007). Glucose sensing by POMC neurons regulates glucose homeostasis and is impaired in obesity. Nature *449*, 228-232.

Pelling, M., Anthwal, N., McNay, D., Gradwohl, G., Leiter, A.B., Guillemot, F., and Ang, S.L. (2010). Differential requirements for neurogenin 3 in the development of POMC and NPY neurons in the hypothalamus. Dev Biol.

Phillips, C.T., and Palmiter, R.D. (2008). Role of agouti-related protein-expressing neurons in lactation. Endocrinology *149*, 544-550.

Plagemann, A. (2005). Perinatal programming and functional teratogenesis: impact on body weight regulation and obesity. Physiol Behav *86*, 661-668.

Plum, L., Ma, X., Hampel, B., Balthasar, N., Coppari, R., Munzberg, H., Shanabrough, M., Burdakov, D., Rother, E., Janoschek, R.*, et al.* (2006). Enhanced PIP(3) signaling in POMC neurons causes K(ATP)

channel activation and leads to diet-sensitive obesity. The Journal of clinical investigation *116*, 1886-1901.

Popkin, B.M. Recent dynamics suggest selected countries catching up to US obesity. Am J Clin Nutr *91*, 284S-288S.

Price, M., Lazzaro, D., Pohl, T., Mattei, M.G., Ruther, U., Olivo, J.C., Duboule, D., and Di Lauro, R. (1992). Regional expression of the homeobox gene Nkx-2.2 in the developing mammalian forebrain. Neuron *8*, 241-255.

Qian, S., Chen, H., Weingarth, D., Trumbauer, M.E., Novi, D.E., Guan, X., Yu, H., Shen, Z., Feng, Y., Frazier, E.*, et al.* (2002). Neither agouti-related protein nor neuropeptide Y is critically required for the regulation of energy homeostasis in mice. Mol Cell Biol *22*, 5027-5035.

Ring, L.E., and Zeltser, L.M. Disruption of hypothalamic leptin signaling in mice leads to early-onset obesity, but physiological adaptations in mature animals stabilize adiposity levels. The Journal of clinical investigation *120*, 2931-2941.

Risold, P.Y., Thompson, R.H., and Swanson, L.W. (1997). The structural organization of connections between hypothalamus and cerebral cortex. Brain Res Brain Res Rev *24*, 197-254.

Root, C.M., Velazquez-Ulloa, N.A., Monsalve, G.C., Minakova, E., and Spitzer, N.C. (2008). Embryonically expressed GABA and glutamate drive electrical activity regulating neurotransmitter specification. J Neurosci *28*, 4777-4784.

Roselli-Rehfuss, L., Mountjoy, K.G., Robbins, L.S., Mortrud, M.T., Low, M.J., Tatro, J.B., Entwistle, M.L., Simerly, R.B., and Cone, R.D. (1993). Identification of a receptor for gamma melanotropin and other proopiomelanocortin peptides in the hypothalamus and limbic system. Proc Natl Acad Sci U S A *90*, 8856-8860.

Rosenbaum, M., and Leibel, R.L. (1999). The role of leptin in human physiology. N Engl J Med *341*, 913-915.

Routh, V.H. (2002). Glucose-sensing neurons: are they physiologically relevant? Physiol Behav *76*, 403-413.

Saper, C.B. (2002). The central autonomic nervous system: conscious visceral perception and autonomic pattern generation. Annu Rev Neurosci *25*, 433-469.

Schwartz, M.W., Sipols, A.J., Marks, J.L., Sanacora, G., White, J.D., Scheurink, A., Kahn, S.E., Baskin, D.G., Woods, S.C., Figlewicz, D.P.*, et al.* (1992). Inhibition of hypothalamic neuropeptide Y gene expression by insulin. Endocrinology *130*, 3608-3616.

Scott, M.M., Lachey, J.L., Sternson, S.M., Lee, C.E., Elias, C.F., Friedman, J.M., and Elmquist, J.K. (2009). Leptin targets in the mouse brain. J Comp Neurol *514*, 518-532.

Shimamura, K., Hartigan, D.J., Martinez, S., Puelles, L., and Rubenstein, J.L. (1995). Longitudinal organization of the anterior neural plate and neural tube. Development *121*, 3923-3933.

Shimamura, K., and Rubenstein, J.L. (1997). Inductive interactions direct early regionalization of the mouse forebrain. Development *124*, 2709-2718.

Shimogori, T., Lee, D.A., Miranda-Angulo, A., Yang, Y., Wang, H., Jiang, L., Yoshida, A.C., Kataoka, A., Mashiko, H., Avetisyan, M.*, et al.* (2010). A genomic atlas of mouse hypothalamic development. Nat Neurosci.

Shin, J.W., Geerling, J.C., and Loewy, A.D. (2008). Inputs to the ventrolateral bed nucleus of the stria terminalis. J Comp Neurol *511*, 628-657.

Shutter, J.R., Graham, M., Kinsey, A.C., Scully, S., Luthy, R., and Stark, K.L. (1997). Hypothalamic expression of ART, a novel gene related to agouti, is up-regulated in obese and diabetic mutant mice. Genes Dev *11*, 593-602.

Silverman, B.L., Rizzo, T.A., Cho, N.H., and Metzger, B.E. (1998). Long-term effects of the intrauterine environment. The Northwestern University Diabetes in Pregnancy Center. Diabetes Care *21 Suppl 2*, B142-149.

Sipols, A.J., Baskin, D.G., and Schwartz, M.W. (1995). Effect of intracerebroventricular insulin infusion on diabetic hyperphagia and hypothalamic neuropeptide gene expression. Diabetes *44*, 147-151.

Smart, J.L., Tolle, V., and Low, M.J. (2006). Glucocorticoids exacerbate obesity and insulin resistance in neuron-specific proopiomelanocortin-deficient mice. The Journal of clinical investigation *116*, 495-505.

Stanley, B.G., and Leibowitz, S.F. (1985). Neuropeptide Y injected in the paraventricular hypothalamus: a powerful stimulant of feeding behavior. Proc Natl Acad Sci U S A *82*, 3940-3943.

Sternson, S.M., Shepherd, G.M., and Friedman, J.M. (2005). Topographic mapping of VMH --> arcuate nucleus microcircuits and their reorganization by fasting. Nat Neurosci *8*, 1356-1363.

Sussel, L., Marin, O., Kimura, S., and Rubenstein, J.L. (1999). Loss of Nkx2.1 homeobox gene function results in a ventral to dorsal molecular respecification within the basal telencephalon: evidence for a transformation of the pallidum into the striatum. Development *126*, 3359-3370.

Swanson, L.W. (2000). Cerebral hemisphere regulation of motivated behavior. Brain Res *886*, 113-164.

Swanson, L.W., and Kuypers, H.G. (1980). A direct projection from the ventromedial nucleus and retrochiasmatic area of the hypothalamus to the medulla and spinal cord of the rat. Neurosci Lett *17*, 307-312.

Tartaglia, L.A., Dembski, M., Weng, X., Deng, N., Culpepper, J., Devos, R., Richards, G.J., Campfield, L.A., Clark, F.T., Deeds, J.*, et al.* (1995). Identification and expression cloning of a leptin receptor, OB-R. Cell *83*, 1263-1271.

Tatemoto, K. (1982). Neuropeptide Y: complete amino acid sequence of the brain peptide. Proc Natl Acad Sci U S A *79*, 5485-5489.

Tatemoto, K., Carlquist, M., and Mutt, V. (1982). Neuropeptide Y--a novel brain peptide with structural similarities to peptide YY and pancreatic polypeptide. Nature *296*, 659-660.

Tong, Q., Ye, C.P., Jones, J.E., Elmquist, J.K., and Lowell, B.B. (2008). Synaptic release of GABA by AgRP neurons is required for normal regulation of energy balance. Nat Neurosci.

van de Wall, E., Leshan, R., Xu, A.W., Balthasar, N., Coppari, R., Liu, S.M., Jo, Y.H., MacKenzie, R.G., Allison, D.B., Dun, N.J.*, et al.* (2008). Collective and individual functions of leptin receptor modulated neurons controlling metabolism and ingestion. Endocrinology *149*, 1773-1785.

Wardlaw, S.L. (2011). Hypothalamic proopiomelanocortin processing and the regulation of energy balance. Eur J Pharmacol.

Watson, S.J., Akil, H., Richard, C.W., 3rd, and Barchas, J.D. (1978). Evidence for two separate opiate peptide neuronal systems. Nature *275*, 226-228.

Wiesel, T.N., and Hubel, D.H. (1963). Single-Cell Responses In Striate Cortex Of Kittens Deprived Of Vision In One Eye. J Neurophysiol *26*, 1003-1017.

Williams, K.W., Margatho, L.O., Lee, C.E., Choi, M., Lee, S., Scott, M.M., Elias, C.F., and Elmquist, J.K. (2010). Segregation of acute leptin and insulin effects in distinct populations of arcuate proopiomelanocortin neurons. J Neurosci *30*, 2472-2479.

Wilson, S.W., and Houart, C. (2004). Early steps in the development of the forebrain. Dev Cell *6*, 167-181.

Wolff, G.L. (1963). Growth of Inbred Yellow (Aya) and Non-Yellow (Aa) Mice in Parabiosis. Genetics *48*, 1041-1058.

Wu, Q., Boyle, M.P., and Palmiter, R.D. (2009). Loss of GABAergic signaling by AgRP neurons to the parabrachial nucleus leads to starvation. Cell *137*, 1225-1234.

Wu, Q., Howell, M.P., Cowley, M.A., and Palmiter, R.D. (2008). Starvation after AgRP neuron ablation is independent of melanocortin signaling. Proc Natl Acad Sci U S A *105*, 2687-2692.

Xu, Q., Tam, M., and Anderson, S.A. (2008). Fate mapping Nkx2.1-lineage cells in the mouse telencephalon. J Comp Neurol *506*, 16-29.

Yaswen, L., Diehl, N., Brennan, M.B., and Hochgeschwender, U. (1999). Obesity in the mouse model of pro-opiomelanocortin deficiency responds to peripheral melanocortin. Nat Med *5*, 1066-1070.

Yen, T.T., Gill, A.M., Frigeri, L.G., Barsh, G.S., and Wolff, G.L. (1994). Obesity, diabetes, and neoplasia in yellow A(vy)/- mice: ectopic expression of the agouti gene. FASEB J *8*, 479-488.

Zhang, Y., Kerman, I.A., Laque, A., Nguyen, P., Faouzi, M., Louis, G.W., Jones, J.C., Rhodes, C., and Munzberg, H. (2011). Leptin-receptor-expressing neurons in the dorsomedial hypothalamus and median preoptic area regulate sympathetic brown adipose tissue circuits. J Neurosci *31*, 1873-1884.

Zhang, Y., Proenca, R., Maffei, M., Barone, M., Leopold, L., and Friedman, J.M. (1994). Positional cloning of the mouse obese gene and its human homologue. Nature *372*, 425-432.

Zheng, H., Patterson, L.M., Rhodes, C.J., Louis, G.W., Skibicka, K.P., Grill, H.J., Myers, M.G., Jr., and Berthoud, H.R. (2010). A potential role for hypothalamomedullary POMC projections in leptin-induced suppression of food intake. Am J Physiol Regul Integr Comp Physiol *298*, R720-728.

CHAPTER 2 "*Pomc*-expressing Progenitors Give Rise to Antagonistic Neuronal Populations in Hypothalamic Feeding Circuits."

Introduction

It is well established that the maternal environment can program body weight phenotypes in offspring, yet little is known regarding the underlying mechanism of this programmed effect (reviewed in (Levin, 2006)). Recent findings suggest that the establishment of leptin-sensing neurons in the hypothalamus may be vulnerable to an obese gestational environment. Specifically, Simerly and Bouret et al. (2008) have shown that obesity prone offspring reared in an obese gestational environment have fewer leptin-sensing neurons (~20% fewer P-STAT3 positive cells upon acute fasted leptin injection) in the arcuate nucleus of the hypothalamus (ARH) compared to controls (Bouret et al., 2008). This work suggests that alterations in the differentiation and specification leptin-sensing neurons in the ARH may underlie body weight programming. Because AgRP and a subset of POMC neurons are leptin-sensing, we believe that the ontogeny of these two primary feeding centers may represent a critical node underlying the programmed establishment of obesity in offspring. In the following manuscript we will investigate the profile of *Pomc* and *Npy*-expressing populations over the course of development in a wild-type model.

Manuscript

(Author Contributions: I, SL Padilla, performed experiments, analyzed data, and together with LM Zeltser wrote this manuscript; JS Carmody generated data toward Figure 2.1 (part e); LM Zeltser designed the study.)

***Pomc*-expressing Progenitors Give Rise to Antagonistic Neuronal Populations in Hypothalamic Feeding Circuits.**

***Nature Medicine,* 2010 Apr;16(4):403-5. [PMID: 20348924]**

Padilla SL, Carmody JS and Zeltser LM

Hypothalamic neuron circuits regulating energy balance are highly plastic and develop in response to nutrient and hormonal cues. To identify processes that might be susceptible to gestational influences in mice, we characterized the ontogeny of proopiomelanocortin (POMC) and neuropeptide Y (NPY) cell populations, which exert opposing influences on food intake and body weight. These analyses revealed that *Pomc* is broadly expressed in immature hypothalamic neurons and that half of embryonic *Pomc*-expressing precursors subsequently adopt a non-POMC fate in adult mice. Moreover, nearly one quarter of the mature NPY^+ cell population shares a common progenitor with $POMC^+$ cells.

The rapid increase in the prevalence of childhood obesity and the concomitant rise in obesity-related medical morbidities and costs lend urgency to the need for new insights into the causes and potential preventive measures for this disease (Ogden et al., 2006). Mounting evidence supports the idea that the maternal environment can impart a lasting effect on the susceptibility of offspring to obesity and type 2 diabetes (Taylor and Poston, 2007). The arcuate nucleus of the hypothalamus (ARH) is a key component of the neuronal network regulating body weight, adiposity and glucose homeostasis, and recent studies suggest that the development of arcuate neurons may be sensitive to maternal metabolic status (Levin, 2006). The discovery that ARH projections are influenced by leptin provided the first insight into potential mechanisms

underlying 'maternal programming' in the perinatal period (Bouret et al., 2004). The gestational environment has also been shown to influence the future metabolic status of offspring (Shankar et al., 2008); however, little is known about the embryonic origins of arcuate lineages.

The two best-characterized arcuate populations—orexigenic neurons expressing NPY (NPY neurons) and agouti-related protein (AgRP) and anorexigenic neurons expressing POMC (POMC neurons)—produce antagonistic effects on food intake in response to nutrient and hormonal signals of peripheral energy status (Saper et al., 2002). Signals of positive energy balance, such as leptin and glucose, stimulate subsets of POMC neurons, leading to decreased food intake while inhibiting the release of orexigenic peptides from neighboring NPY neurons (Cowley et al., 2001). NPY neurons are active when the energy supply is not sufficient to meet systemic demands, releasing AgRP and γ-aminobutyric acid (GABA) to inhibit melanocortin-mediated suppression of food intake (Cowley et al., 2001; Ollmann et al., 1997). Together, NPY and POMC neurons integrate signals of energy homeostasis to direct physiological processes that regulate proper body weight (Schwartz and Porte, 2005). We focused our initial efforts on characterizing the ontogeny of NPY and POMC neuronal lineages during gestation because nutrient and hormonal cues influence the formation of NPY and POMC circuits, consistent with the idea that these developmental processes influence future metabolic phenotypes.

Using the GenePaint digital mouse atlas, we found that *Pomc* expression starts at E10.5 and that *Npy* expression begins at E14.5. Given the earlier onset of *Pomc* expression, together with the established lateromedial gradient of hypothalamic neurogenesis (Altman and Bayer, 1978), we predicted that the lateral POMC neurons would differentiate before the medial NPY neurons. To determine the birth dates of POMC and NPY neurons in the ARH, we injected dams with a single pulse of BrdU between E11.5 and E16.5 and assessed the retention of the BrdU label by immunohistochemistry at postnatal day 9 (P9) (Supplementary Methods). We observed that the peak birth date of most cells in the ARH is E11.5–E12.5 (ref. (Shimada and

Nakamura, 1973) and Fig. 2.1a); however, BrdU injections at E13.5 labeled some cells in the lateral ARH (Supplementary Figs. 2.1 and 2.2). Analysis of BrdU labeling in conjunction with *Pomc* or *Npy* expression showed that POMC and NPY neurons are born within the same time window, E11.5–E12.5, and that later-born ARH populations are distinct (Fig. 2.1a–c).

The shared birth dates of POMC and NPY neurons led us to consider whether the origins of these two antagonistic populations of neurons may be related. We characterized *Pomc* and *Npy* expression by two-color FISH across gestation (Fig. 2.1d,e). We first observed *Pomc* expression in the hypothalamic ventricular zone at E10.5–E11.5; from E12.5 on, expression was restricted to differentiated neurons, consistent with our birth-dating studies (Fig. 2.1d). The number of *Pomc*$^+$ cells reached a maximum at E13.5, after which its expression was extinguished in more than half of the population between E14.5 and E18.5 (Fig. 2.1f). We did not observe *Npy* expression in the ventricular zone; we first detected it in laterally situated cells in the rostral aspect of the presumptive ARH at E13.5 (Fig. 2.1d). Subsequently, *Npy*$^+$ cells are predominantly situated in the ventromedial ARH. We did not detect appreciable numbers of apoptotic cells by TUNEL staining (data not shown), which is consistent with the idea that *Pomc* expression is turned off in a large percentage of immature hypothalamic neurons (Broad et al., 2009). These data argue that *Pomc* expression does not reflect the acquisition of a terminal cell fate. Rather, the gradual extinction of *Pomc* and progressive onset of *Npy* represent an ongoing maturation process that extends throughout gestation. Supporting this idea, POMC and NPY neurons do not acquire their terminal peptidergic phenotype until the postnatal period in rodents, as reflected by the gene encoding cocaine- and amphetamine-regulated transcript and *Agrp* expression, respectively (Cottrell et al., 2009; Nilsson et al., 2005).

Pomc and *Npy* are expressed in mutually exclusive cell populations in adults (Pinto et al., 2004), yet we detected *Pomc*$^+$ and *Npy*$^+$ colocalization at midgestation (Fig. 2.1e). To substantiate this unexpected finding that a subset of neurons express both *Pomc* and *Npy*, we

compared the expression profiles of NPY neurons isolated from embryonic and postnatal stages. We used FACS to collect GFP$^+$ cells from *Npy*-hrGFP embryos, which express humanized *Renilla* green fluorescent protein (hr-GFP) under the control of *Npy* promoter and enhancer elements (van den Top et al., 2007). We detected *Pomc* transcripts by PCR on sorted cells from E14.5 but not from P9 (Fig. 2.1g and Supplementary Fig. 2.3a,b). These observations support the idea that during gestation a subset of *Pomc*-expressing cells can differentiate into NPY neurons.

Next we used a genetic lineage tracing strategy (Zinyk et al., 1998) to visualize the mature POMC neuronal population, defined by *Pomc* expression in adults, in relation to the broad immature *Pomc*-expressing population in the embryo (Fig. 2.2). In this strategy, we used mice with Cre recombinase driven by *Pomc* regulatory elements to direct the excision of a *loxP*-flanked stop codon (*Pomc*-Cre) upstream of a *Gfp* reporter knocked into the constitutively active *ROSA26* locus (*R26*-GFP). In this way, cells that express *Pomc* from gestation are permanently marked (Balthasar et al., 2004). To assess *Pomc* transcriptional activity in conjunction with a GFP reporter, we developed a technique to combine images of direct GFP fluorescence with FISH (Supplementary Figs. 2.4 and 2.5). When we performed this assay on adult tissue from *Pomc*-GFP transgenic mice, 95% of *Pomc*-GFP$^+$ neurons also expressed *Pomc* (Fig. 2.2a), validating the sensitivity of this technique (Cowley et al., 2001). In contrast, only half of the GFP$^+$ cells in *Pomc*-Cre;*R26*-GFP mice expressed *Pomc* (Fig. 2.2b and Supplementary Fig. 2.6). *Pomc*-negative GFP$^+$ cells in *Pomc*-Cre;*R26*-GFP adults probably represent cells that turned off *Pomc* expression at some point after E13.5. GFP$^+$ cell counts in *Pomc*-Cre;*R26*-GFP mice were consistently twice as high as those generated by *Pomc* FISH or direct fluorescence in *Pomc*-GFP–transgenic mice (Fig. 2.2d).

Given our finding that *Npy* and *Pomc* colocalize in a subset of embryonic neurons, we considered whether some of the *Pomc*-negative GFP$^+$ neurons in *Pomc*-Cre;*R26*-GFP adults

are NPY neurons. We detected *Npy* expression in 17% ± 2% of GFP^+ neurons in adult *Pomc*-Cre;*R26*-GFP mice (Fig. 2.2b). We used two strategies to independently verify this observation. First, confocal images of immunohistochemistry on *Npy*-GFP;*Pomc*-Cre;*R26*-LacZ mice confirmed that 25% of NPY (GFP^+) neurons also express the *Pomc*-Cre lineage trace (β-galactosidase immunohistochemistry) (Fig. 2.2c,e). Second, RT-PCR on FACS-purified GFP^+ cells from *Pomc*-Cre;*R26*-GFP mice showed that some cells marked by the lineage trace express *Npy* (Fig. 2.2f and Supplementary Fig. 2.3c).

These data provide evidence that a subpopulation of NPY neurons are derived from progenitors that are distinct from other ARH NPY neurons, raising the possibility that they serve different functions within the hypothalamic feeding circuit and, thus, may underlie the known heterogeneous electrophysiological properties of NPY neurons (Fioramonti et al., 2007). Although the origins of NPY subpopulations may differ, their subsequent differentiation converges on an orexigenic, GABAergic phenotype, as we found that all ARH NPY neurons express *Agrp* and the gene encoding glutamic acid decarboxylase-67, a rate-limiting enzyme in GABA synthesis (Cowley et al., 2001). A key area for future research is to use labeling techniques that distinguish between *Pomc*-derived and *Pomc*-nonderived NPY neurons in conjunction with analyses of gene expression profiles, neuronal architecture and electrophysiological properties. Classification of functionally distinct subsets of neurons derived from a $Pomc^+$ lineage is crucial for elucidating how hormonal and nutrient signals are sensed by ARH neurons and relayed to downstream targets that regulate body weight and energy homeostasis.

In this study, we have shown that *Pomc* is transiently expressed by the vast majority of cells in the developing ventral hypothalamus (Fig. 2.1d,f). During gestation, *Pomc* transcription is extinguished in more than half of these cells, some of which subsequently differentiate into NPY neurons and some of which adopt alternative terminal fates. Consistent with our FISH analyses,

when we used *Pomc*-Cre;*R26*-GFP mice to trace *Pomc*-derived lineages in the adult hypothalamus, we found that half of the GFP-labeled neurons are non-POMC neurons. This *Pomc*-Cre driver was developed as a tool to investigate the physiological consequences of POMC-specific loss or gain of gene function. As we demonstrated that recombination of floxed alleles is not limited to mature POMC neurons and includes a substantial portion of mature NPY neurons, previous functional studies using this Cre driver should be reanalyzed. Indeed, some functions ascribed to POMC neurons might be mediated by non-POMC neurons that expressed *Pomc* at one time in development.

The observation that several functionally distinct cell types arise from a *Pomc*-expressing lineage raises the possibility that factors that influence cell fate decisions within the immature population during gestation could permanently affect the neuronal composition of circuits regulating energy homeostasis. Dietary manipulations during gestation have been associated with increased *Pomc* expression at postnatal stages, supporting the idea that maternal signals can influence the differentiation of the *Pomc*-expressing lineage (Chen et al., 2008). Two major areas for future research are to determine whether specific maternal nutrient or hormonal signals influence the differentiation or the architecture of neuronal lineages in hypothalamic circuits and, if so, to assess how these changes affect metabolic phenotypes in the offspring.

Figures:

Figure 2.1

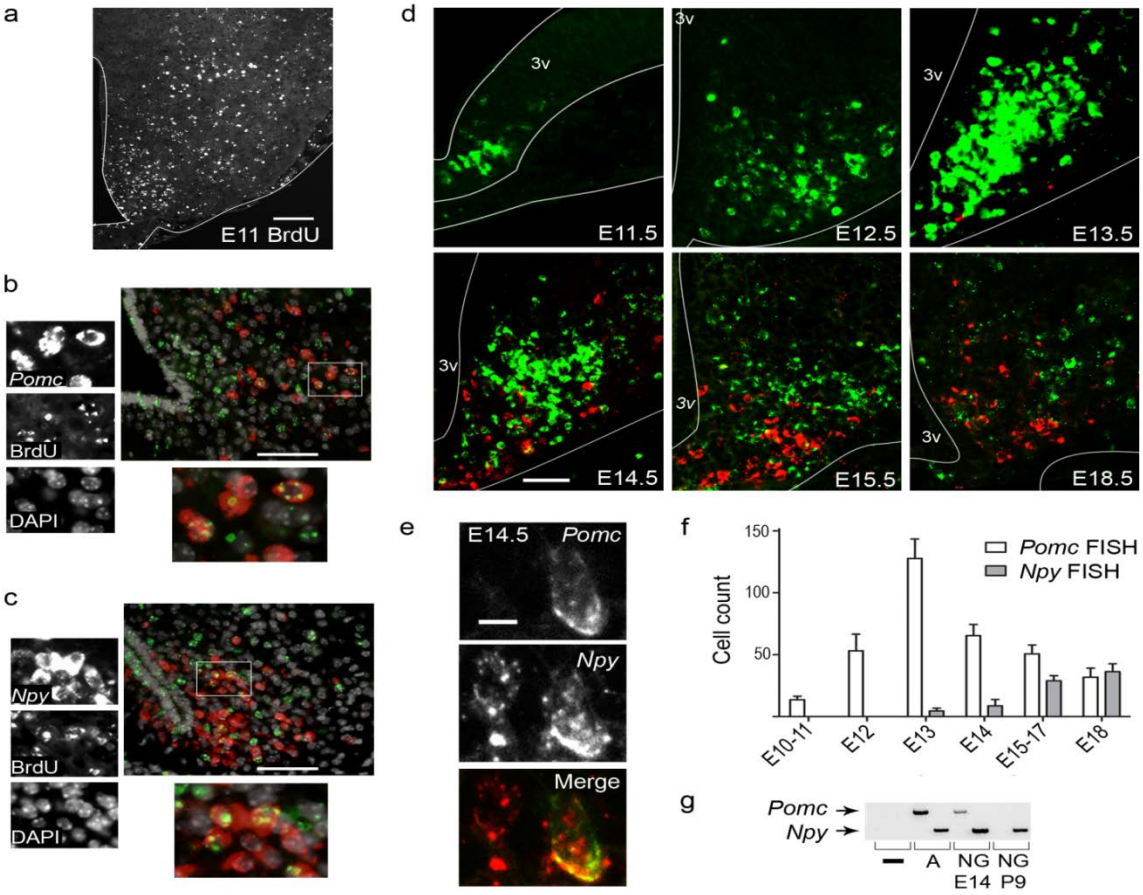

Figure 2.1. *Pomc* is transiently expressed in a broad population of hypothalamic neurons during embryonic development. (**a**–**c**) We injected wild-type dams once with 200 mg per kg body weight BrdU at E11.5 and killed the offspring at P9 for analysis. (**a**) BrdU Immunohistochemistry. (**b**,**c**) Combined FISH with immunohistochemistry with probes against *Pomc* (**b**) or *Npy* (**c**) in conjunction with an antibody against BrdU and counterstained for DAPI. Magnified view of the boxed areas in the composite are shown at the bottom; individual layers from the boxed regions are shown at the left. (**d**) FISH for *Pomc* (green) and *Npy* (red) in ventral hypothalamus from E11.5 to E18.5. 3V, third ventricle. (**e**) Confocal image of a cell containing both *Npy* and *Pomc* transcripts at E14.5. (**f**) We counted cells expressing *Pomc* and *Npy* as described in Supplementary Figure 2.3. Each group represents the average counts of at least five coronal sections per mouse, spanning the rostrocaudal extent of the presumptive ARH, with error bars representing means ± s.e.m. ($n \geq 3$ mice for each group). (**g**) *Pomc* and *Npy* expression, as assessed by PCR on cDNA generated from sorted GFP^+ cells. We dissociated cells from transgenic *Npy*-hrGFP hypothalami and FACS-purified GFP^+ cells at E14.5 and P9. –, no cDNA control; A, adult hypothalamus positive control; NG, *Npy*-hrGFP. Scale bars: **a**, 100 μm; **b**,**c**, 50 μm (low magnification), 10 μm (high magnification); **d**, 50 μm; **e**, 5 μm; all tissues are 10-μm cryosections.

Figure 2.2

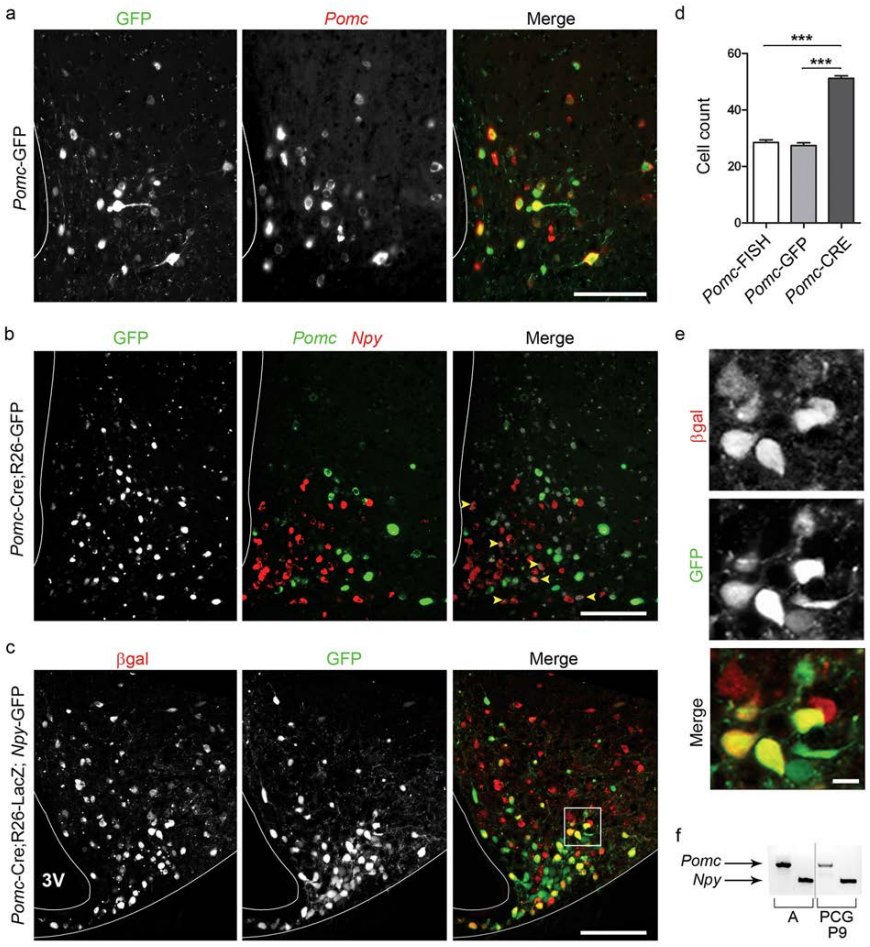

Figure 2.2. NPY neurons derived from a *Pomc*-expressing lineage persist to adulthood. (**a,b**) Images of direct GFP fluorescence obtained prior to FISH processing in *Pomc*-GFP (a left) or *Pomc*-Cre;*R26*-GFP (b left) adults, followed by FISH with *Pomc* alone (a center) or *Pomc* (green) plus *Npy* (red) probes (b center) or, composite images (a, b right) (technique described in Supplementary Fig. 2.5). (**b**) Cells expressing *Npy* and the *Pomc*-Cre lineage marker, GFP, are indicated with arrowheads. Because of its perinuclear localization, the FISH signal appears as a ring around the GFP signal. (**a,b**) All images acquired with a Nikon Eclipse 80i fluorescent microscope. (**c**) Confocal images of β-GAL IHC (red) in conjunction with direct GFP fluorescence (green) in *Pomc*-Cre;*R26*-LacZ;*Npy*-GFP adults. (**d**) Cell counts across the rostral-caudal axis of the ARH for *Pomc* transcript (*Pomc*-FISH), direct fluorescence of GFP from *Pomc*-GFP adults or from *Pomc*-Cre;*R26*-GFP (*Pomc*-CRE) adults are compared. (**e**) High magnification image of the region boxed in **c**. (**f**) We dissociated hypothalamic cells from transgenic *Pomc*-Cre;*R26*-GFP mice and FACS-purified GFP^+ cells at P9. *Pomc* and *Npy* expression, as assessed by PCR on cDNA generated from sorted GFP^+ cells. Adjacent lane doublets separated by the grey bar were run simultaneously on the same gel but not in neighboring lanes; they have been juxtaposed for the purposes of this figure. Abbreviation for sources of cDNA: adult hypothalamus positive control (A); *Pomc*-Cre;*R26*-GFP (PCG). 3V, third ventricle; Scale bar (**a**–**c**) 100 µm, (**e**) 10 µm. Error bars representing mean ± SEM ($n \geq 42$ sections for each group, from $n \geq 6$ animals), *** denotes $p < 0.0001$.

Methods

Animals

Animals were housed in temperature controlled rooms at 21 °C and subject to a 12 h light-dark cycle. Mice had *ad libitum* access to standard chow diet (Lab Diet: PicoLab Rodent Diet 5053) and water. C57BL/6 and (*ROSA*)*26Sor-EGFP* reporter (*R26*-GFP) mice were obtained from the Jackson Laboratory and bred at the Russ Berrie Animal Facility (Soriano, 1999). *Pomc*-Cre (Balthasar et al., 2004), *Pomc*-GFP (Cowley et al., 2001) and *Npy*-hrGFP (van den Pol et al., 2009) transgenic animals were generously provided by Joel Elmquist, Malcolm Low and Bradford Lowell respectively. All analyses were performed on mice which were *Pomc*-Cre Tg^+ and homozygous for the *R26*-GFP allele. All procedures were performed in accordance with the guidelines of the Institutional Animal Care and Use Committee at the Columbia University Health Sciences Division.

Genotyping

Genotyping at the *ROSA26* locus was performed using the following three-primer set: oIMR 0883: 5'-AAAGTCGCTCTGAGTTGTTAT-3'; oIMR 0315 5'-GCGAAGAGTTTGTCCTCAACC-3'; oIMR 0316 5'-GGAGCGGGAGAAATGGATATG-3' (Soriano, 1999). Genotyping of *Npy*-hrGFP transgenic mice was performed using: NPY-ata-S-F: 5'-TATGTGGACGGGGCAGAAGATCCAGG-3', NPY-ata-S-R: 5'-CCCAGCTCACATATTTATCTAGAG-3' and AA33 5'-GGTGCGGTTGCCGTACTGGA-3' (van den Pol et al., 2009). The *Cre* transgene was assessed with: 5'-GCGGTCTGGCAGTAAAAACTATC-3', 5'-GTGAAACAGCATTGCTGTCACTT-3'.

Tissue Processing

P9 and adult mice were anesthetized and perfused transcardially with 0.9% NaCl followed by 4% paraformaldehyde (PFA) in phosphate buffer (PB). Brains were post-fixed at 4°C overnight and cryoprotected with 30% sucrose for 48 h. For embryonic tissue, dams were

anesthetized with Avertin and embryos were dissected in cold PBS and fixed at 4 °C overnight and cryoprotected with 30% sucrose for 24 h. Tissue was embedded in O.C.T (Tissue Tek) and frozen at –80°C. 10 µm-thick coronal sections were collected across the rostral–caudal extent of the ARH on Superfrost Plus slides (Fisher).

Fluorescent *In Situ* Hybridization

Frozen sections were processed as described in the TSA Plus Cy3 System manual (Perkin Elmer). Antisense digoxigenin- or fluorescein-labeled riboprobes were generated from plasmids containing PCR fragments of *Npy* and *Pomc* using the following primers sets: (NPY) 5'-TGCTAGGTAACAAGCGAATGG-3'/5'-CAACAACAACAAGGGAAATGG-3; (POMC) 5'-GTTAAGAGCAGTGACTAAGAGAGGC-3'/5'-CCTAACACAGGTAACTCTAAGAGGC-3'.

Imaging and Quantification

Fluorescent microscopy was performed using a Nikon Eclipse 80i equipped with a Retiga EXi camera and X cite 120 fluorescent illumination system. TIFF files were acquired using Q Capture Pro software (Qimaging) and analyzed using Adobe Photoshop. Because our studies involved comparisons of images of the same tissue captured at different times, we used a diamidino-2-phenylindole (DAPI) stain to establish a reference focal plane. Images were separated into independent RGB channels using Photoshop, and Cy3 or GFP signals were compared to signals in the DAPI channel (Supplementary Fig. 2.4). Cy3 or GFP signals that did not have a corresponding DAPI-stained nucleus were excluded from our counts.

GFP fluorescence is lost during the high temperature hybridization step; thus, we pre-imaged direct GFP fluorescence in conjunction with DAPI. Following FISH, the tissue was re-stained with DAPI and imaged. Using Photoshop, pre- and post-FISH images were aligned using the common DAPI stain as a reference to generate a composite image (**Supplementary Fig. 2.4**).

Combined BrdU Immunohistochemistry and FISH

To label proliferating cells, dams were given a single intraperitoneal (i.p.) injection of 5-Bromo-2-deoxyuridine (BrdU) (200 mg kg^{-1} Sigma) on E11.5, E12.5, E13.5, E14.5 and E15.5. Offspring were sacrificed at P9 and processed as described above (cyroprotection in sucrose was reduced to 24 h). Detection of BrdU-labeled DNA by IHC requires DNA denaturation, which can be accomplished in many ways (Wojtowicz and Kee, 2006). We compared two pretreatment methods: standard 2.0 N HCl at 37 °C for 1 h, versus 50% formamide at 68 °C overnight. We found that both methods yield similar numbers of BrdU-positive cells with fluorescent IHC (Supplementary Fig. 2.1a,b). Because the same formamide treatment is also used in FISH hybridization step, we used this method to combine BrdU IHC with FISH.

Day one of the FISH protocol was followed directly, except the permeabilization step was performed with 0.1% Triton X-100 (in PBS, 30 min) instead of proteinase K. Following the overnight hybridization plus denaturation step, sections were blocked for one hour in 2% normal horse serum; 0.1% Triton X-100 (Block Buffer) at room temperature. Sections were then incubated overnight at 4 °C with the combination sheep anti-DIG-POD and rat anti-BrdU antibody (1:400, Novus Biologicals) in Block Buffer. The following day, sections were treated with tyramide Cy3 for 10 min room temperature (described in Perkin Elmer TSA amplification kit), washed 3X in PBS and then incubated with goat anti-rat Alexa-488 (1:500, Invitrogen) for one hour at room temperature. IHC with goat anti-β-Gal (1:4,000, Biogenesis) was performed without tyramide amplification. Slides were counterstained with DAPI (Invitrogen) and mounted with VectaShield (Vector Labs).

FACS and PCR Analysis

Hypothalamic tissue was dissociated as described by the Papain Dissociation System manual (Worthington). GFP^+ cells were collected using a BD FACS Aria Cell Sorter by the Herbert Irving Cancer Institute facility, total RNA was isolated (Invitrogen) and cDNA was

reversed transcribed (Invitrogen). PCR was performed using the *Npy* and *Pomc* primers sets described above.

Statistical Analysis

Significance was calculated using 2-tailed Student's t-tests, and defined as $P<0.05$.

Supplimentary Figures

Supplementary Figure 2.1

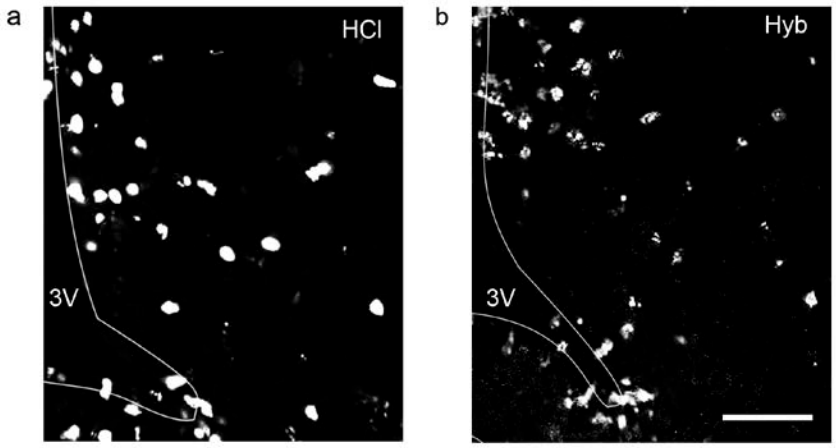

Supplementary Fig. 2.1 Overnight incubation at 70 °C in 50% formamide can substitute for HCl pre-treatment to detect BrdU by IHC. (**a,b**) IHC detection of BrdU label retained at P9 in adjacent hypothalamic sections resulting from a single BrdU injection at E11.5. Similar numbers of BrdU-labeled cells were detected using the standard HCl pre-treatment at 37 °C for 1 h (**a**) and 50% formamide overnight at 70 °C (**b**). 3V, third ventricle. Scale bar: 50 µM

Supplementary Figure 2.2

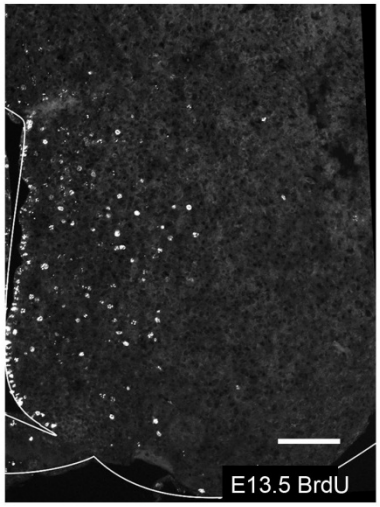

Supplementary Fig. 2.2 A population of laterally situated cells in the ARH is born at E13.5. IHC on P9 hypothalamic sections to detect BrdU-labeled cells resulting from an E13.5 injection. 3V, third ventricle. Scale bar: 100 µM

Supplementary Figure 2.3

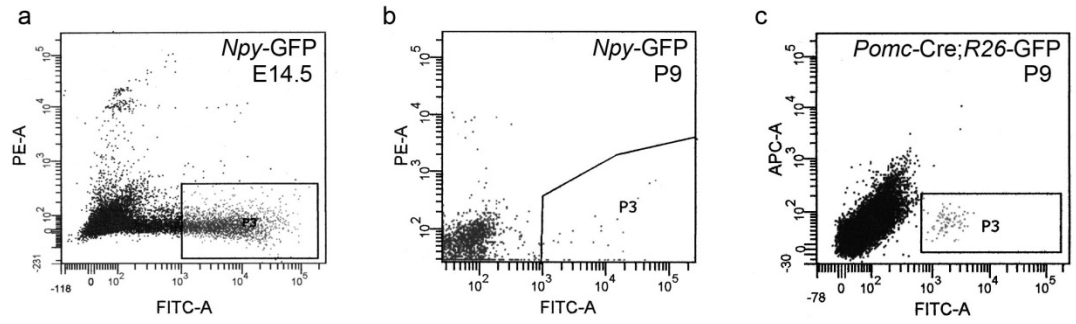

Supplementary Fig. 2.3 FACS isolation of GFP positive populations from dissociated ventral hypothalamic tissue. (**a,b)** Cells collected from *Npy*-hrGFP animals at E14.5 and P9 respectively (see Figure 2.1g for corresponding PCR data). (**c)** Cells collected from *Pomc*-Cre*;R26*-GFP animals at P9 (see **Fig. 2.2f** for corresponding PCR data).

Supplementary Figure 2.4

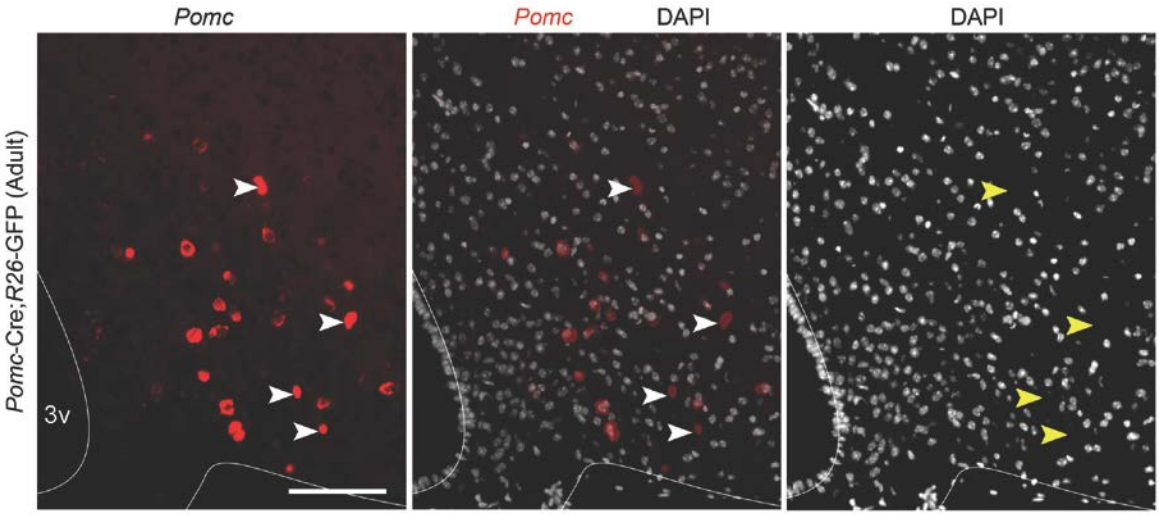

Supplementary Fig. 2.4 Using DAPI stain as a criterion for cell counts. (**Left**) *Pomc* FISH image alone. **(Center**) The fluorescent signal from *Pomc* FISH (red) was imaged in conjunction with a DAPI counterstain (gray). To facilitate our analyses, the channel containing the DAPI image was copied to a separate layer, converted to grayscale and made semi-transparent in Photoshop. (**Right**) DAPI image alone. Fluorescent signals that did not overlap with DAPI stain (marked by arrows) were excluded from the cell counts. 3V, third ventricle. Scale bar: 100 µM

Supplementary Figure 2.5

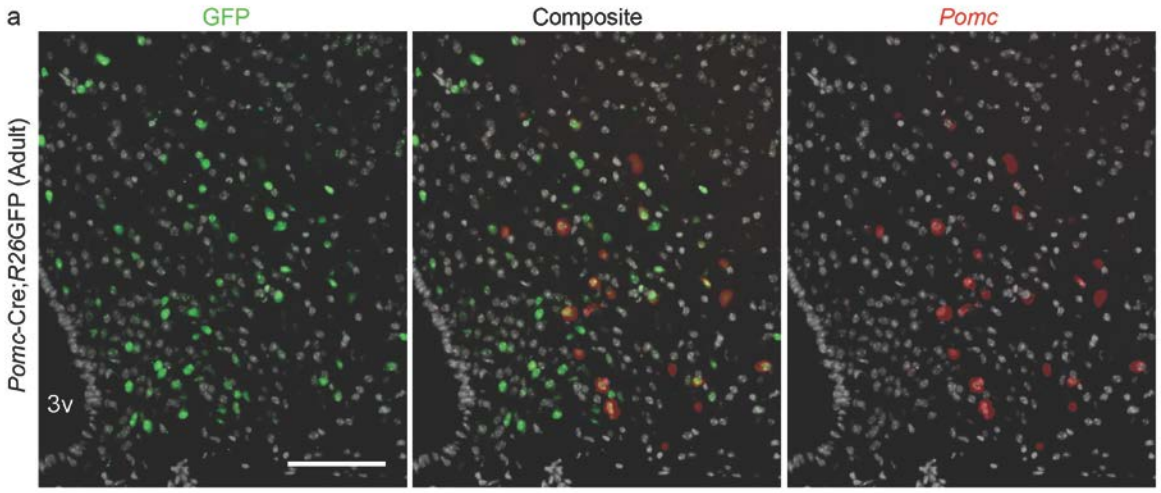

Supplementary Fig. 2.5 Technique to analyze GFP expression in conjunction with FISH at the single cell level. (**Left**) Section from a *Pomc*-Cre*;R26*-GFP adult hypothalamus was pre-imaged for direct GFP fluorescence (green) in conjunction with a DAPI counterstain (gray). (**Right**) FISH with a *Pomc* probe (red) was subsequently performed on the same section and imaged in conjunction with DAPI (gray). (**Center**) Using the DAPI stains as a guide, images in (A) and (C) were aligned and merged in Photoshop. 3V, third ventricle. Scale bar: 100 µM

Supplementary Figure 2.6

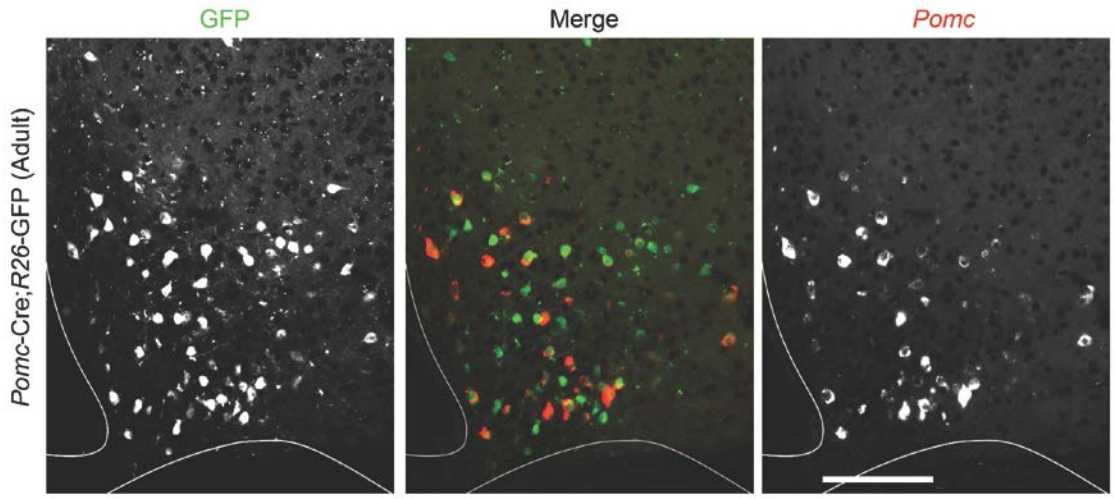

Supplementary Fig. 2.6 Only half of the GFP-labeled cells marked by a *Pomc*-Cre*;R26*-GFP genetic trace express *Pomc* in adults. Sectioned tissue from adult *Pomc*-Cre*;R26*-GFP animals was pre-imaged for direct GFP (green) fluorescence (**Left**), processed using FISH with a *Pomc* (red) probe (**Right**), and aligned on the basis of DAPI stain as described in (**Supplementary Fig. 2.5**) (**Center**). Scale bar: 100 µM; tissue 10 µm cryo-sections.

Acknowledgements

We thank L. Sussel, H. Wichterle and D. Accili for critical reading of our manuscript and helpful comments; R. Leibel for support and critical funding for this project (RO1 DK52431-16); J. Overton for help with confocal imaging; L. Yang of the DERC Pathology Core for cryosectioning and C. Liu of the Irving Institute CTSA FACS core (NCRR UL1 RR024156); M. Low (University of Michigan Health Center), J. Elmquist (UT Southwestern Medical Center), and B. Lowell (Beth Israel Deaconess Medical Center) for generously providing mouse reagents. This work was supported by F31DK079372 (SLP), Institute of Human Nutrition Training Grant 2T32DK007647-21 (JSC), ADA 7-07RA-195 (LMZ), and Columbia DERC Pilot and Feasibility Award P30 DK63608-07 (LMZ), NY Obesity Research Center Pilot and Feasibility P30 DK26687-26 (LMZ).

References

Altman, J., and Bayer, S.A. (1978). Development of the diencephalon in the rat. I. Autoradiographic study of the time of origin and settling patterns of neurons of the hypothalamus. J Comp Neurol *182*, 945-971.

Balthasar, N., Coppari, R., McMinn, J., Liu, S.M., Lee, C.E., Tang, V., Kenny, C.D., McGovern, R.A., Chua, S.C., Jr., Elmquist, J.K.*, et al.* (2004). Leptin receptor signaling in POMC neurons is required for normal body weight homeostasis. Neuron *42*, 983-991.

Bouret, S.G., Draper, S.J., and Simerly, R.B. (2004). Trophic action of leptin on hypothalamic neurons that regulate feeding. Science *304*, 108-110.

Bouret, S.G., Gorski, J.N., Patterson, C.M., Chen, S., Levin, B.E., and Simerly, R.B. (2008). Hypothalamic neural projections are permanently disrupted in diet-induced obese rats. Cell Metab *7*, 179-185.

Broad, K.D., Curley, J.P., and Keverne, E.B. (2009). Increased apoptosis during neonatal brain development underlies the adult behavioral deficits seen in mice lacking a functional paternally expressed gene 3 (Peg3). Dev Neurobiol *69*, 314-325.

Chen, H., Simar, D., Lambert, K., Mercier, J., and Morris, M.J. (2008). Maternal and postnatal overnutrition differentially impact appetite regulators and fuel metabolism. Endocrinology.

Cottrell, E.C., Cripps, R.L., Duncan, J.S., Barrett, P., Mercer, J.G., Herwig, A., and Ozanne, S.E. (2009). Developmental changes in hypothalamic leptin receptor: relationship with the postnatal leptin surge and energy balance neuropeptides in the postnatal rat. Am J Physiol Regul Integr Comp Physiol *296*, R631-639.

Cowley, M.A., Smart, J.L., Rubinstein, M., Cerdan, M.G., Diano, S., Horvath, T.L., Cone, R.D., and Low, M.J. (2001). Leptin activates anorexigenic POMC neurons through a neural network in the arcuate nucleus. Nature *411*, 480-484.

Fioramonti, X., Contie, S., Song, Z., Routh, V.H., Lorsignol, A., and Penicaud, L. (2007). Characterization of glucosensing neuron subpopulations in the arcuate nucleus: integration in neuropeptide Y and pro-opio melanocortin networks? Diabetes *56*, 1219-1227.

Levin, B.E. (2006). Metabolic imprinting: critical impact of the perinatal environment on the regulation of energy homeostasis. Philos Trans R Soc Lond B Biol Sci *361*, 1107-1121.

Nilsson, I., Johansen, J.E., Schalling, M., Hokfelt, T., and Fetissov, S.O. (2005). Maturation of the hypothalamic arcuate agouti-related protein system during postnatal development in the mouse. Brain Res Dev Brain Res *155*, 147-154.

Ogden, C.L., Carroll, M.D., Curtin, L.R., McDowell, M.A., Tabak, C.J., and Flegal, K.M. (2006). Prevalence of overweight and obesity in the United States, 1999-2004. Jama *295*, 1549-1555.

Ollmann, M.M., Wilson, B.D., Yang, Y.K., Kerns, J.A., Chen, Y., Gantz, I., and Barsh, G.S. (1997). Antagonism of central melanocortin receptors in vitro and in vivo by agouti-related protein. Science *278*, 135-138.

Pinto, S., Roseberry, A.G., Liu, H., Diano, S., Shanabrough, M., Cai, X., Friedman, J.M., and Horvath, T.L. (2004). Rapid rewiring of arcuate nucleus feeding circuits by leptin. Science *304*, 110-115.

Saper, C.B., Chou, T.C., and Elmquist, J.K. (2002). The need to feed: homeostatic and hedonic control of eating. Neuron *36*, 199-211.

Schwartz, M.W., and Porte, D., Jr. (2005). Diabetes, obesity, and the brain. Science *307*, 375-379.

Shankar, K., Harrell, A., Liu, X., Gilchrist, J.M., Ronis, M.J., and Badger, T.M. (2008). Maternal obesity at conception programs obesity in the offspring. Am J Physiol Regul Integr Comp Physiol *294*, R528-538.

Shimada, M., and Nakamura, T. (1973). Time of neuron origin in mouse hypothalamic nuclei. Exp Neurol *41*, 163-173.

Soriano, P. (1999). Generalized lacZ expression with the ROSA26 Cre reporter strain. Nat Genet *21*, 70-71.

Taylor, P.D., and Poston, L. (2007). Developmental programming of obesity in mammals. Exp Physiol *92*, 287-298.

van den Pol, A.N., Yao, Y., Fu, L.Y., Foo, K., Huang, H., Coppari, R., Lowell, B.B., and Broberger, C. (2009). Neuromedin B and gastrin-releasing peptide excite arcuate nucleus neuropeptide Y neurons in a novel transgenic mouse expressing strong Renilla green fluorescent protein in NPY neurons. J Neurosci *29*, 4622-4639.

van den Top, M., Lyons, D.J., Lee, K., Coderre, E., Renaud, L.P., and Spanswick, D. (2007). Pharmacological and molecular characterization of ATP-sensitive K(+) conductances in CART and NPY/AgRP expressing neurons of the hypothalamic arcuate nucleus. Neuroscience *144*, 815-824.

Wojtowicz, J.M., and Kee, N. (2006). BrdU assay for neurogenesis in rodents. Nat Protoc *1*, 1399-1405.

Zinyk, D.L., Mercer, E.H., Harris, E., Anderson, D.J., and Joyner, A.L. (1998). Fate mapping of the mouse midbrain-hindbrain constriction using a site-specific recombination system. Curr Biol *8*, 665-668.

Chapter 3 “Defining POMC neurons utilizing transgenic reagents: Impact of transient *Pomc* expression in diverse immature neuronal populations.”

Introduction

In our previous study we detected transient *Pomc*-expression in many immature neurons of the mediobasal hypothalamus during the last week of embryogenesis. Furthermore, we found that as these cells differentiate into a variety of distinct functional populations, some of which inversely determine hypothalamic mediated effects on energy homeostasis. These studies have yet to conclude on role that *Pomc* expression plays during development or on the lineages of distinct populations in the ARH; however, one immediate goal based on these initial findings was to utilize *Pomc*-Cre reporters to investigate the properties of terminal cell fate decisions of immature *Pomc*-expressing cells.

Hypothalamic POMC neurons function to mediate an anorexigenic effect on energy expenditure and food intake via the transmission of POMC-derived peptides to downstream secondary targets. While it has long been noted that *Pomc* is expressed in the mediobasal hypothalamus during embryogenesis, at a time prior to circuit formation, it has been generally disregarded by the field and otherwise noted as an early marker of cells destined for a mature POMC terminal fate. However, considering our findings in Chapter 2, it is unlikely that early *Pomc*-expressing cells indicate a POMC fate, exclusively. Literature focused on the developing retina and spinal cord demonstrate a role for POMC-derived proteins during cellular maturation, implicating these peptides in the differentiation and specification of cell fates in these aspects of the brain (Cossu et al., 1989; Eriksson et al., 1991; Hauser et al., 1996; Ilyinsky et al., 1987; Isayama et al., 1991; Lindqvist et al., 2003; Satoh and Ide, 1987; Vernadakis and Kentroti, 1990).

This chapter consists of a manuscript in preparation that aims to provide a comprehensive description of all neuronal populations in the CNS that are derived from *Pomc*-expressing

precursors. Importantly this data will provide a foundation to interpret previous studies using the *Pomc*-Cre driver.

Manuscript

(Author Contributions: I, SL Padilla, performed experiments, analyzed data, and together with LM Zeltser wrote this manuscript; D Reef worked as my summer student and helped generate the dot renderings in Fig. 3.3; LM Zeltser designed the study.)

Defining POMC neurons utilizing transgenic reagents: Impact of transient *Pomc* expression in diverse immature neuronal populations.

Manuscript in preparation

Padilla SL[1,2], Reef D[2,3] and Zeltser LM[2,4*]

Abstract

Melanocortin signaling plays a central role in the regulation of phenotypes related to body weight and energy homeostasis. To specifically target and study the function of POMC neurons, *Pomc* promoter elements have been utilized to generate reporter and Cre recombinase transgenic reagents. Across gestation, we find that *Pomc* is dynamically expressed in many sites in the developing mouse forebrain, midbrain, hindbrain, spinal cord and retina. While *Pomc* expression in most embryonic brain regions is transient, it is sufficient to direct Cre-mediated recombination of floxed alleles. We visualize the populations affected by this transgene by crossing *Pomc*-Cre mice to *ROSA* reporter strains and identify 62 sites of recombination throughout the adult brain, including several nuclei implicated in energy homeostasis regulation. To compare the relationship between acute *Pomc* promoter activity and *Pomc*-Cre-mediated recombination at the single cell level, we crossed *Pomc*-eGFP and *Pomc*-Cre;*ROSA*-tdTomato lines. We detect the highest concentration of *Pomc*-eGFP+ cells in the arcuate nucleus of the hypothalamus and dentate gyrus, but also observe smaller populations of labeled cells in the nucleus of the solitary tract, periventricular zone of the third ventricle and cerebellum. Consistent with the dynamic nature of *Pomc* expression in the embryo, the vast majority of neurons marked with the tdTomato reporter do not express GFP in

the adult. Thus, recombination in off-target sites could contribute to physiological phenotypes using *Pomc-Cre* transgenics. For example, we find that roughly half of the leptin-induced phospho-STAT3+ cells in the ARH are marked with *Pomc*-Cre;*ROSA*-tdTomato; only 15% of these are GFP+ POMC neurons.

Introduction

Severe obesity in mice lacking the *Pro-opioimelanocortin* (*Pomc*) or *Melanocortin receptor 4* (*Mc4r*) genes led to the widely-held belief that POMC neurons play a central role in regulating body weight (Huszar et al., 1997; Yaswen et al., 1999). POMC and agouti-related peptide (AgRP) neurons located in the ARH are thought to be the principal source of MC4R ligands in the brain; however the contribution of signals from POMC neurons in the nucleus of the solitary tract (NTS) has not been well-defined. A cleavage product of the POMC peptide, α-melanocyte stimulating hormone, and AgRP induce opposite effects on signaling via MC4R (Fan et al., 1997; Ollmann et al., 1997). Observations that leptin signaling induces the expression of the POMC-derived agonist and inhibits the expression of the AgRP antagonist, led to the hypothesis that melanocortin (MC) circuits mediate leptin's effects on energy homeostasis (Cowley et al., 2001; Mizuno and Mobbs, 1999; Schwartz et al., 1996; Schwartz et al., 1997). As these early seminal studies relied on pharmacological administration of leptin and/or MC antagonists and agonists, they could not distinguish between the contributions of discrete neuronal populations to energy homeostasis.

Two types of genetically engineered mouse strains were generated to specifically target and interrogate the role of POMC neurons in leptin-responsive circuits. GFP reporters driven by *Pomc* promoter elements (*Pomc*-eGFP) (Cowley et al., 2001; Pinto et al., 2004) have been used to identify POMC neurons for electrophysiological and immunohistochemical analyses. In addition, a *Pomc*-Cre BAC transgenic strain was developed to restrict genetic manipulations to POMC neurons and thus evaluate their function *in vivo* (Balthasar et al., 2004). These seminal

studies using *Pomc* transgenic reagents serve as the basis for prevailing models of hypothalamic regulation of body weight and energy homeostasis.

Previously we demonstrated that the *Pomc*-Cre transgene activity during gestation directs recombination of floxed alleles in many ARH neurons that do not express POMC in adulthood (Padilla et al., 2010). In follow-up studies, we observed that *Pomc* is broadly expressed throughout the central nervous system **(**CNS) during development. These observations raise the possibility that off-target effects in diverse populations in the CNS could contribute to physiological outcomes of genetic manipulations intended for POMC neurons. To assist in interpreting experiments utilizing *Pomc*-Cre mice, we provide a comprehensive map of brain nuclei marked by *Pomc*-Cre-mediated combination of *ROSA26*-(loxSTOPlox)-LacZ (*R26R*-LacZ) or *ROSA26*-(loxSTOPlox)-tdTOMATO *(R26R*-TOM*)* reporter strains (Madisen et al., 2010; Soriano, 1999). As MC and leptin pathways likely interact to regulate energy homeostasis, we characterized the relationship between leptin-induced phospho-STAT3 (P-STAT3) immunoreactivity, neurons marked by a *Pomc*-Cre reporter, and those that express *Pomc* or *Neuropeptide Y* (*Npy*).

As newer approaches to temporally restrict *Pomc*-Cre expression to adulthood are developed, it is important to determine whether off-target expression of *Pomc*-Cre reporters results from transient expression of *Pomc* during an earlier developmental stage or ectopic expression of the transgenic construct. Thus, we compare the relationship between endogenous *Pomc* transcription, expression of a *Pomc*-eGFP reporter, and *Pomc*-Cre reporters at the single cell level in *Pomc*-eGFP; *Pomc*-Cre;*R26R*-TOM mice. Going forward, temporal and spatial patterns of *Pomc*-eGFP and *Pomc*-Cre reporter expression should inform analysis and design of functional studies using these reagents.

Results

Dynamic *Pomc* expression in the embryonic CNS

Off-target sites of *Pomc*-Cre-mediated recombination could result from 1) early transient expression; 2) sub-threshold expression in the adult; or 3) ectopic expression in cells that do not express endogenous *Pomc* transcripts. Distinguishing between these possibilities is critical to developing reagents and strategies that accurately target POMC neurons. Initially we characterized *Pomc* expression in the developing embryo using a *Pomc*-eGFP reporter (Cowley et al., 2001). In two independent transgenic lines, *Pomc*-eGFP reporter expression accurately reflects endogenous *Pomc* transcription in ARH neurons (Cowley et al., 2001; Padilla et al., 2010; Pinto et al., 2004). At embryonic day 12.5 (E12.5), we observe robust GFP signals in the presumptive ARH, retina, optic tract, midbrain and in a broad domain in the ventral hindbrain and spinal cord (Fig. 3.1A). We first detect expression in the isthmus and pituitary at E13.5 (Fig. 3.1B). We confirmed that these sites of GFP fluorescence correlate with *Pomc* expression, as visualized by *in situ* hybridization (Fig. 3.2, A-D). Prominent domains of GFP expression persist through E14.5 in the optic tract, ventral hypothalamus and isthmus; however, the fluorescent signal is dramatically decreased in the midbrain and hindbrain (Fig. 3.1C). *Pomc* expression in the developing pituitary steadily increases throughout gestation, in parallel with the maturation of this organ (Fig. 3.1, B and C).

Distribution of *Pomc*-Cre activity

We next examined whether transient *Pomc* expression in the embryo is sufficient to drive Cre-mediated recombination of floxed reporter allele. At E16.5, we detect X-Gal-labeled cells in the hypothalamus, thalamus, midbrain, hindbrain, retina, olfactory bulb, spinal cord and dorsal root ganglia in *Pomc*-Cre*;R26R*-LacZ embryos (Fig. 3.2, E–H). In the periphery, we observe X-Gal+ cells in the pituitary and duodenum, consistent with previously identified melanocyte and corticotrophic reservoirs (Cohen-Cory, 2002; Wolter, 1984) (Fig. 3.2, E and H). Despite a

dramatic down-regulation of *Pomc* expression in caudal brain regions at E14.5 (Fig. 3.1C), we detect extensive X-Gal staining at E16.5, indicating that the transient burst of expression is sufficient to drive recombination of floxed alleles in many brain regions.

To capture the cumulative distribution of cells that expressed *Pomc* at any point during development, we performed X-Gal staining on serial sections of *Pomc*-Cre*;R26R*-LacZ adult brains in both sagittal and coronal planes. A comprehensive map of the density and distribution of X-Gal + neurons is presented in Table 1. The lowest score, +/-, denotes regions with very few cells (significantly above background), while the highest score of +++++, represents regions with a majority of cells stained in a particular area (Table 1). Analysis of the density and distribution of stained neurons is rendered into dot-plot diagrams in 8 rostrocaudal and 2 mediolateral planes of section, as described in the Methods section (Fig. 3.3).

Hypothalamus and thalamus

In the hypothalamus, we detect the highest density of X-Gal staining in the ARH and the posterior periventricular nucleus. In the ARH, X-Gal+ cells are distributed throughout the nucleus; with notable saturation along the ventral and lateral borders. We observe moderate staining density in the suprachiasmatic nucleus (SCN) and tuberal area, and low density staining in the ventromedial division of the ventral medial nucleus (VMH), retrochiasmatic nucleus and paraventricular nucleus (PVH). There are a few stained cells in the anterior hypothalamus, lateral and medial preoptic areas, medial mammillary nucleus, ventral premammilary nucleus and posterior hypothalamus. We consistently find sparse X-Gal staining in the zona incerta, supraoptic nucleus, dorsal medial hypothalamus and lateral hypothalamic area (Fig. 3.3 *Bregma 0 to -1.4*, and Table 1). In addition to the ARH, other hypothalamic nuclei that contain a substantial number of X-Gal+ cells also contribute to energy homeostasis. The SCN nucleus is the master regulator of circadian rhythms; disruption of circadian inputs leads to hyperphagia, obesity and insulin resistance (Turek et al., 2005). The VMH is thought to integrate

metabolic and reproductive functions and to modulate physiological responses to high fat diet (King, 2006; Yi et al., 2011). Homeostatic, circadian and hedonic inputs from the hypothalamus and brainstem are integrated in the PVH and relayed to the periphery via neuroendocrine signals and efferent projections to the sympathetic nervous system (Tolson et al., 2010).

In the rostral thalamus, we observe moderate X-Gal staining in the central medial and lateral dorsal nuclei, along with the nucleus of the reunions and paraventricular nucleus. We detect very low levels of expression in the medial habenula and mediodorsal nucleus (Fig. 3.3 *Bregma -0.1*, and Table 1).

Hippocampus, olfactory bulb and septum

Outside of the ARH, we find the densest region of X-Gal staining in the granule cell layer of the dentate gyrus (DG), particularly in the medial and lateral blades. We observe moderate staining density in the presubiculum and in layers 1,2 and 3 of the subiculum, and a few X-Gal+ cells in the entorhinal area and in the parsubiculum. In the rostral hippocampus, we detect a few X-Gal+ cells in the CA3 region. We observe sparse staining in the postsubiculum (Fig. 3.3 Bregma -0.1, -1.4, -4.5, Lateral 0.2, 2.6, and Table 1). Processing of cognitive factors by the hippocampus is reported to influence feeding behavior and body weight, in part through effects on learning and memories related to food . For example, hippocampal ablations result in increased food intake and body weight, while leptin injections into the ventral hippocampus are reported to suppress food intake and processing of food-related memories (Davidson et al., 2009; Forloni et al., 1986; Kanoski et al., 2011).

In the olfactory bulb, we observe low levels of X-Gal stain in layers 1 and 2 of the cortical amygdalar area and also in layers 2 and 3 of the piriform area. We also detect staining in the taenia tecta and in the rostroventral aspect of the lateral septal nucleus (Fig. 3.3 Bregma 1.4, 0 and Table 1). Olfactory circuits modulate appetite and food intake in response to select odors

(Shen et al., 2005), and in turn, the sensitivity of odor detection is influenced by prandial state and leptin signaling (Aime et al., 2007; Prud'homme et al., 2009).

Cerebral cortex

We observe moderate levels of expression in the bed nucleus of the stria terminalis (BNST) and the medial amygdalar nucleus. The BNST receives afferent input the parabrachial nucleus (PB), which is reported to elicit potent orexigenic effects on food intake (Wu et al., 2009), and also from NPY/AgRP neurons in the ARH (Saper and Loewy, 1980; Shin et al., 2008). The medial amygdala plays a critical role in regulating behavioral stress response, and lesions of the medial amygdala significantly attenuate chronic stress-induced weight gain (Solomon et al., 2010). In addition, we detect a few X-Gal+ cells in the basomedial amygdalar nucleus, the primary somatosensory area (layers 3 and 4) and in layer 4 of the cerebral cortex. We find sparse staining in the primary motor area and in the primary somatosensory barrel field (Fig. 3.3 *Bregma* -0.1, -1.4 and Table 1).

Midbrain, pons and medulla

In the midbrain, we find a moderate density of X-Gal staining in the limbic interpeduncular fossa. We also observe a few stained cells in the inferior colliculus, parabigeminal, medial basal reticular nucleus and the superior colliculus. The periaqueductal gray and the ventral tegmental area contain sparse staining (Fig. 3.3 *Bregma* -5.0, -5.7 and Table 1).

In the pons, we detect a low density of X-Gal staining in the external lateral division of the lateral PB (lPB). The PB nucleus mediates conditioned taste aversion and more recently, has been shown to receive inhibitory inputs from ARH neurons that influence feeding behavior (Wu et al., 2009). We detect a few X-Gal+ cells in the pontine central gray, with sparse staining in the pontine reticular nucleus and the principal sensory nucleus of the trigeminal (Fig. 3.3, Bregma -4.5, -5.0, -5.7 and Table 1).

In the medulla, we observe strong staining in the cochlear nucleus and moderate staining in the area postrema (AP). The facial motor nucleus, the medial aspect of the nucleus of the solitary tract (NTS) and the spinal nucleus of the trigeminal have low levels of X-Gal+ staining. We find sparse staining in the parvicellular reticular and vestibular nuclei (Fig. 3.3, Bregma -7.8, Lateral, 0.2, 2.6 and Table 1). The caudal brain stem integrates hypothalamic and vagal inputs with circulating gut and satiety signals, and influences processes related to food intake and energy expenditure in the periphery via the autonomic nervous system (Crawley and Schwaber, 1983; Grill et al., 2002; Munzberg et al., 2003). Lesions of the AP and NTS independently result in hypophagia accompanied by substantial reductions in body weight (Contreras et al., 1982; Menani et al., 1996).

Cerebellum

We detect X-Gal+ cells in the cerebellum of the mature brain (Fig. 3.4). To determine which cerebellar subtypes are affected by the *Pomc*-Cre transgene, we performed fluorescent immunohistochemistry (IHC) in sections from *Pomc*-Cre;*R26R*-TOM mice. First we confirmed that the distribution of cells labeled in *Pomc*-Cre;*R26R*-TOM mice matches/recapitulates the pattern observed in *Pomc*-Cre;*R26R*-LacZ mice. Next we assessed TOM reporter expression in conjunction with NeuN and parvalbumin (PV) immunoreactivity, to identify granule cells and stellate cells, respectively (Doyle et al., 2008). TOM+ cells are found throughout both the nuclear and molecular layers of the cerebellum. TOM+ cells in the nuclear layer co-express the granule cell marker NeuN (Fig. 3.4A), whereas many TOM+ cells in the molecular layer co-express PV (Fig. 3.4, B and C). While Purkinje cells are not marked with the lineage trace, TOM+ fibers (Fig. 3.4 B arrows) are observed in close proximity to their large soma.

Comparison of *Pomc*-eGFP vs. *Pomc*-Cre reporters

As both *Pomc*-eGFP and *Pomc*-Cre transgenic lines have been used as the basis for studies of POMC neuronal activity, connectivity and function, we directly compared sites of

Pomc promoter activity with those marked by *Pomc*-Cre-mediated recombination in *Pomc*-eGFP;*Pomc*-Cre*;R26R*-TOM mice, which express both types of reporter. Confirming previous reports, we observe *Pomc*-eGFP+ cells in the ARH, DG, AP and NTS (Bronstein et al., 1992; Knigge et al., 1981; Overstreet et al., 2004) (Figs. 3.5 and 3.6). In the ARH, all GFP+ cells co-express the *Pomc*-Cre;*R26R*-TOM reporter. Consistent with our previous analyses/studies, we find that many TOM+ cells do not express the *Pomc*-eGFP reporter (Fig. 3.5, A-C) (Padilla et al., 2010). The only other site where we observe *Pomc*-eGFP+ cells in the hypothalamus is in the ependymal zone of the third ventricle, adjacent to the PVH and DMH; however, cells in this region are not marked with the *Pomc*-Cre;*R26R*-TOM reporter (Fig. 3.6 C).

In addition to the periventricular hypothalamus, we can identify *Pomc*-eGFP+ cells that do not express TOM in the DG, cerebellum and caudal brainstem. In the DG and CA3, we find that GFP and TOM reporter expression is nearly mutually exclusive, with GFP+ cells in the subgranular zone and TOM+ cells in the adjacent granular layer of the DG and CA3 at both P9 and in adulthood (Fig. 3.6, A and D). *Pomc*-eGFP+ cells in the subgranular region of the DG are reported to be/purported/may represent a transient population of immature neurons derived from a neurogenic niche in adults (Overstreet et al., 2004).

The physiological properties of POMC neurons in the AP and caudal NTS are a subject of ongoing debate, as some studies found that subsets of these cells are stimulated by the anorexigenic hormones cholecystokinin and leptin, while others reported that *Pomc*-eGFP+ cells in the NTS do not transduce leptin signals (Ellacott et al., 2006; Huo et al., 2006). We detect *Pomc*-eGFP+ cells in both the AP and NTS. In the AP a minority of GFP+ cells co-express TOM (35%± 8 of GFP+ are TOM+, Fig. 3.5 D-arrows), whereas in the NTS we find that TOM and GFP label mutually exclusive/non-overlapping neuronal populations (Fig. 3.6 F). In the cerebellum we also detect *Pomc*-eGFP+ cells that do not express the *Pomc*-Cre reporter, similar to the cells described in the ependymal zone of the third ventricle, the subgranular region

of the DG and in the NTS. These GFP+ cells are localized to the medial and caudal cerebellum at P9, a period of external granule layer proliferation (Hatten and Heintz, 1995); however, in the adult, GFP+ cells are distributed throughout the rostro-caudal extent of the molecular cell layer (Fig. 3.6, B and E).

In contrast to ARH, where nearly all *Pomc*-eGFP+ neurons are also labeled with a *Pomc*-Cre reporter, GFP and TOM expression patterns in the hypothalamic periventricular zone, DG and NTS are largely discordant/complementary. We used two *in situ* hybridization protocols to determine whether we can detect a *Pomc* signal in any of these sites - a tyramide-based amplification system (TSA-kit, Perkin-Elmer) and a more sensitive neutravidin-based amplification system (Lein et al., 2007). In the NTS, we are able to detect the presence of/visualize *Pomc* transcripts using the Neutravidin system, but not with TSA system (Fig. 3.7). We did not detect a *Pomc* signal using either *in situ* system in the AP, DG or lPB (data not shown).

Peptidergic identities of leptin-sensing neurons in the ARH and caudal brainstem

Pomc-expressing populations in both the ARH and NTS have been implicated in the regulation of energy balance, in part, through transduction of leptin signals. To determine whether cells expressing *Pomc*-eGFP and/or *Pomc*-Cre reporter cells are leptin-sensing, we assessed P-STAT3 immunoreactivity in conjunction with GFP and TOM in adult brains following a peripheral leptin injection. Consistent with published analyses (Munzberg et al., 2003; Williams et al., 2010), we find that approximately 40 percent of mature POMC neurons in the ARH are P-STAT3+ following leptin treatment (Fig. 3.8 A, of 18±4 GFP+ cells, 7±3 cells are P-STAT3+). We also observe that approximately half of the TOM+ cells that do not co-express GFP in the ARH are leptin-sensing (Fig. 3.8 A, of 87±4 TOM-only, 47±2 are P-STAT3+); 35% of these non-POMC TOM+/P-STAT3+ cells are NPY neurons (Fig. 3.8 A, of 47±2 TOM only/P-STAT3+, 13±3 also express NPY). Thus, whereas POMC neurons represent a mere 14% of the

total number of leptin-sensing neurons in the ARH, the *Pomc*-Cre transgenic affects 70% of this population.

In the AP, we find that 30 percent of the TOM+ population is leptin-sensing (Fig. 3.8 D, of 20±3 TOM+, 11.8±4 are P-STAT3+). In the NTS, there are relatively few TOM+ cells compared to GFP+, none of which are leptin sensing. However, consistent with previously published reports, we find that approximately 50 percent of the GFP+ population in the medial NTS are leptin-sensing (Fig. 3.8 E, in an average of 21±2 GFP-only cells, 10±1 are P-STAT3+) (Ellacott et al., 2006).

Discussion

Pomc-eGFP and *Pomc*-Cre transgenic mouse lines have been used extensively to investigate the role of melanocortin circuits in regulating energy homeostasis. In previous studies, we demonstrated that nearly all *Pomc*-eGFP+ cells in the adult ARH express *Pomc* transcript, whereas many cells marked with a *Pomc*-Cre reporter are devoid of a *Pomc* ISH signal and/or *Pomc*-eGFP reporter expression (Padilla et al., 2010). Our data further indicated that this phenomenon was due to down-regulation of *Pomc*-expression in a broad region of the mediobasal hypothalamus during embryogenesis. Similar findings of transient *Pomc* expression have been reported in the embryonic spinal cord, where POMC processing products/derivatives may promote/regulate differentiation and proliferation of motor neurons (Berry and Haynes, 1989; Haynes, 1990). In our initial assessment/characterization of *Pomc*-eGFP and *Pomc*-Cre;*R26R*-LacZ reporter distribution at embryonic stages, we noticed that X-Gal+ neurons were widely distributed throughout the brain, spinal cord and retina. As recombination of a floxed allele is permanent, analyses of functional studies using the *Pomc*-Cre transgenic line could be complicated due to overlapping expression patterns of the transgene and gene of interest in other CNS sites at an earlier developmental stage. To assist in the analysis of completed/existing studies involving the *Pomc*-Cre transgene, as well as to facilitate the design

of future experiments, we systematically characterized the distribution of cells marked with *Pomc*-Cre and *Pomc*-eGFP reporters across the murine brain at E16.5 and in the adult.

Pomc-eGFP reporter as a marker of endogenous Pomc transcription

Consistent with previous studies, we find that nearly all *Pomc*-eGFP+ cells in the embryonic and adult ARH express *Pomc* transcript (Cowley et al., 2001; Padilla et al., 2010; Pinto et al., 2004). Moreover, we observe a close correspondence between domains of *Pomc*-eGFP+ cells and *Pomc* expression in the embryonic pituitary, midbrain and hindbrain and spinal cord (Figs. 3.1B and 3.2A). Therefore, these transgenic lines are well-suited for use in neuroanatomical or electrophysiological studies of POMC neurons in the ARH.

In several brain regions outside of the ARH (including the DG, periventricular zone of the dorsal hypothalamus, and cerebellum) we and others have identified *Pomc*-eGFP+ cells that do not express detectable levels of *Pomc* transcript (Fig. 3.6, (Overstreet et al., 2004)). We considered three possible explanations for these findings: 1) *Pomc* is expressed below the level of detection for this assay; 2) transient bursts of transcription are preserved by the persistence of GFP protein after transcription is extinguished; and 3) ectopic activation of the transgene. Using highly sensitive ISH methods, such as radioactive and Neutravidin-amplified detection systems, we and others detect *Pomc* transcripts in the NTS (Fig. 3.7 and (Bronstein et al., 1992). As the integrity of fluorescent reporter staining is not maintained under the conditions needed for Neutravidin-amplified detection, we could not assess the relationship between the *Pomc*-expressing cells in the NTS and those marked with either *Pomc*-eGFP or a *Pomc*-Cre reporter. We were unable to detect a *Pomc* signal in the DG, ependymal layer of the 3rd ventricle, or cerebellum using the Neutravidin-based system; however, others have reported low levels of *Pomc* transcription by PCR amplification from the rat cortex and cerebellum (Grauerholz et al., 1998). Together these data support the idea that *Pomc*-eGFP expression in the NTS and in some extra-ARH brain regions reflect sub-threshold or transient *Pomc*

transcription, but we cannot exclude the possibility that some sites of GFP+ cells result from ectopic expression of the transgene.

Interpretation and design of functional studies using *Pomc*-Cre transgenic lines

Pomc-Cre transgenic mice have been utilized to conditionally target and study the function of POMC neurons in the hypothalamus. The phenotypes reported in these studies include effects on lipid metabolism, fertility, sexually dimorphic effects on glucose homeostasis and body weight phenotypes, food intake, locomotor activity, energy expenditure and alterations in soma size (Balthasar et al., 2004; Banno et al., 2010; Hill et al., 2010; Huo et al., 2009; Mori et al., 2009; Shi et al., 2010; Xu et al., 2007). We find that not only does this Cre line direct recombination to more cells than expected in the ARH, it is also present in other regions of the brain implicated in energy homeostasis including: PVH, VMH, subiculum, medial amygdala, lPB and AP (Table 3.1, Fig. 3.3).

Previously we determined that *Pomc*-Cre directs recombination to a subset of AgRP/NPY neurons in the ARH (Padilla et al., 2010). In this study we find that the absolute number of NPY/AgRP neurons labeled with the *Pomc*-Cre lineage trace varies, depending on the reporter allele used (25% with Rosa-eGFP vs. 70% with Rosa-LacZ and/or Rosa-tdTOM), ((Padilla et al., 2010) and Fig 3.8B). Approximately 40% of ARH neurons are labeled with the TOM reporter; many of these do not express *Pomc* or *Npy* in adulthood (Padilla et al., 2010). As distinct ARH neuronal subpopulations are physically intermingled and project to similar downstream targets, the use of *Pomc*-Cre transgenes as part of a strategy to genetically label cell bodies or projection patterns or to characterize electrophysiological properties of POMC neurons is not advisable.

Depending on the experimental design, off-target *Pomc*-Cre-mediated recombination could complicate the interpretation of conditional gain- or loss-of gene function studies. The two most important considerations in analyzing phenotypes from genetic manipulations using *Pomc*-Cre

transgenes are: 1) the endogenous expression pattern of the gene of interest in relation to sites listed in Table 1; and 2) the timing of *Pomc*-Cre expression. When the gene of interest is broadly expressed in the CNS, off-target effects in nuclei with moderate to high X-Gal staining could also contribute to body composition and metabolic outcomes. If a target gene is not expressed in any of the neurons marked with the lineage trace, all resulting phenotypes can be attributed to POMC neurons.

Even if a gene of interest has a restricted expression pattern, the severity of phenotypes could be mitigated by simultaneous genetic manipulations in NPY/AgRP and POMC neurons, which are thought to play opposing functions in circuits regulating body composition and energy homeostasis. In addition, non-POMC/NPY neurons marked with *Pomc*-Cre could also contribute to physiological outcomes. In our analysis of the peptidergic identities of leptin-sensing cells in the ARH, we find that 70% of P-STAT3+ cells are TOM+ (of 65±4 P-STAT3+ cells, 54±2 are TOM+, Fig. 3.8). Of the leptin-sensing neurons affected by the *Pomc*-Cre transgene, 30% express *Pomc*, 55% express *Npy*, and the remaining 15% have yet to be defined (of 54±2 P-STAT3+/TOM+, 14±1 are POMC+, 30±6 are NPY+).

As many off-target sites of *Pomc*-Cre reporter activity result from transient *Pomc* expression during gestation, delaying transgene expression to adulthood would reduce the opportunity for unintended *Pomc*-Cre-mediated recombination events. For example, by injecting a viral construct expressing a floxed target gene into the adult ARH of *Pomc*-Cre mice, recombination should be limited to POMC neurons (Aponte et al., 2011). In theory, activation of an inducible *Pomc*-Cre transgene in adulthood should also reduce off-target recombination. While strategies to spatially and/or temporally restrict *Pomc*-Cre expression can limit unintended recombination events, consideration should be given to extra-ARH sites of *Pomc*-Cre activity in the adult, discussed below.

Discordace between *Pomc* transcription, *Pomc*-eGFP and *Pomc*-Cre reporter expression

In the ARH we conclude that *Pomc*-expressing cells, marked by *Pomc*-eGFP, co-express the *Pomc*-Cre reporter; however, in extra-ARH regions of the brain including the DG, periventricular zone of the dorsal hypothalamus, NTS and cerebellum, *Pomc*-eGFP+ cells do not follow this trend. For example, in the DG, GFP and TOM are expressed in mutually exclusive neighboring cellular populations, whereas in the cerebellum we detect TOM in a subset of the broad GFP+ population. Some possibilities to explain these observations are discussed below and involve both the potential role of POMC processing products in the maturation of immature neurons and/or the potential of extopic reporter expression.

In the DG, *Pomc*-eGFP is expressed in an immature population in the subgranular zone, while the *Pomc*-Cre reporter is detected in a juxta-population of cells in the granular layer (Fig. 3.6D). These findings are consistent with previous reports that *Pomc*-eGFP is transiently expressed in newly-born neurons in the adult hippocampus, which extinguish the *Pomc* driven transgene as they mature and migrate out into the granular layer (Overstreet et al., 2004). The most parsimonious explanation of the pattern of reporter expression we observe in the DG is that the *Pomc*-eGFP and *Pomc*-Cre transgenes are transiently expressed in immature neurons in the subgranular layer, which are extinguished upon maturation and migration to the granular layer. Detection of the *Pomc*-Cre lineage trace in the granular layer and not in the subgranular layer could be a result of the delay in Cre-mediated recombination of floxed reporter alleles relative to the onset of Cre expression (Branda and Dymecki, 2004). While we cannot exclude the possibility that the *Pomc*-eGFP and *Pomc*-Cre transgenes are ectopically expressed in the subgranular layer and the granular layer of the DG, respectively, it is striking to find the expression of both *Pomc* transgenes in adjacent populations that reflect different stages of maturation of the same cell type.

The neighboring pattern of cells expressing Pomc-eGFP and Pomc-Cre reporters found in the DG, is similarly reflected in the periventricular zone of the dorsal hypothalamus and in NTS. GFP+ cells in the hypothalamus are adjacent to the ventricular zone – a proposed site of neurogenesis (Xu et al., 2005) – while *Pomc*-Cre reporter+ cells occupy more dorsal and lateral aspects of the PVN and DMH (Fig. 3.6C). In the medulla, GFP+ cells are located in a medial cluster of the commissural NTS, while *Pomc*-Cre reporter+ cells occupy the more dorsolateral regions of this nucleus (Fig. 3.6F). Unlike the DG, neither of these neighboring populations are immediately adjacent to one another, therefore determining the origin of the *Pomc*-Cre reporter+ cells remains speculative. Because the GFP+ hypothalamic periventricular cells are near a proposed neurogenic niche, it is likely that *Pomc* is expressed transiently in immature neurons, playing a role in the maturation of these newly born cells. While it is also possible that the GFP+ cells in the NTS are immature, we also detect low levels of *Pomc* expression in the medial commissural NTS (Fig. 3.7B), and thus it is also possible that such low levels of transcript are not sufficient to drive recombination. In this case, *Pomc*-Cre reporter+ cells in the NTS may be derived from *Pomc*-expressing precursors at an earlier stage of development, consistent with the detection of transient *Pomc* expression in the hindbrain during embryogenesis (Figs. 3.1 and 3.2, A and D).

Unlike the situations described above, *Pomc*-eGFP and *Pomc*-Cre reporters are not entirely mutually exclusive of one another in the cerebellum but rather are co-expressed in subsets of these reporter-expressing cells. During development at P9 – a stage of external germinal layer proliferation in the cerebellum (Hatten and Heintz, 1995) – GFP and TOM reporters are present in adjacent cell populations (Fig. 3.6B), consistent with the idea of transient expression. In adult, GFP expression is not as restrictive but rather scattered throughout all layers of the cerebellum, and is not particularly localized near the reported site of neurogenesis in the subpial layer (Ponti et al., 2006, 2008). While we cannot detect *Pomc* expression in the cerebellum under any

condiditions, others have found low levels of transcript using quantitave PCR. If the q-PCR data is accurate, very low levels of expression may be present in the GFP population, while *Pomc*-Cre reporter+ cells devoid of GFP reporter may have been derived from transient *Pomc* expression during earlier stages of development.

Together, these observations raise the intriguing possibility that *Pomc*-eGFP expression outside the ARH regions could be a marker for immature neurons that were born in the adult or may also represent cells that express very low levels of *Pomc* transcript (perhaps below the level necessary to drive recombination via *Pomc*-Cre. Further studies are needed to explore this hypothesis; however, if proven true*, Pomc*-eGFP expression could provide a powerful new tool to investigate the contribution of adult-born hypothalamic neurons to obesity-related outcomes.

Methods

Animals

Animals were housed in temperature controlled rooms at 21 °C and subject to a 12 h light-dark cycle. Mice had *ad libitum* access to standard chow diet (Lab Diet: PicoLab Rodent Diet 5053) and water. C57BL/6, *ROSA(26R)*-TOM and *ROSA(26R)*-LacZ mice were obtained from the Jackson Laboratory and bred at the Russ Berrie Animal Facility (Madisen et al., 2010; Soriano, 1999). *Pomc*-Cre (Balthasar et al., 2004) and *Pomc*-eGFP (Cowley et al., 2001) transgenic animals were generously provided by Joel Elmquist/Bradford Lowell and Malcolm Low, respectively. All procedures were performed in accordance with the guidelines of the Institutional Animal Care and Use Committee at the Columbia University Health Sciences Division.

Genotyping

Genotyping at the *ROSA26* locus for LacZ was performed using the following three-primer set: oIMR 0316 (wt-F) 5'-GGAGCGGGAGAAATGGATATG-3'; oIMR 0883 (wt-R): 5'-

AAAGTCGCTCTGAGTTGTTAT-3'; oIMR (mutant-LacZ) 0315 5'-GCGAAGAGTTTGTCCTCAACC-3'; (Soriano, 1999). Genotyping at the *ROSA26* locus for TOM was performed using a three-primer set including both wild type (wt) primers (0316 & 0883) above and, oIMR (mutant-TOM) 5'-CTGTTCCTGTACGGCATGG-3' (Madisen et al., 2010). The *Cre* transgene was assessed with: 5'-GCGGTCTGGCAGTAAAAACTATC-3', 5'-GTGAAACAGCATTGCTGTCACTT-3'.

Tissue processing

P9 and adult mice were anesthetized and perfused transcardially with 0.9% NaCl followed by 4% paraformaldehyde (PFA) in phosphate buffer (PB). Brains were post-fixed at 4°C for 3 hours and cryoprotected using a 30% sucrose gradient. For embryonic tissue, dams were anesthetized with Avertin and embryos were dissected in cold PBS and fixed at 4 °C overnight and cryoprotected. Tissue used for IHC and/or FISH was embedded in O.C.T. (Tissue Tek) and frozen at –80°C. 10 µm-thick coronal sections were collected across the rostral–caudal extent of the ARH on Superfrost Plus slides (Fisher). Alternatively, tissue used for X-Gal staining was not cryoprotected following fixation, but rather immediately processed for whole mount staining.

X-Gal staining

Following fixation, whole mount tissue was washed thoroughly in PBS at 4°C, and then permeabilized using 2 mM $MgCl_2$, 0.001% sodium deoxycholate, and 0.02% NP-40 buffer, at room temperature for 2 hours. X-Gal staining was performed using 5 mM potassium ferricyanide, 5 mM potassium ferrocyanide, 20 mM Tris, and 1 mg/ml X-Gal, overnight at room temperature. After staining, the tissue was rinsed in PBS and fixed in 4% paraformaldehyde overnight. Embryonic tissue was subsequently cleared in glycerol and imaged as a whole mount preparation. Adult brains were vibrabome-sectioned (200 µm) and mounted on slides for imaging.

Scoring

The density of positive X-Gal staining in each brain nucleus, expressed as a percentage of total nuclear area, was used to determine the scores assigned to the nuclei as follows: 0-2 percent scored +/-, 2-8% +, 8-14% ++, 14-30% +++, 30-50% ++++, and >50% +++++.

Imaging

Fluorescent microscopy was performed using both a Zeiss LSM5 Pascal Confocal or a Nikon Eclipse 80i equipped with a Retiga EXi camera and an Xcite 120 fluorescent illumination system. Bright field microscopy was performed with a Nikon Eclipse 80i camera. Tiled images acquired for dot renderings were obtained using an automated stage with Q Capture Pro imaging software (Qimaging).

Dot rendering

Regions with X-Gal+ cells categorized relative to the Allen Reference Atlas (http://www.brain-map.org, (Lein et al., 2007)). Stain density in each designated nucleus was quantified and rendered into dots using Adobe Photoshop. Within each individual nucleus, dot number is proportional to the area of the stain and dot placement reflects the spatial distribution of stained cells (note: dots were not assigned to nuclei with <2% total stain).

IHC

Fixed slide-mounted sections were blocked in 2% normal horse serum; 0.1% Triton X-100 (Block Buffer) at room temperature. Primary antibody incubation was performed using either guinea pig anti-GFP (1:2000; Molecular Probes) or rabbit anti-P-STAT3 (1:800; Cell Signaling) at 4 °C overnight. Tissue was then washed in PBS and incubated in with secondary using either goat anti-guinea pig Alexa-488 (1:500 Invitrogen) or goat anti-rabbit cy5 (1:100 Jackson ImmunoResearch), for one hour at room temperature. Note, for P-STAT3 IHC an additional unmasking step was performed prior to blocking and primary antibody incubation by the

following sequential pretreatment: 1% NaOH with 1% H_2O_2 solution, 0.3% glycine, and 0.3% SDS.

Combined IHC and FISH

Procedures performed according to previously published methods (Padilla et al., 2010).

FISH and NeutrAvidin amplified ISH

Frozen sections were processed as described in the TSA Plus Cy3 System manual (Perkin Elmer). Antisense digoxigenin- or fluorescein-labeled riboprobes were generated from plasmids containing PCR fragments of *Npy* and *Pomc* using the following primers sets: (NPY) 5'-TGCTAGGTAACAAGCGAATGG-3'/5'-CAACAACAACAAGGGAAATGG-3; (POMC) 5'-GTTAAGAGCAGTGACTAAGAGAGGC-3'/5'-CCTAACACAGGTAACTCTAAGAGGC-3'. NeutrAvidin amplified ISH was achieved using biotinylated-tyramide (Perkin Elmer) in conjunction with NeutrAvidin Protein, Alkaline Phosphatase Conjugated (Thermo Scientific) followed by BCIP/NBT staining.

Acknowledgements

We thank J.P. Pardere for helping to establish the technique used for dot plot renderings, M. Madra for assistance with tissue preparation and ISH staining, L. Yang of the DERC Pathology Core for cryosectioning (NCRR UL1 RR024156); M. Low (University of Michigan Health Center), J. Elmquist (UT Southwestern Medical Center), and B. Lowell (Beth Israel Deaconess Medical Center) for generously providing mouse reagents. This work was supported by F31DK079372 (SLP), Institute of Human Nutrition Training Grant 2T32DK007647-21 (JSC), ADA 7-07RA-195 (LMZ), and Columbia DERC Pilot and Feasibility Award P30 DK63608-07 (LMZ), NY Obesity Research Center Pilot and Feasibility P30 DK26687-26 (LMZ).

Figures and Tables:

Table 3.1

Hypothalamus (layers)	Score
Anterior hypothalamus	+
Arcuate nucleus	+++++
Dorsal medial hypothalamus	+/-
Lateral preoptic area	+
Medial mammillary nucleus	+
Medial preoptic area	+
Median preoptic nucleus	++++
Lateral hypothalamic area	+/-
Paraventricular nucleus	++
Periventricular (posterior)	+++++
Posterior hypothalamus	+
Retrochiasmatic area	++
Suprachiasmatic nucleus	+++
Supraoptic nucleus	+/-
Tuberal nucleus	+++
Ventral medial nucleus (ventromedial)	++
Ventral premammilary nucleus	+
Zona incerta	+/-
Thalamus	
Central medial nucleus	+
Lateral dorsal nucleus	+
Medial habenula	+/-
Mediodorsal nucleus	+/-
Nucleus of reunions	+
Paraventricular nucleus	+
Hippocampus	
CA3 (pyramidal cell layer)	+
Dentate gyrus (granular cell)	+++++
Entorhinal area (2a,2b,3)	+
Parsubiculum	+
Postsubiculum	+/-
Presubiculum	+++
Subiculum (1,2,3)	+++

Olfactory Bulb	
Cortical amygdalar area (1,2)	++
Piriform area (2,3)	++
Taenia tecta	+
Septum	
Lateral septal nucleus (rostroventral)	+
Cerebral cortex	
Amygdalar nucleus, basomedial	+
Bed nuclei of the stria terminalis	++
Cerebral cortex (layer 4)	+
Amygdalar nucleus, medial	++
Primary motor area (1,2,3)	+/-
Primary somatosensory area (3,4)	+
Primary somatosensory barrel field (2,3,4)	+/-
Midbrain	
Inferior colliculus (dorsal/external)	++
Interpeduncular fossa	+++
Medial prectectal area	
Parabigeminal	++
Periaqueductal gray	+/-
Superior colliculus	+/-
Ventral tegmental area	+/-
Pons	
Lateral parabrachial, external lateral	++
Pontine central gray	+
Pontine reticular nucleus	+/-
Principal sensory nucleus of the trigeminal	+/-
Medulla	
Area postrema	+++
Cochlear nucleus	++++
Facial motor nucleus	++
Intermediate reticular nucleus	+/-
NTS, medial	++
Nucleus of the solitary tract, total	+
Parvicellular reticular nucleus	+/-
Spinal nucleus of the trigeminal	+
Vestibular nucleus	+/-

Figure 3.1

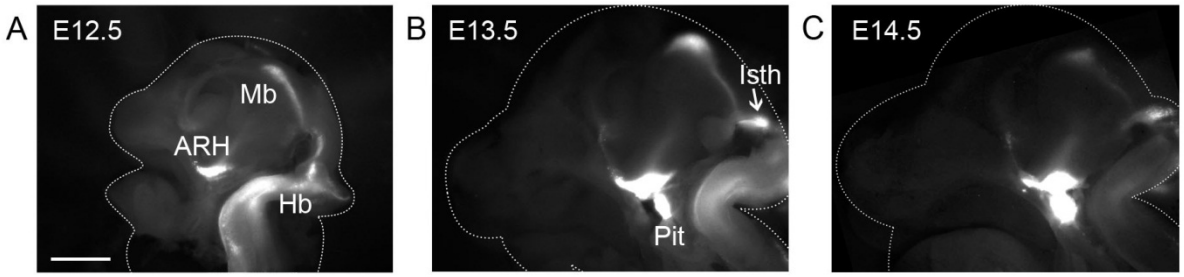

FIG. 3.1. Transient expression of a *Pomc*-eGFP transgenic reporter during gestation. Representative fluorescent images (magnification 1.6X) of the ventricular surface of hemisected embryonic brains at (A) E12.5; (B) E13.5; and (C) E14.5. All images are presented rostral, left. Abbreviations: Pit, pituitary; Mb, midbrain; Isth, isthmus; Hb, hindbrain. Scale bar, 1mm.

Figure 3.2

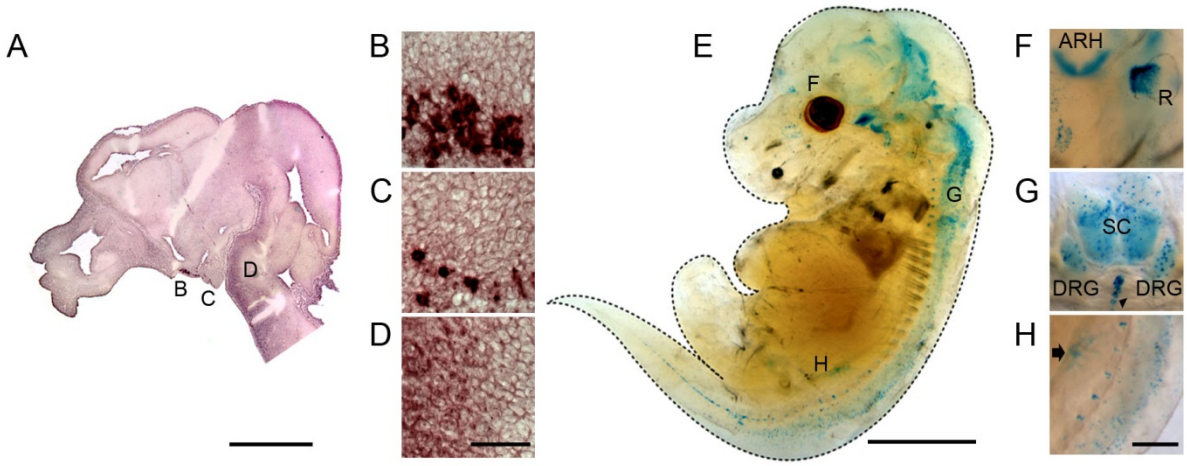

FIG. 3.2. Pomc is broadly distributed in the embryonic CNS and periphery. (A) E13.5 *Pomc* ISH. (B-D) Magnified views of the ARH (A), Pituitary (B) and hindbrain (C). (E) E16.5 *Pomc*-Cre*;R26R*-LacZ embryo stained with X-Gal. (B-D) Magnified views at the level of the retina (B), hindbrain (C) and spinal cord (D) denoted in (A). Abbreviations: ARH, arcuate nucleus of the hypothalamus; R, retina; SC, spinal cord; DRG, dorsal root ganglia; arrowhead (C) developing vertebrae; arrow (D) duodenal melanocyte. Scale bars: (A) 1mm; (D, H) 100μm; (E) 2mm.

Figure 3.3

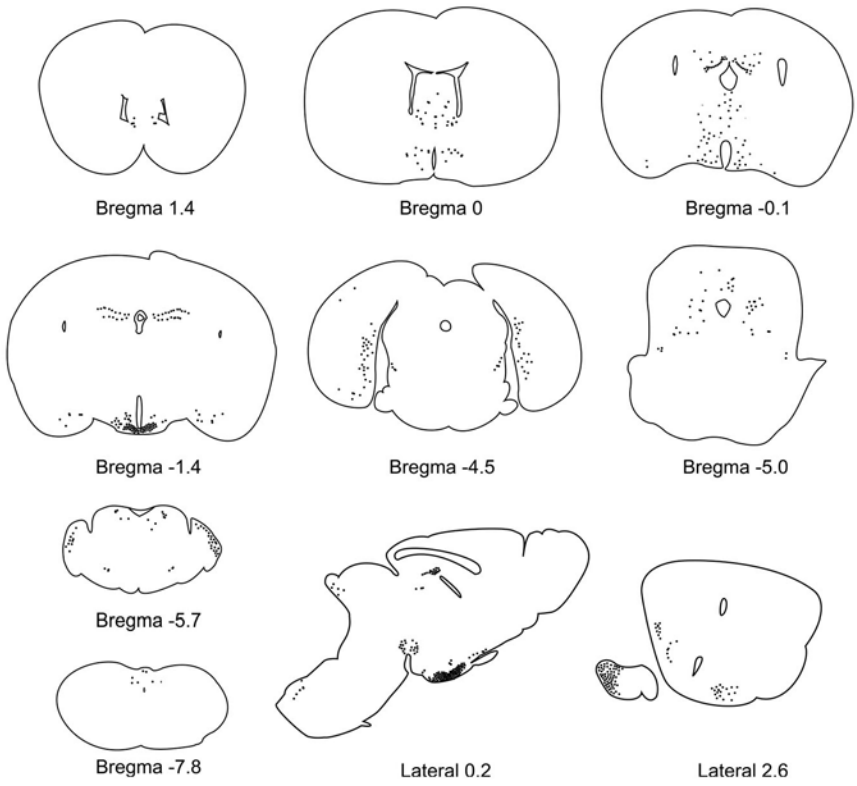

FIG. 3.3. Line drawings to illustrate the distribution of neurons labeled with the *Pomc*-Cre;*R26R*-LacZ reporter in the adult brain. Dot plots are rendered from X-Gal-stained *Pomc*-Cre;*R26R*-LacZ brains (200μm thick sections in the coronal and sagittal planes) and labeled with atlas coordinates (Lein et al., 2007). The density of dots directly corresponds to the density of X-Gal staining in each brain region. See Table 3.1 for complete listing and scoring.

Figure 3.4

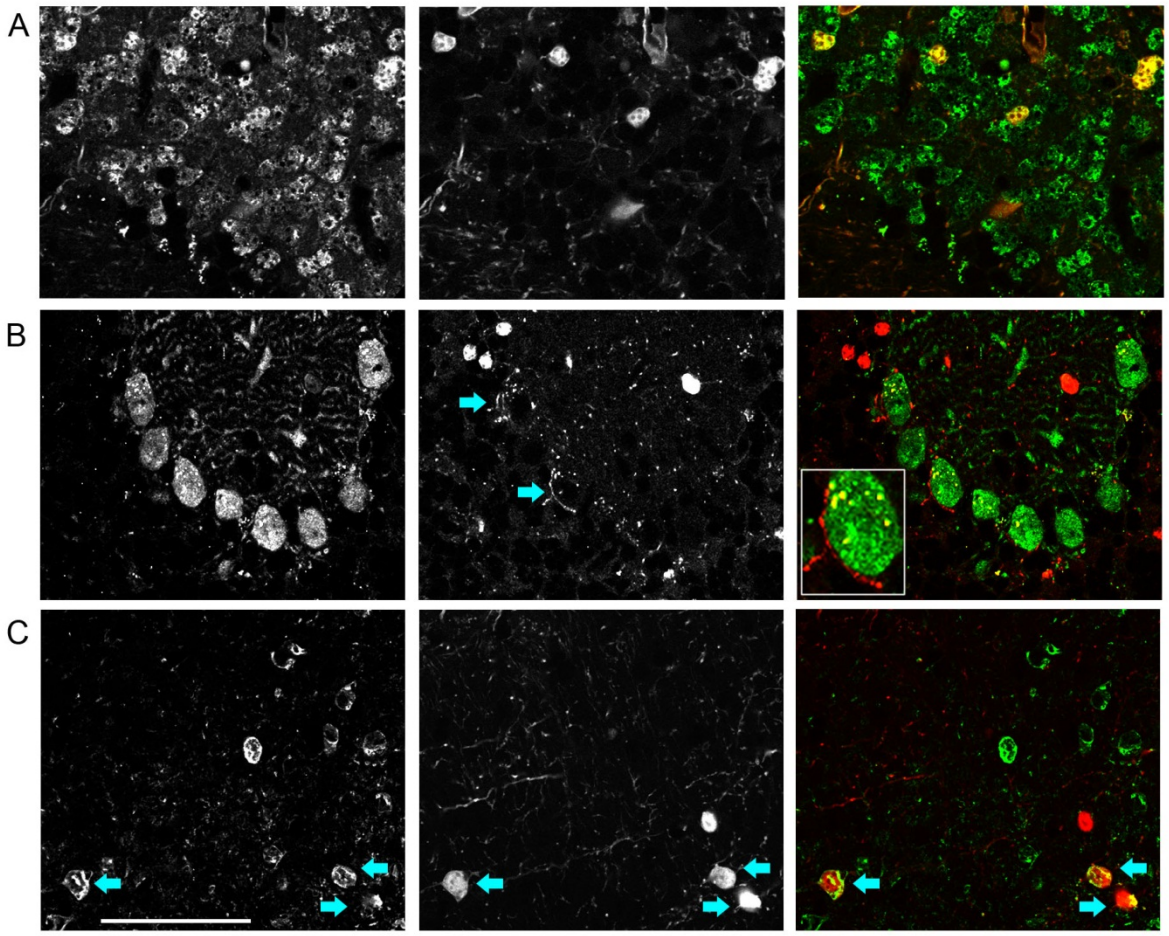

FIG. 3.4. *Pomc*-Cre;*R26*R-TOM reporter is observed in the molecular and nuclear layers of the adult cerebellum. (A-C) Direct TOM fluorescence is visualized in conjunction with IHC for: NeuN (A); Calbindin (B); Parvalbumin (C) IHC staining (left panels) appears green in the merged image (right panels), while TOM fluorescence (center panels) appears red in merged images (right panels) (B) Arrows indicate TOM+ fibers. (C) Arrows indicate TOM/Parvalbumin co-expression. Scale bar, 50μm.

Figure 3.5

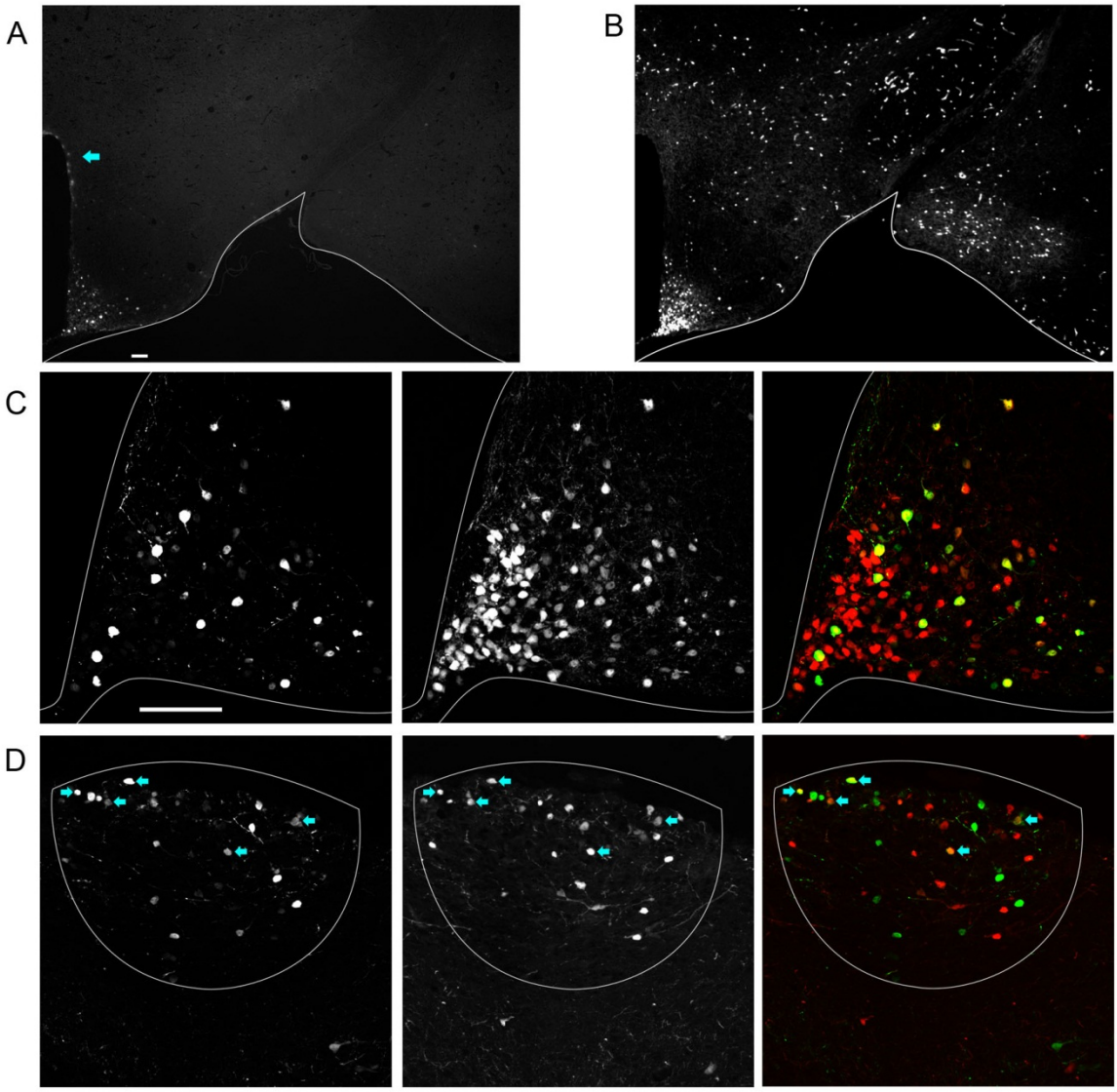

FIG. 3.5. POMC neurons represent a minority of the cells labeled with a *Pomc*-Cre;*R26R*-TOM reporter in adulthood. (A-F) Confocal images of direct TOM fluorescence in conjunction with IHC for GFP in 10μm sections from adult *Pomc*-eGFP;*Pomc*-Cre*;R26R*-TOM animals. (A, B) Low magnification (4X) images of GFP+ (A) and TOM+ (B) populations in the hypothalamus at the level of the ARH. (C,D) Higher magnification (20X) images of the ARH (C) and AP (D). For each section, GFP IHC is in the left panel, direct TOM fluorescence is in the center panel, and merged composites are in the right panels. (D) Arrows indicate double positive GFP/TOM cells. Scale bars, 100μm.

Figure 3.6

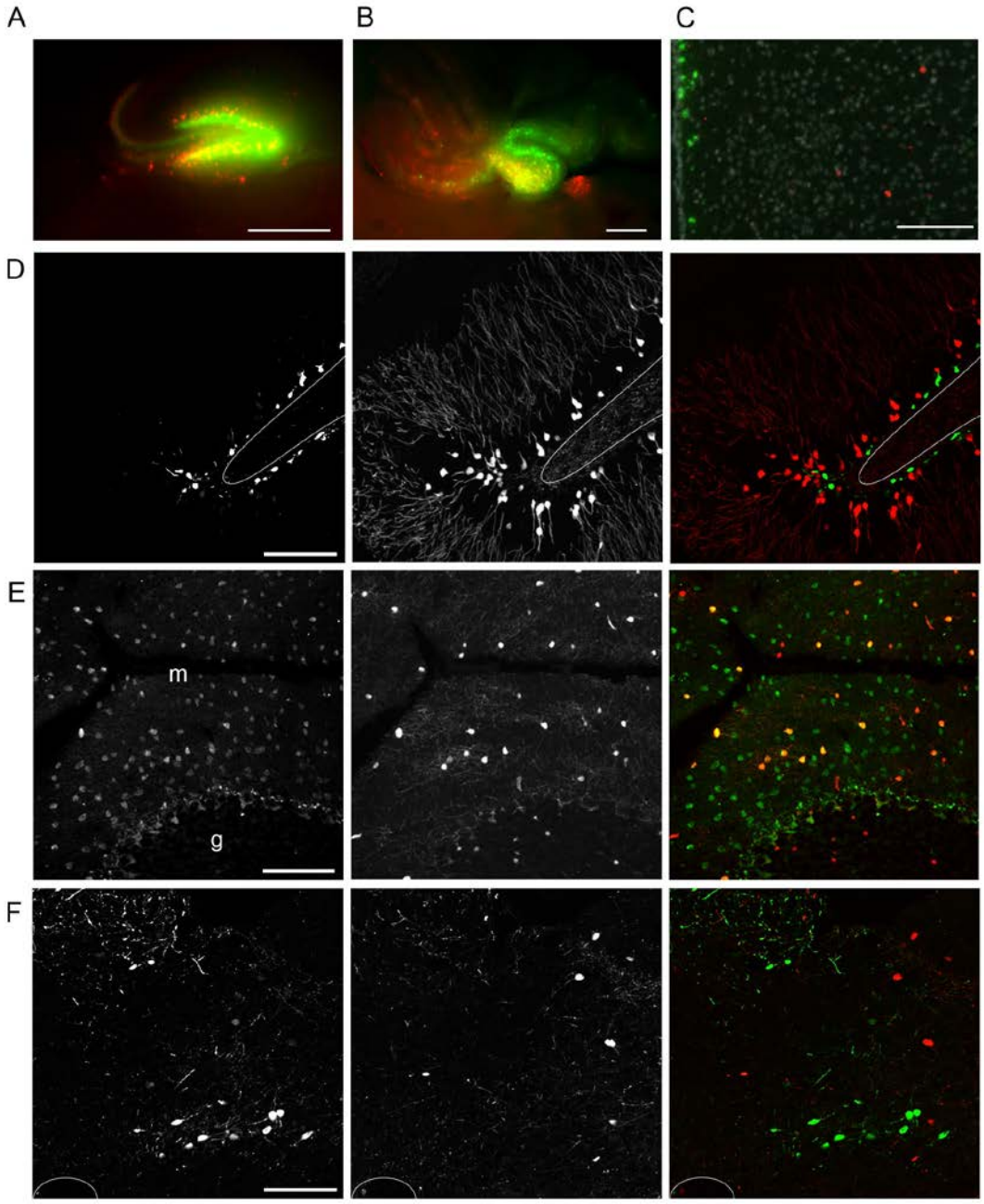

FIG. 3.6. Expression of the *Pomc*-eGFP reporter in the absence of a *Pomc*-Cre*;R26R*-TOM reporter is observed in several brain regions in *Pomc*-eGFP;*Pomc*-Cre*;R26R-TOM* mice. (A, B) 2X images of direct GFP and TOM fluorescence visualized from the ventricular surface in hemisected brains from P9. (A) hippocampus; (B) cerebellum. (C) 3rd ventricle of an adult hypothalamus, dorsal to the ARH; DAPI staining is presented in grey. (D-F) 20X of GFP IHC (left, green in merge), direct TOM fluorescence (center, red in merge) and the merged image (right) in 10µm sections from adult animals. (D) cerebellum, (E) DG, (F) NTS. Scale bars: (A,B) 500µm; (C-F) 100µm.

Figure 3.7

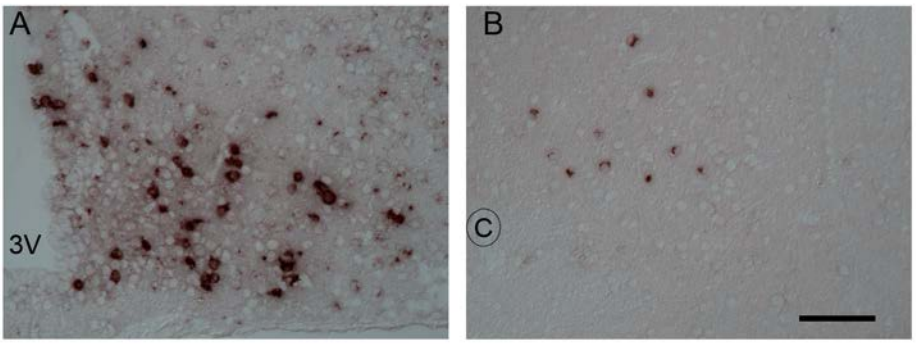

FIG. 3.7. *Pomc* transcript can be detected in the NTS using Neutravidin-amplified ISH. (A,B) AP stain of Pomc transcript. (A) ARH; (B) NTS. Abbreviations: 3V, 3rd ventricle; C, central cannal. Scale bar, 100um

Figure 3.8

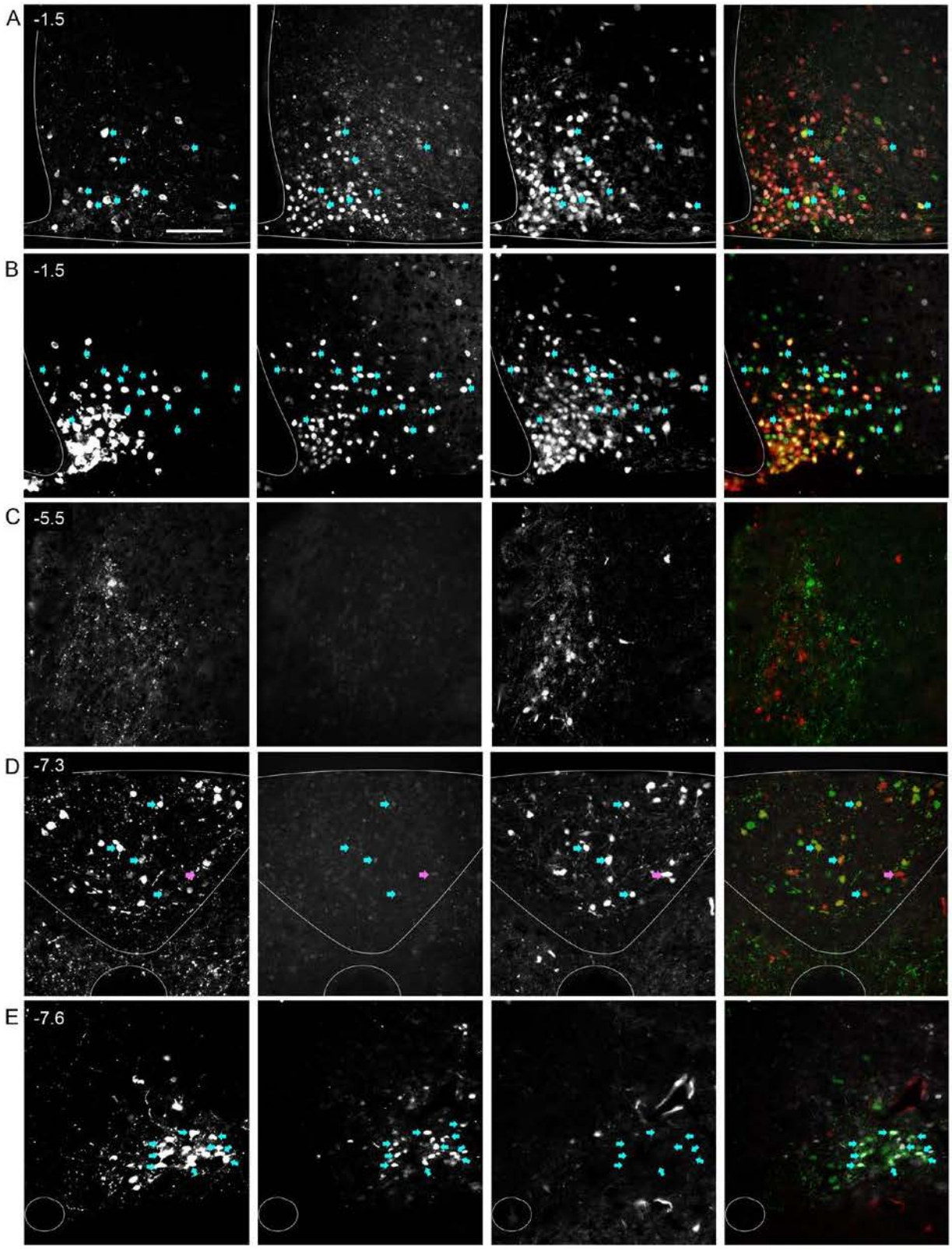

FIG. 3.8. Peptidergic identities of leptin-sensing neurons in the ARH and brainstem. Adult *Pomc*-eGFP ;*Pomc*-Cre*;R26R*-TOM animals were injected with leptin (4mg/kg i.p.) following an overnight fast. 20X images of GFP IHC (left, green in merged image), P-STAT3 IHC (center-left, white in merged image), direct TOM fluorescence (center-right, red in merged image), and merged image (right) in 10µm sections. Exception (B-left) represents *Npy* transcript by FISH; this technique is combined with IHC for P-STAT3, TOM is detected by direct fluorescence. (A, B) ARH. (A) Arrows represent leptin-sensing GFP+ cells, note; in the merged image pink cells (red & white) represent leptin sensing non-POMC neurons that are labeled with the TOM reporter. (B) Arrows represent leptin-sensing NPY cells that are marked with the TOM reporter. (C) PB (D) Brainstem at the level of the AP. Blue arrows indicate leptin-sensing POMC neurons in the AP, note; pink arrow represents a leptin-sensing non-POMC neuron that is labeled with the TOM reporter. (E) Caudal brainstem. Blue arrows indicate leptin-sensing POMC neurons in the NTS. Stereotactic coordinates defined according to Allen Brain Atlas are indicated in the top left. Scale bar; 100µm.

References

Aime, P., Duchamp-Viret, P., Chaput, M.A., Savigner, A., Mahfouz, M., and Julliard, A.K. (2007). Fasting increases and satiation decreases olfactory detection for a neutral odor in rats. Behav Brain Res *179*, 258-264.

Aponte, Y., Atasoy, D., and Sternson, S.M. (2011). AGRP neurons are sufficient to orchestrate feeding behavior rapidly and without training. Nat Neurosci *14*, 351-355.

Balthasar, N., Coppari, R., McMinn, J., Liu, S.M., Lee, C.E., Tang, V., Kenny, C.D., McGovern, R.A., Chua, S.C., Jr., Elmquist, J.K*., et al.* (2004). Leptin receptor signaling in POMC neurons is required for normal body weight homeostasis. Neuron *42*, 983-991.

Banno, R., Zimmer, D., De Jonghe, B.C., Atienza, M., Rak, K., Yang, W., and Bence, K.K. (2010). PTP1B and SHP2 in POMC neurons reciprocally regulate energy balance in mice. The Journal of clinical investigation *120*, 720-734.

Berry, S., and Haynes, L.W. (1989). The opiomelanocortin peptide family: neuronal expression and modulation of neural cellular development and regeneration in the central nervous system. Comp Biochem Physiol A Comp Physiol *93*, 267-272.

Branda, C.S., and Dymecki, S.M. (2004). Talking about a revolution: The impact of site-specific recombinases on genetic analyses in mice. Dev Cell *6*, 7-28.

Bronstein, D.M., Schafer, M.K., Watson, S.J., and Akil, H. (1992). Evidence that beta-endorphin is synthesized in cells in the nucleus tractus solitarius: detection of POMC mRNA. Brain Res *587*, 269-275.

Cohen-Cory, S. (2002). The developing synapse: construction and modulation of synaptic structures and circuits. Science *298*, 770-776.

Contreras, R.J., Fox, E., and Drugovich, M.L. (1982). Area postrema lesions produce feeding deficits in the rat: effects of preoperative dieting and 2-deoxy-D-glucose. Physiol Behav *29*, 875-884.

Cossu, G., Cusella-De Angelis, M.G., Senni, M.I., De Angelis, L., Vivarelli, E., Vella, S., Bouche, M., Boitani, C., and Molinaro, M. (1989). Adrenocorticotropin is a specific mitogen for mammalian myogenic cells. Dev Biol *131*, 331-336.

Cowley, M.A., Smart, J.L., Rubinstein, M., Cerdan, M.G., Diano, S., Horvath, T.L., Cone, R.D., and Low, M.J. (2001). Leptin activates anorexigenic POMC neurons through a neural network in the arcuate nucleus. Nature *411*, 480-484.

Crawley, J.N., and Schwaber, J.S. (1983). Nucleus tractus solitarius lesions block the behavioral actions of cholecystokinin. Peptides *4*, 743-747.

Davidson, T.L., Chan, K., Jarrard, L.E., Kanoski, S.E., Clegg, D.J., and Benoit, S.C. (2009). Contributions of the hippocampus and medial prefrontal cortex to energy and body weight regulation. Hippocampus *19*, 235-252.

Doyle, J.P., Dougherty, J.D., Heiman, M., Schmidt, E.F., Stevens, T.R., Ma, G., Bupp, S., Shrestha, P., Shah, R.D., Doughty, M.L.*, et al.* (2008). Application of a translational profiling approach for the comparative analysis of CNS cell types. Cell *135*, 749-762.

Ellacott, K.L., Halatchev, I.G., and Cone, R.D. (2006). Characterization of leptin-responsive neurons in the caudal brainstem. Endocrinology *147*, 3190-3195.

Eriksson, P.S., Hansson, E., and Ronnback, L. (1991). Mu and delta opiate receptors in neuronal and astroglial primary cultures from various regions of the brain--coupling with adenylate cyclase, localisation on the same neurones and association with dopamine (D1) receptor adenylate cyclase. Neuropharmacology *30*, 1233-1239.

Fan, W., Boston, B.A., Kesterson, R.A., Hruby, V.J., and Cone, R.D. (1997). Role of melanocortinergic neurons in feeding and the agouti obesity syndrome. Nature *385*, 165-168.

Forloni, G., Fisone, G., Guaitani, A., Ladinsky, H., and Consolo, S. (1986). Role of the hippocampus in the sex-dependent regulation of eating behavior: studies with kainic acid. Physiol Behav *38*, 321-326.

Grauerholz, B.L., Jacobson, J.D., Handler, M.S., and Millington, W.R. (1998). Detection of pro-opiomelanocortin mRNA in human and rat caudal medulla by RT-PCR. Peptides *19*, 939-948.

Grill, H.J., Schwartz, M.W., Kaplan, J.M., Foxhall, J.S., Breininger, J., and Baskin, D.G. (2002). Evidence that the caudal brainstem is a target for the inhibitory effect of leptin on food intake. Endocrinology *143*, 239-246.

Hatten, M.E., and Heintz, N. (1995). Mechanisms of neural patterning and specification in the developing cerebellum. Annu Rev Neurosci *18*, 385-408.

Hauser, K.F., Stiene-Martin, A., Mattson, M.P., Elde, R.P., Ryan, S.E., and Godleske, C.C. (1996). mu-Opioid receptor-induced Ca2+ mobilization and astroglial development: morphine inhibits DNA synthesis and stimulates cellular hypertrophy through a Ca(2+)-dependent mechanism. Brain Res *720*, 191-203.

Haynes, L.W. (1990). Immunocytochemical detection of beta-endorphin in mouse spinal motoneurons cocultured with astrocytes from spinal cord and forebrain. Mol Chem Neuropathol *12*, 27-35.

Hill, J.W., Elias, C.F., Fukuda, M., Williams, K.W., Berglund, E.D., Holland, W.L., Cho, Y., Chuang, J., Xu, Y., Choi, M.*, et al.* (2010). Direct insulin and leptin action in pro-opiomelanocortin neurons is required for normal glucose homeostasis and fertility. Cell Metabolism *In Press*.

Huo, L., Gamber, K., Greeley, S., Silva, J., Huntoon, N., Leng, X.H., and Bjorbaek, C. (2009). Leptin-dependent control of glucose balance and locomotor activity by POMC neurons. Cell Metab *9*, 537-547.

Huo, L., Grill, H.J., and Bjorbaek, C. (2006). Divergent regulation of proopiomelanocortin neurons by leptin in the nucleus of the solitary tract and in the arcuate hypothalamic nucleus. Diabetes *55*, 567-573.

Huszar, D., Lynch, C.A., Fairchild-Huntress, V., Dunmore, J.H., Fang, Q., Berkemeier, L.R., Gu, W., Kesterson, R.A., Boston, B.A., Cone, R.D.*, et al.* (1997). Targeted disruption of the melanocortin-4 receptor results in obesity in mice. Cell *88*, 131-141.

Ilyinsky, O.B., Kozlova, M.V., Kondrikova, E.S., Kalentchuk, V.U., Titov, M.I., and Bespalova, Z.D. (1987). Effects of opioid peptides and naloxone on nervous tissue in culture. Neuroscience *22*, 719-735.

Isayama, T., McLaughlin, P.J., and Zagon, I.S. (1991). Endogenous opioids regulate cell proliferation in the retina of developing rat. Brain Res *544*, 79-85.

Kanoski, S.E., Hayes, M.R., Greenwald, H.S., Fortin, S.M., Gianessi, C.A., Gilbert, J.R., and Grill, H.J. (2011). Hippocampal leptin signaling reduces food intake and modulates food-related memory processing. Neuropsychopharmacology *36*, 1859-1870.

King, B.M. (2006). The rise, fall, and resurrection of the ventromedial hypothalamus in the regulation of feeding behavior and body weight. Physiol Behav *87*, 221-244.

Knigge, K.M., Joseph, S.A., and Nocton, J. (1981). Topography of the ACTH-immunoreactive neurons in the basal hypothalamus of the rat brain. Brain Res *216*, 333-341.

Lein, E.S., Hawrylycz, M.J., Ao, N., Ayres, M., Bensinger, A., Bernard, A., Boe, A.F., Boguski, M.S., Brockway, K.S., Byrnes, E.J.*, et al.* (2007). Genome-wide atlas of gene expression in the adult mouse brain. Nature *445*, 168-176.

Lindqvist, N., Napankangas, U., Lindblom, J., and Hallbook, F. (2003). Proopiomelanocortin and melanocortin receptors in the adult rat retino-tectal system and their regulation after optic nerve transection. Eur J Pharmacol *482*, 85-94.

Madisen, L., Zwingman, T.A., Sunkin, S.M., Oh, S.W., Zariwala, H.A., Gu, H., Ng, L.L., Palmiter, R.D., Hawrylycz, M.J., Jones, A.R.*, et al.* (2010). A robust and high-throughput Cre reporting and characterization system for the whole mouse brain. Nat Neurosci *13*, 133-140.

Menani, J.V., Colombari, E., Talman, W.T., and Johnson, A.K. (1996). Commissural nucleus of the solitary tract lesions reduce food intake and body weight gain in rats. Brain Res *740*, 102-108.

Mizuno, T.M., and Mobbs, C.V. (1999). Hypothalamic agouti-related protein messenger ribonucleic acid is inhibited by leptin and stimulated by fasting. Endocrinology *140*, 814-817.

Mori, H., Inoki, K., Munzberg, H., Opland, D., Faouzi, M., Villanueva, E.C., Ikenoue, T., Kwiatkowski, D., MacDougald, O.A., Myers, M.G., Jr.*, et al.* (2009). Critical role for hypothalamic mTOR activity in energy balance. Cell Metab *9*, 362-374.

Munzberg, H., Huo, L., Nillni, E.A., Hollenberg, A.N., and Bjorbaek, C. (2003). Role of signal transducer and activator of transcription 3 in regulation of hypothalamic proopiomelanocortin gene expression by leptin. Endocrinology *144*, 2121-2131.

Ollmann, M.M., Wilson, B.D., Yang, Y.K., Kerns, J.A., Chen, Y., Gantz, I., and Barsh, G.S. (1997). Antagonism of central melanocortin receptors in vitro and in vivo by agouti-related protein. Science *278*, 135-138.

Overstreet, L.S., Hentges, S.T., Bumaschny, V.F., de Souza, F.S., Smart, J.L., Santangelo, A.M., Low, M.J., Westbrook, G.L., and Rubinstein, M. (2004). A transgenic marker for newly born granule cells in dentate gyrus. J Neurosci *24*, 3251-3259.

Padilla, S.L., Carmody, J.S., and Zeltser, L.M. (2010). Pomc-expressing progenitors give rise to antagonistic neuronal populations in hypothalamic feeding circuits. Nat Med *16*, 403-405.

Pinto, S., Roseberry, A.G., Liu, H., Diano, S., Shanabrough, M., Cai, X., Friedman, J.M., and Horvath, T.L. (2004). Rapid rewiring of arcuate nucleus feeding circuits by leptin. Science *304*, 110-115.

Ponti, G., Peretto, P., and Bonfanti, L. (2006). A subpial, transitory germinal zone forms chains of neuronal precursors in the rabbit cerebellum. Dev Biol *294*, 168-180.

Ponti, G., Peretto, P., and Bonfanti, L. (2008). Genesis of neuronal and glial progenitors in the cerebellar cortex of peripuberal and adult rabbits. PLoS ONE *3*, e2366.

Prud'homme, M.J., Lacroix, M.C., Badonnel, K., Gougis, S., Baly, C., Salesse, R., and Caillol, M. (2009). Nutritional status modulates behavioural and olfactory bulb Fos responses to isoamyl acetate or food odour in rats: roles of orexins and leptin. Neuroscience *162*, 1287-1298.

Saper, C.B., and Loewy, A.D. (1980). Efferent connections of the parabrachial nucleus in the rat. Brain Res *197*, 291-317.

Satoh, M., and Ide, H. (1987). Melanocyte-stimulating hormone affects melanogenic differentiation of quail neural crest cells in vitro. Dev Biol *119*, 579-586.

Schwartz, M.W., Baskin, D.G., Bukowski, T.R., Kuijper, J.L., Foster, D., Lasser, G., Prunkard, D.E., Porte, D., Jr., Woods, S.C., Seeley, R.J*., et al.* (1996). Specificity of leptin action on elevated blood glucose levels and hypothalamic neuropeptide Y gene expression in ob/ob mice. Diabetes *45*, 531-535.

Schwartz, M.W., Seeley, R.J., Woods, S.C., Weigle, D.S., Campfield, L.A., Burn, P., and Baskin, D.G. (1997). Leptin increases hypothalamic pro-opiomelanocortin mRNA expression in the rostral arcuate nucleus. Diabetes *46*, 2119-2123.

Shen, J., Niijima, A., Tanida, M., Horii, Y., Maeda, K., and Nagai, K. (2005). Olfactory stimulation with scent of grapefruit oil affects autonomic nerves, lipolysis and appetite in rats. Neurosci Lett *380*, 289-294.

Shi, H., Sorrell, J.E., Clegg, D.J., Woods, S.C., and Seeley, R.J. (2010). The roles of leptin receptors on POMC neurons in the regulation of sex-specific energy homeostasis. Physiol Behav *100*, 165-172.

Shin, J.W., Geerling, J.C., and Loewy, A.D. (2008). Inputs to the ventrolateral bed nucleus of the stria terminalis. J Comp Neurol *511*, 628-657.

Solomon, M.B., Jones, K., Packard, B.A., and Herman, J.P. (2010). The medial amygdala modulates body weight but not neuroendocrine responses to chronic stress. J Neuroendocrinol *22*, 13-23.

Soriano, P. (1999). Generalized lacZ expression with the ROSA26 Cre reporter strain. Nat Genet *21*, 70-71.

Tolson, K.P., Gemelli, T., Gautron, L., Elmquist, J.K., Zinn, A.R., and Kublaoui, B.M. (2010). Postnatal Sim1 deficiency causes hyperphagic obesity and reduced Mc4r and oxytocin expression. J Neurosci *30*, 3803-3812.

Turek, F.W., Joshu, C., Kohsaka, A., Lin, E., Ivanova, G., McDearmon, E., Laposky, A., Losee-Olson, S., Easton, A., Jensen, D.R.*, et al.* (2005). Obesity and metabolic syndrome in circadian Clock mutant mice. Science *308*, 1043-1045.

Vernadakis, A., and Kentroti, S. (1990). Opioids influence neurotransmitter phenotypic expression in chick embryonic neuronal cultures. J Neurosci Res *26*, 342-348.

Williams, K.W., Margatho, L.O., Lee, C.E., Choi, M., Lee, S., Scott, M.M., Elias, C.F., and Elmquist, J.K. (2010). Segregation of acute leptin and insulin effects in distinct populations of arcuate proopiomelanocortin neurons. J Neurosci *30*, 2472-2479.

Wolter, H.J. (1984). alpha-melanotropin and beta-endorphin-like immunoreactivities are contained within neurons and nerve fibers of the rat duodenum. Brain Res *295*, 378-384.

Wu, Q., Boyle, M.P., and Palmiter, R.D. (2009). Loss of GABAergic signaling by AgRP neurons to the parabrachial nucleus leads to starvation. Cell *137*, 1225-1234.

Xu, A.W., Kaelin, C.B., Morton, G.J., Ogimoto, K., Stanhope, K., Graham, J., Baskin, D.G., Havel, P., Schwartz, M.W., and Barsh, G.S. (2005). Effects of hypothalamic neurodegeneration on energy balance. PLoS Biol *3*, e415.

Xu, A.W., Ste-Marie, L., Kaelin, C.B., and Barsh, G.S. (2007). Inactivation of signal transducer and activator of transcription 3 in proopiomelanocortin (Pomc) neurons causes decreased pomc expression, mild obesity, and defects in compensatory refeeding. Endocrinology *148*, 72-80.

Yaswen, L., Diehl, N., Brennan, M.B., and Hochgeschwender, U. (1999). Obesity in the mouse model of pro-opiomelanocortin deficiency responds to peripheral melanocortin. Nat Med *5*, 1066-1070.

Yi, C.X., Scherer, T., and Tschop, M.H. (2011). Cajal revisited: does the VMH make us fat? Nat Neurosci *14*, 806-808.

CHAPTER 4: The Role of POMC Processing Products in Hypothalamic Development

Padilla SL, Meece K, Lachance L, Low MJ, Wardlaw SL, Zeltser LM

(Author Contributions: I, SL Padilla, performed experiments, analyzed data, and have worked on this draft with the helpful advice of LM Zeltser; K Meece performed the radioimmunoassays and has provided suggestions for these experiments; L Lachance worked as my summer student and generated expression data and counts contributing to Figure 4.2; MJ Low provided β-*ep*$^{-/-}$ animals and is collaborating on our effort to characterize these embryos, SL Wardlaw helped design the quantitative protein expression studies and has provided many antibodies used in this work; LM Zeltser designed the study.)

Please Note: The majority of studies in this chapter are preliminary

Abstract

Neuropeptide products of the pro-protein POMC are processed and released from neurons in the hypothalamus. In the mature brain, POMC-derived peptides are relayed to downstream targets to influence food intake. In previous studies we have shown that *Pomc* is expressed at high levels in a broad population of hypothalamic precursors during embryogenesis (prior to the establishment of circuits regulating food intake). During development, products of POMC processing are reported to promote differentiation and specification of neurons and glia in extra-hypothalamic regions of the brain. We hypothesize that POMC-derived products influence the ontogeny of feeding centers in ARH. In these studies we find that both α-MSH and β-EP are present during embryogenesis in the MBH and adjacent pituitary anlage. Our current efforts are aimed at determining the influence of these POMC-derived peptides on the establishment of the ARH. Using a genetic loss-of-function strategy we will assess the composition of the ARH in the absence of *Pomc* (*Pomc-GFP;Pomc*$^{-/-}$) and in the absence of *β-ep*$^{-/-}$ alone. As metabolic

baselines are largely determined by orexigenic/anorexigenic tone initiated in the ARH, these findings may provide key targets toward altering body weight homeostasis and combating obesity.

Introduction

Obesity is implicated in the dysregulation of many homeostatic processes that lead to the life threatening complications of diabetes, hypertension, and dyslipidemia (Bjorntorp, 1992). Despite concerted efforts toward dietary intervention, the prevalence of obesity over the past 40 years has increased dramatically (Ogden et al., 2010). There is a large body of evidence to support the idea that the maternal gestational environment can impart lasting effects on metabolic outcomes in offspring. Models of both over- and under- nutrition during pregnancy have been shown to program susceptibility for obesity in offspring (Dabelea et al., 2000; Kral et al., 2006; Silverman et al., 1998). One hypothesis to explain this aspect of maternal programming is that the hypothalamus (a critical determinant of anorexigenic/orexigenic tone) develops in response to the hormonal and nutrient environment during gestation. In support of this, Simerly et al. (2008) find that obesity-prone offspring reared in an obese gestational environment have significantly fewer leptin-sensing cells in the ARH compared to controls (Bouret et al., 2008). We hypothesize that nutrient and hormonal signals specific to the obese gestational environment can influence the establishment of cellular identity during embryogenesis, a consequence that remains intact for the life of the animal. Studies in motor neurons find that the establishment of neurotransmitter identity can be biased during sensitive periods of differentiation, establishing molecular precedence for our hypothesis in the hypothalamus (Root et al., 2008). Terminal fate decisions of neurons in the ARH that mediate energy homeostasis are established during embryogenesis. Previous work from our lab indicates that functionally opposing anorexigenic POMC and a subset of orexigenic neuropeptide-Y/agouti-related peptide (NPY/AgRP) terminal cell fates are derived from a

common progenitor. Thus we hypothesize that the signaling events involved in the differentiation of these two opposing cell types from a common progenitor establish a basis for orexigenic/anorexigenic tone which will determine body weight outcomes, and may explain why some individuals, in the face of a Western type diet (characterized by a dietary pattern rich in fat, sugar, and red meat, but poor in fiber, fruits and vegetables), are programmed to regulate around altered body weight set-points (Fung et al., 2001).

In previous studies we demonstrated that during embryogenesis, *Pomc*-expressing progenitors give rise to functionally distinct neuronal populations, the minority of which maintain a terminal *Pomc*-expressing cell fate (Padilla SL et al. (2011) manuscript in preparation) (Carmody et al., 2010; Padilla et al., 2010). Specifically, we found that during mid-gestation at embryonic day (E) 13.5, *Pomc* is expressed at high levels in most cells of the MBH. From E13.5 through the end of gestation, *Pomc* expression is down-regulated in the majority of these cells, which subsequently differentiate into non-POMC terminal identities (Padilla et al., 2010).

POMC is functionally inert as a pro-peptide. Post-translational processing of POMC into the functional derivatives of the opioid, β-EP and the melanocortin peptides: adrenocorticotropic hormone (ACTH), α-MSH, β-MSH and γ-MSH, occurs in a tissue specific manner (reviewed in: (Wardlaw, 2011)). Developmental expression analyses via immunohistochemistry and quantitative radioimmunoassays have defined the onset of MC peptides to be one of the earliest peptidergic systems in brain. β-EP and ACTH related peptides are, detected as early as E10.5 in the mouse (Angelogianni et al., 2000; Rius et al., 1991b). Along with this, binding studies have shown that both the melanocortin receptors, MC3R and MC4R, and the opioid receptors, μ and κ, are not only expressed, but occupied by ligands in the brain during embryogenesis (Kistler-Heer et al., 1998; Rius et al., 1991a; Tong et al., 2000). It should be noted that the opioid receptor isoforms, μ and κ, are expressed and ligand-occupied as early as E15.5, while

the melanocortin receptors, MC3R and MC4R, are induced later, first detected at E18.5 in the MBH (Rius et al., 1991b).

During embryogenesis, i*n vivo* studies support that opioid ligands, including β-EP, are involved in stimulating neurite outgrowth from neurons in the sympathetic ganglia and spinal cord, and also stimulates proliferation cells of the retina (Ilyinsky et al., 1987; Isayama et al., 1991). MSH variants including α-MSH have also been shown to be involved in neurite outgrowth in retinal ganglion cells (Lindqvist et al., 2003). *In vitro* studies further support that both β-EP and ACTH related peptides can act as trophic factors and are involved in specification of both neurons and astrocytes (Cossu et al., 1989; Eriksson et al., 1991; Hauser et al., 1996; Satoh and Ide, 1987; Vernadakis and Kentroti, 1990). Together, this work supports a role for POMC-derived peptides, prior to circuit formation, in the differentiation and specification of cell types. In the mature brain, hypothalamic derived α-MSH signaling is relayed via axonal projections to distant melanocortin receptors, eliciting an anorexigenic effect with respect to food intake and energy expenditure (Campfield et al., 1995; Fan et al., 1997; Huszar et al., 1997; Yaswen et al., 1999). Neurite outgrowth from neurons in the ARH occurs during perinatal development, while mature projection patterns from the ARH are achieved by postnatal day (P) 18 (Bouret et al., 2004). Because we identify high levels of *Pomc* expression in the MBH during embryogenesis, prior to circuit formation, and because POMC-derived peptides have been shown to participate in differentiation and specification of neurons and glia in extra-hypothalamic regions of the brain, we hypothesize that POMC-derived peptides participate in early developmental events. In this study we will characterize the temporal profile of POMC-derived peptides in the MBH and will also examine the effects of these products on differentiation and cell fate decisions in the mature ARH.

Recent data supports the idea that *Ngn3* is involved in the differentiation of the *Pomc* lineage. Using a genetically null *Ngn3* mouse model, Pelling et al, describe a diminished

number of POMC neurons concomitant with an expansion of both NPY and TH+ cells, such that the total number of ARH neurons was the same (Pelling et al., 2010). This study exemplifies that disruptions during differentiation can affect cell fate choices, which ultimately alter cellular composition of the ARH. We hypothesize that POMC signaling, like Ngn3, will impact the differentiation of cells in the ARH and determine the cellular composition in these offspring.

Results

Ontogeny of POMC-derived Processing Products and Receptors

Because POMC-derived peptides can influence differentiation and specification of extra-hypothalamic cells, and given that *Pomc* is expressed at high levels during embryogenesis in the presumptive MBH, we first developed a strategy to quantify POMC-derived peptides in the MBH across gestation and early postnatal development. In the literature, studies have attempted to quantify products of POMC processing in the MBH during embryogenesis (Kistler-Heer et al., 1998; Rius et al., 1991b). However, *Pomc* is expressed at high levels in both the hypothalamus and adjacent anterior pituitary during embryogenesis (Padilla et al., 2010; Poulin et al., 1997), therefore, it is possible that previously analyzed hypothalamic tissue may have contained *Pomc*-expressing pituitary cells. In this study we have developed a strategy to visually define the hypothalamic/pituitary border using a fluorescent reporter driven off the regulatory elements of *Pomc* (*Pomc-GFP*). This fluorescent marker provides a means to define the hypothalamic/pituitary border, allowing for precise dissection of each region by fluorescent microscopy of whole mount embryos (Figure 4.1) (Cowley et al., 2001).

Hypothalamic and pituitary isolates were analyzed by radioimmunoassay (RIA) for α-MSH and β-EP. In preliminary studies, we observed β-EP protein in the hypothalamus as early as E13.5, but first detected small amounts of αMSH at E16.5 (table 4.1). Efforts to increase numbers and time-points are necessary to achieve statistical significance are underway. We will perform repeated measures at each stage (n≥3 for each stage analyzed), and also expand this

data set to include E11.5–E18.5 for β-EP, E15.5–E18.5 for α-MSH, also including a complete workup from E11.5-E18.5, P9 for ACTH.

These RIA quantification studies will provide a timeline of ligand presence and, in conjunction with similar studies using PCR and IHC for ligand receptors, will serve as the foundation to investigate the role of POMC-derived proteins in differentiation and cell fate determination in ARH neurons. Our data indicating the early detection of β-EP at E13.5 are consistent with literature investigating the onset of opioid system activity in the embryo (Rius et al., 1991b). We determined the expression of one relevant opioid receptor, μ-opioid receptor (MOR), by IHC. Preliminary stains demonstrate a dynamic profile of MOR distribution at: E13.5, E18.5 and in the mature ARH. At E13.5 the staining of MOR appeared to mark narrow fiber-like cells throughout the mantle layer of the ventral hypothalamus and in the proliferating verntricular zone (3V). We did not detect MOR-IR in the MBH at E18.5 (positive staining was identified in the habenular region of the thalamus (data not shown)). In the adult, MOR staining distinctly labeled cell bodies in the ARH and medial VMH (Fig. 4.2). Additional IHC and PCR studies are underway to confirm these findings. Also, we are working to determine the identity of E13.5 MOR-labeled cells, and hypothesize that these cells may be immature glia based on their morphology.

Table 4.1

	Hypothalamus (fmol/MBH)			Pituitary (fmol/pituitary)		
	POMC	αMSH	βEP	POMC	αMSH	βEP
E13.5	**	‡	15.4	**	‡	17.2
E14.5	68.1	‡	8.9	250.4	3.65	71.5
E16.5	15.3	1.7	6.1	374.4	221.6	>294.1
E18.5	59.5	20.8	37.8	2,064.1	743.2	1,746.2
P9	74.8	26.2	55.6	14,011.8	>9,400.0	>17,646.0

Table 4.1. POMC-derived peptides, α-MSH and β-EP are expressed in the hypothalamus and pituitary during embryogenesis. Quantitative analysis of: unprocessed POMC by ELISA and α-MSH and β-EP by RIA in tissue extracts of *Pomc-GFP* transgenic animals. Note: E13.5, 15.5, 18.5, P9 (n=1); E14.5 (n=2). **, has not been analyzed; ‡, sample recording below the level of the curve; **>**, greater than the highest value of the curve

Composition of Neuronal Cell Fates in the ARH

Using a loss-of-function model, we will investigate the effects of POMC and β-EP on the development and establishment of cell populations in the ARH. To facilitate these analyses, we characterized the composition and relationships of the known terminal cell fates in the ARH. Using fluorescent in-situ hybridization (FISH) we characterized the quantity and distribution of: *Pomc*, neuropeptide-Y/agouti-related protein (*Npy/Agrp*), cocaine-amphetamine related transcript (*Cart*), tyrosine hydroxylase (*Th*), growth hormone related hormone (*Ghrh*), gonadotropin-releasing hormone (*Gnrh*), somatostatin (*Sst*), kisspeptin (*Kiss*) and galenin (*Gal*) expressing cells in the ARH (Figure 4.3, Table 4.2). *Kiss* is not included in Table 4.2 because it is expressed at low levels and can only be identified by single process colorimetric ISH. The numbers and distribution patterns found in this data set provide a foundation for which evaluating the influence of POMC processing products on the differentiation of terminal cell fates in the ARH.

Table 4.2

	Npy %N (X)	*Pomc* %P (X)	TH %T (X)	*Sst* %S (X)	*Gal* %G (X)	*Cart* %C (X)	*Ghrh* %Gh (X)
Npy		0.0%		0.0%		0.0%	
Pomc	0.0%		7.0 ± 1.4%	0.0%	30.9 ± 4.4%	37.8 ± 4.3%	0.0%
TH		7.5 ± 1.5%			30.9 ± 4.6%	7.3 ± 1.6%	48.2 ± 9.9%
Sst	0.0%	0.0%					
Gal		2.2 ± 0.8%	13.7 ± 1.6%			8.6 ± 2.6%	
Cart	0.0%	38.9 ± 4.7%	24.1 ± 6.4%		7.1 ± 3.1%		
Ghrh		0.0%	22.8 ± 4.3%				

Table 4.2. Comparative analysis of distinct terminal cell fates in the ARH. Double expression analysis was evaluated and overlapping expression patterns are notated as a percentage of row/column. Deviation is calculated as standard error. Grey boxes; comparison has not been performed.

Developmental Consequences of POMC Loss-of-function

To investigate the roles of POMC-derived products in the differentiation of cell types in the MBH, we will utilize two genetic loss-of-function models targeted to the *Pomc* locus. We have begun to analyze the neuronal phenotypes in the global *Pomc*$^{-/-}$ null animal. To facilitate the visualization of -expressing neurons in the absence of POMC transcript, we crossed both both *Pomc*$^{-/-}$ and β-*Ep*$^{-/-}$ null animals to a *Pomc-GFP* reporter. In a preliminary analysis, we found a nearly three-fold expansion of GFP+ cells in *Pomc*$^{-/-}$*; Pomc-GFP* animals versus controls (Fig. 4.4) (GFP-KO: 57±7, GFP-WT: 24±2) .

We have obtained β-*Ep*$^{-/-}$ null tissue from Malcolm Low and will track the fate of POMC cells using ACTH-IR (Rubinstein et al., 1996)

Working Hypotheses and Future Studies

POMC-derived peptides have been shown to play a role in the differentiation and specification of both neuronal and glial cell fates in the retina and spinal cord (Cossu et al., 1989; Eriksson et al., 1991; Hauser et al., 1996; Ilyinsky et al., 1987; Isayama et al., 1991; Lindqvist et al., 2003; Satoh and Ide, 1987; Vernadakis and Kentroti, 1990). In the ARH,

differentiation and acquisition of terminal fate identity occurs during embryogenesis, while axonal outgrowth and synaptic connectivity are established in the perinatal period (Bouret et al., 2004; Markakis, 2002; Shimada and Nakamura, 1973). In previous work we established that *Pomc* is expressed in most cells of the presumptive ARH at E13.5 and is subsequently down-regulated in the majority of these early progenitors, as the lineage differentiates into distinct terminal identities. In this work we detect immunoreactivity of both β-EP and MOR in the hypothalamus at E13.5 (Table 4.1, Fig. 4.2), and anticipate that this opioid system will influence the differentiation of hypothalamic cells.

Using a combination genetic ablation/reporter strategy (*Pomc*$^{-/-}$*; Pomc-GFP*), we have begun to investigate the influence of POMC-derived proteins on cell fate decisions in the ARH. Primarily we find that *Pomc* expression is not imperative for cellular survival, as we detect GFP+ cells in *Pomc*$^{-/-}$*; Pomc-GFP* tissue (GFP-KO). Next, we demonstrate that GFP-KO cell numbers are approximately 3 times that of *Pomc*-GFP+ cells on a wild-type background (GFP-WT). Considering that the relative area of the ARH is not changed in the null mutant compared to wild-type, we anticipate compensatory alterations in the composition of terminal cell fates in the *Pomc*$^{-/-}$ ARH.

The distribution and number of GFP-KO cells are comparable to those detected in *Pomc* lineage tracing assays (Fig. 4.5) (Padilla et al., 2010). One hypothesis to explain this outcome, is that β-EP acts on *Pomc*-expressing progenitors at E13.5 to direct the differentiation of non-POMC terminal fates. In the absence of this signaling molecule, the *Pomc*-derived lineage may be held in an immature state. To confirm this hypothesis we will need to verify an immature neuronal marker that is present in the immature *Pomc*-expressing population at E13. One potential marker of this population is Doublecortin (DCX), a marker of immature neurons, that is present in the presumptive ARH at E13.5 (Lein et al., 2007). If DCX overlaps a significant population of *Pomc*-expressing cells at E13, then we will perform double IHC/FISH (DCX/*Pomc*)

at E13.5 and will then evaluate DCX relative to the mature GFP KO population by IHC. If DCX co-localizes with all GFP-KO cells in the adult, then we will assume that these cells have not differentiated into a terminal fate and would expect this to come at the consequence of obtaining markers of a terminal identity. In this case, we would expect to find a decrease in the number of NPY/AgRP neurons, as a subset of this population is derived from a *Pomc*-expressing lineage.

It is also possible that the *Pomc*-expressing lineage differentiates into terminal cell fates, but does not inhibit the regulatory elements driving *Pomc*-transcriptional activity upon differentiation. In this case we would expect to see an increase in non-POMC terminal fates derived from a Pomc-expressing lineage (X-POMCs), compensatory to the loss of POMC neurons. This may be reflected in higher NPY numbers, however, approximately 30 percent of the XPOMC population are yet undefined and therefore an increase in these “other” X-POMCs cannot be ruled out in the absence of an NPY phenotype.

While our data supports that POMC-derived proteins influence *Pomc*-expressing lineage, it is also possible that these products influence the differentiation of neighboring cell fates via local diffusion. Using a lineage tracing strategy, we have determined that *Sst*, *Gal*, and *Ghrh*-expressing cells are independent of the *Pomc*-expressing lineage (data not shown). In future studies we will quantify and compare the composition of these terminal cell fates in *Pomc*$^{-/-}$ tissue, compared to Table 4.2.

In vitro studies support that POMC processing products are required for the differentiation of ACTH- and α-MSH-expressing terminal fates and also that opiod peptides, namely β-EP, can inhibit *Pomc* transcription (Daikoku et al., 1983; Hermesz et al., 2003; l'Hereault and Barden, 1991). Consistent with this idea, our data support that β-EP is involved in the down-regulation of *Pomc* transcript. To strengthen this argument we will perform IHC for ACTH on β-*Ep*$^{-/-}$ null embryonic tissue compared to controls (characterizing tissue from E13.5 through E18.5). Because the β-*Ep*$^{-/-}$ specific mutation does not disrupt POMC processing to ACTH/related

products, we can use this expression profile to investigate the effects of β-EP on *Pomc* activity. Furthermore, in previous work we have determined cell counts for *Npy* in the MBH across embryogenesis. We will evaluate this expression profile in *Pomc*$^{-/-}$ and *β-Ep*$^{-/-}$ null animals to get a broad sense of the contribution of α-MSH versus β-EP on differentiation decisions.

In conclusion, we have established a system and developed tools to investigate the influence of POMC-derived peptides on the differentiation of cells in the ARH. Our data so far are consistent with the hypothesis that β-EP influences developmental decisions of *Pomc*-expressing progenitors. In previous studies we have defined that *Pomc*-expressing progenitors differentiate into numerous distinct cell types, two of which are thought to mediate opposing roles in food intake and energy expenditure. Furthermore, we also detect the presence of α-MSH at E15.5, a time in which many terminal identities, including *Npy*, are obtained in the ARH. Finally, both α-MSH and β-EP are implicated in stimulating axonal outgrowth and are in the perinatal ARH when axonal outgrowth occurs. While further experiments are needed, we believe that POMC-derived peptides are critical to the differentiation and specification of cells that determine food intake and energy expenditure in the ARH. Future prospect of this work may reveal pharmacologic targets toward obesity intervention.

Figures

Figure 4.1

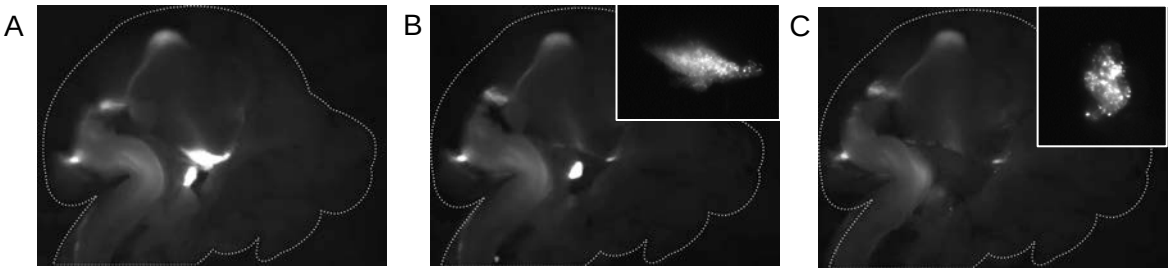

Fig. 4.1. Discrete hypothalamic and pituitary dissections of *Pomc*-GFP reporter tissue at E13.5. (A-C) Whole mount hemisection from the ventricular surface (magnification 1.6X). (A) prior to dissection; (B) post hypothalamic dissection; and (C) following pituitary dissection. All images are presented rostral, right. (B,C) zoom boxes in the top right contain images of the dissected tissue (B) hypothalamus; (C) pituitary.

Figure 4.2

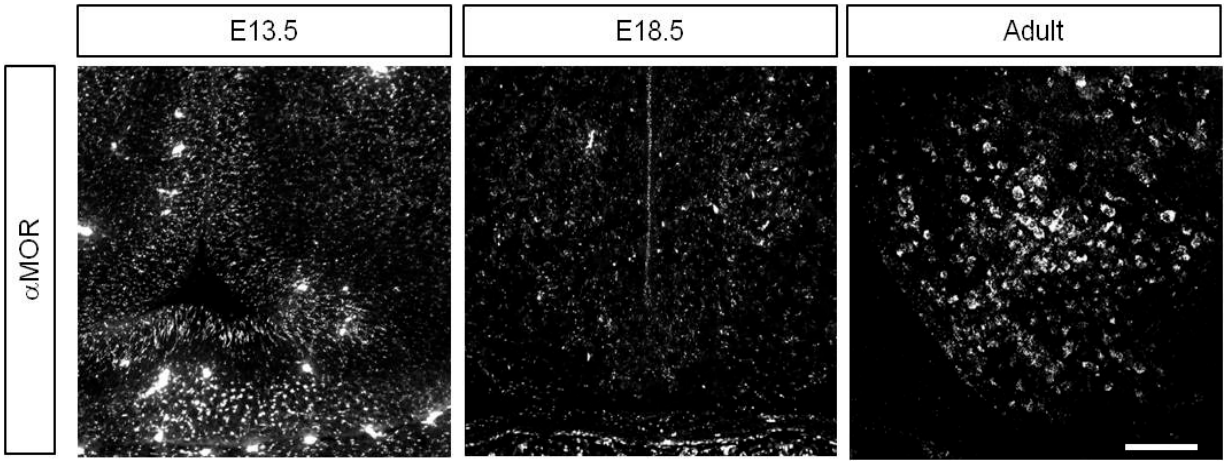

Fig. 4.3. MOR is dynamically expressed during embryogenesis and is subsequently up-regulated in the mature state. MOR-IR performed on wilt-type tissue at: E13.5 (Left), E18.5 (Center) and in the Adult (right). Scale bar: 100 µM; tissue 10 µm cryo-sections; 3V, third ventricle. Note: E13.5 (n=3), E18.5 (n=1), Adult (n=1)

Figure 4.3

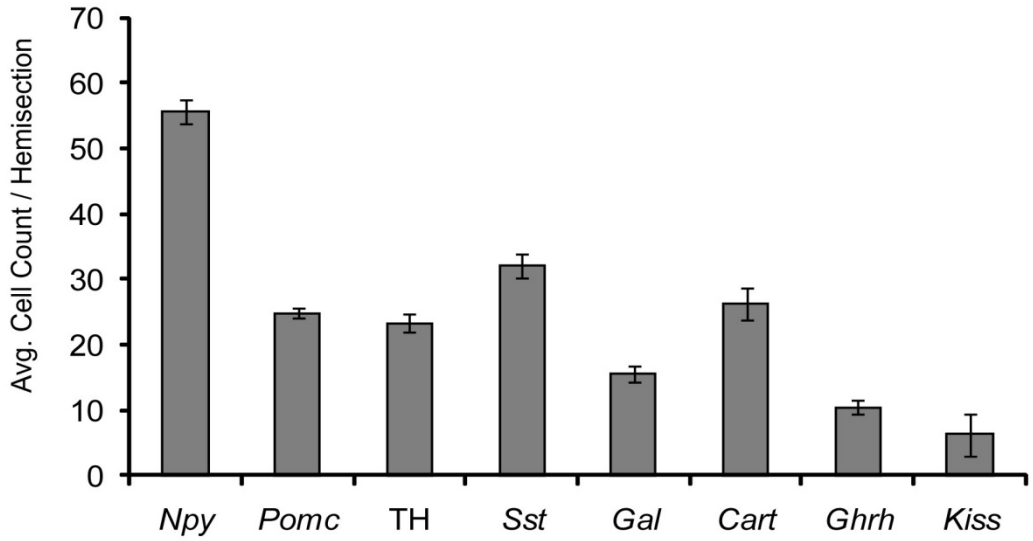

	Npy	Pomc	TH	Sst	Gal	Cart	Ghrh	Kiss
(Percent DAPI count)	24.4	10.8	10.1	14.0	6.8	11.4	4.6	2.7

Fig. 4.3. Relative numbers of distinct terminal cell fates in the ARH. We used FISH to define cells in the ARH that expressed *Npy, Pomc, Sst, Gal, Cart, Ghrh* and *Kiss*. TH was detected by IHC. Single cell counts were qualified by co-locolization with the nuclear marker DAPI. Each group represents the average counts of at least five coronal sections per mouse, spanning the rostrocaudal extent of the ARH (Bregma -1.3 to -2.0). Error bars calculated as standard error of the mean.

Figure 4.4

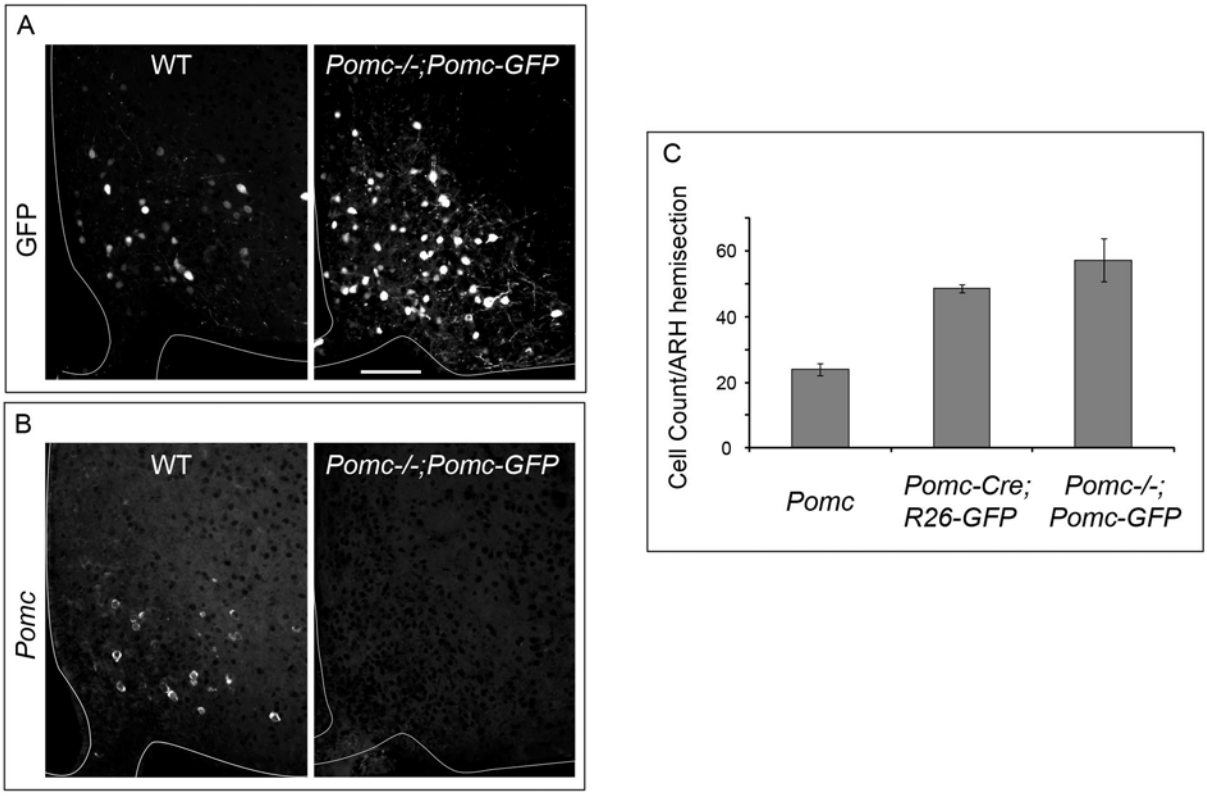

Fig. 4.4. Pomc-expression is not required for the survival of POMC neurons; in the absence of *Pomc* transcript, there is an expansion of the *Pomc-GFP*+ population. (A,B) Histologocial analysis of *Pomc-GFP* (left) versus *Pomc*$^{-/-}$*;Pomc-GFP* (right) tissue. (A) Endogenous GFP expression. (B) *Pomc* expression by FISH. (C) Quantitation of cell numbers (by FISH or endogenous GFP) per ARH hemi-section, averaged across the rostral-caudal extent of the ARH. Scale bar, 100um; error bars calculated as standard deviation; cell counts: *Pomc* (n=20); *Pomc-Cre;R26R-GFP* (n=13); *Pomc*$^{-/-}$*;Pomc-GFP* (n=1; 9 hemisections averaged from one animal)

Methods

Animals

Animals were housed in temperature controlled rooms at 21 °C and subject to a 12 h light-dark cycle. Mice had *ad libitum* access to standard chow diet (Lab Diet: PicoLab Rodent Diet 5053) and water. C57BL/6 mice were obtained from the Jackson Laboratory and bred at the Russ Berrie Animal Facility. *Pomc*-GFP (Cowley et al., 2001) transgenic animals were generously provided by Malcolm Low. All procedures were performed in accordance with the guidelines of the Institutional Animal Care and Use Committee at the Columbia University Health Sciences Division.

Genotyping

Genotyping for GFP was performed using primer set:

Gfp-F 5'-AAGTTC ATCTGCACCACCG-3'

Gfp-R 5'-TCCTTGAAGAAGATGGTGCG-3'

Fluorescent *In Situ* Hybridization

Tissue Processing: FISH: Adult mice were anesthetized and perfused transcardially with 0.9% NaCl followed by 4% paraformaldehyde (PFA) in phosphate buffer (PB). Brains were post-fixed at 4°C overnight and cryoprotected with 30% sucrose for 48 h. For embryonic tissue, dams were anesthetized with Avertin and embryos were dissected in cold PBS and fixed at 4 °C overnight and cryoprotected with 30% sucrose for 24 h. Tissue was embedded in O.C.T (Tissue Tek) and frozen at –80°C. 10 µm-thick coronal sections were collected across the rostral–caudal extent of the ARH on Superfrost Plus slides (Fisher).

FISH: Frozen sections were processed as described in the TSA Plus Cy3 System manual (Perkin Elmer). Antisense digoxigenin-labeled riboprobes were generated for: *Npy*, *Pomc,Th, Sst, Gal, Ghrh, pDny, Cart* using the following primers sets:

Npy-F 5'-TGCTAGGTAACAAGCGAATGG-3'

Npy-R 5’-CAACAACAACAAGGGAAATGG-3

Pomc-F 5’-GTTAAGAGCAGTGACTAAGAGAGGC-3’

Pomc-R 5’-CCTAACACAGGTAACTCTAAGAGGC-3’

Th-F 5’-GATTGCAGAGATTGCCTTCC-3’

Th-R 5’-CCTGTGGGTGGTACCCTATG-3’

Sst-F 5’-GAGGCAAGGAAGATGCTGTC-3’

Sst-R 5’-GGGCCAGGAGTTAAGGAAGA-3’

Gal-F 5’-ATCCTGCACTGACCAGCC-3’

Gal-R 5’-TTGGCTTGAGGAGTTGGC-3’

Ghrh-F 5’-ACAGAGTCCCACCCAGGAGT-3’

Ghrh-R 5’-CAGAGGACGGAAAAGGTCAG-3’

Cart-F 5’-GCTACCTTTGCTGGGTGC-3’

Cart-R 5’-CAACAGGGAAAGAGCCCA-3’

Kiss-F 5’-CTTCCTCCCAGAATGATCTCAA-3’

Kiss-R 5’-CACAAGTCTAGAAGCTCCCTGC-3’

Imaging and Quantification

Fluorescent microscopy was performed using a Nikon Eclipse 80i equipped with a Retiga EXi camera and X cite 120 fluorescent illumination system. TIFF files were acquired using Q Capture Pro software (Qimaging) and analyzed using Adobe Photoshop. We used a diamidino-2-phenylindole (DAPI) stain to establish a reference focal plane. Images were separated into independent RGB channels using Photoshop, and fluorescent signals were compared relative to DAPI (as described in (Padilla et al., 2010)).

GFP fluorescence is lost during the high temperature hybridization step; thus, we pre-imaged direct GFP fluorescence in conjunction with DAPI. Following FISH, the tissue was re-stained with DAPI and imaged. Using Photoshop, pre- and post-FISH images were aligned

using the common DAPI stain as a reference to generate a composite image (as described in (Padilla et al., 2010)).

Immunohistochemistry (IHC)

Fixed slide-mounted sections were blocked in 2% normal horse serum; 0.1% Triton X-100 (Block Buffer) at room temperature. Primary antibody incubation was performed using either mouse anti-TH (1:1000; Chemicon MAB318) or rabbit anti-MOR (1:4000; AbCam ab10275) at 4 °C overnight. Tissue was then washed in PBS and incubated in with secondary using either goat anti-guinea pig Alexa-488 (1;500 invitrogen) or goat anti-rabbit cy5 (1;100 invitrogen), for one hour at room temperature.

Radioimmunoassay (RIA)

Tissue was extracted into 0.1N HCL at 4deg C, homogenized via sonication and the 4K X g supernatant was used for quantitative RIA analysis. Pomc-GFP+ embryos from each litter were pooled for RIA analysis. β-EP and α-MSH antibodies were generated in the Wardlaw laboratory (Jaffe et al., 1994).

References

Angelogianni, P., Li, H.L., and Gianoulakis, C. (2000). Ontogenesis of proopiomelanocortin and its processing to beta-endorphin by the fetal and neonatal rat brain. Neuroendocrinology *72*, 231-241.

Bjorntorp, P. (1992). Abdominal obesity and the metabolic syndrome. Ann Med *24*, 465-468.

Bouret, S.G., Draper, S.J., and Simerly, R.B. (2004). Formation of projection pathways from the arcuate nucleus of the hypothalamus to hypothalamic regions implicated in the neural control of feeding behavior in mice. J Neurosci *24*, 2797-2805.

Bouret, S.G., Gorski, J.N., Patterson, C.M., Chen, S., Levin, B.E., and Simerly, R.B. (2008). Hypothalamic neural projections are permanently disrupted in diet-induced obese rats. Cell Metab *7*, 179-185.

Campfield, L.A., Smith, F.J., Guisez, Y., Devos, R., and Burn, P. (1995). Recombinant mouse OB protein: evidence for a peripheral signal linking adiposity and central neural networks. Science *269*, 546-549.

Carmody, J.S., Wan, P., Accili, D., Zeltser, L.M., and Leibel, R.L. (2010). Respective Contributions of Maternal Insulin Resistance and Diet to Metabolic and Hypothalamic Phenotypes of Progeny. Obesity (Silver Spring).

Cossu, G., Cusella-De Angelis, M.G., Senni, M.I., De Angelis, L., Vivarelli, E., Vella, S., Bouche, M., Boitani, C., and Molinaro, M. (1989). Adrenocorticotropin is a specific mitogen for mammalian myogenic cells. Dev Biol *131*, 331-336.

Cowley, M.A., Smart, J.L., Rubinstein, M., Cerdan, M.G., Diano, S., Horvath, T.L., Cone, R.D., and Low, M.J. (2001). Leptin activates anorexigenic POMC neurons through a neural network in the arcuate nucleus. Nature *411*, 480-484.

Dabelea, D., Knowler, W.C., and Pettitt, D.J. (2000). Effect of diabetes in pregnancy on offspring: follow-up research in the Pima Indians. J Matern Fetal Med *9*, 83-88.

Daikoku, S., Chikamori, M., Adachi, T., Okamura, Y., Nishiyama, T., and Tsuruo, Y. (1983). Ontogenesis of hypothalamic immunoreactive ACTH cells in vivo and in vitro: role of Rathke's pouch. Dev Biol *97*, 81-88.

Eriksson, P.S., Hansson, E., and Ronnback, L. (1991). Mu and delta opiate receptors in neuronal and astroglial primary cultures from various regions of the brain--coupling with adenylate cyclase, localisation on the same neurones and association with dopamine (D1) receptor adenylate cyclase. Neuropharmacology *30*, 1233-1239.

Fan, W., Boston, B.A., Kesterson, R.A., Hruby, V.J., and Cone, R.D. (1997). Role of melanocortinergic neurons in feeding and the agouti obesity syndrome. Nature *385*, 165-168.

Fung, T.T., Rimm, E.B., Spiegelman, D., Rifai, N., Tofler, G.H., Willett, W.C., and Hu, F.B. (2001). Association between dietary patterns and plasma biomarkers of obesity and cardiovascular disease risk. Am J Clin Nutr *73*, 61-67.

Hauser, K.F., Stiene-Martin, A., Mattson, M.P., Elde, R.P., Ryan, S.E., and Godleske, C.C. (1996). mu-Opioid receptor-induced Ca2+ mobilization and astroglial development: morphine inhibits DNA synthesis and stimulates cellular hypertrophy through a Ca(2+)-dependent mechanism. Brain Res *720*, 191-203.

Hermesz, E., Williams-Simons, L., and Mahon, K.A. (2003). A novel inducible element, activated by contact with Rathke's pouch, is present in the regulatory region of the Rpx/Hesx1 homeobox gene. Dev Biol *260*, 68-78.

Huszar, D., Lynch, C.A., Fairchild-Huntress, V., Dunmore, J.H., Fang, Q., Berkemeier, L.R., Gu, W., Kesterson, R.A., Boston, B.A., Cone, R.D*., et al.* (1997). Targeted disruption of the melanocortin-4 receptor results in obesity in mice. Cell *88*, 131-141.

Ilyinsky, O.B., Kozlova, M.V., Kondrikova, E.S., Kalentchuk, V.U., Titov, M.I., and Bespalova, Z.D. (1987). Effects of opioid peptides and naloxone on nervous tissue in culture. Neuroscience *22*, 719-735.

Isayama, T., McLaughlin, P.J., and Zagon, I.S. (1991). Endogenous opioids regulate cell proliferation in the retina of developing rat. Brain Res *544*, 79-85.

Jaffe, S.B., Sobieszczyk, S., and Wardlaw, S.L. (1994). Effect of opioid antagonism on beta-endorphin processing and proopiomelanocortin-peptide release in the hypothalamus. Brain Res *648*, 24-31.

Kistler-Heer, V., Lauber, M.E., and Lichtensteiger, W. (1998). Different developmental patterns of melanocortin MC3 and MC4 receptor mRNA: predominance of Mc4 in fetal rat nervous system. J Neuroendocrinol *10*, 133-146.

Kral, J.G., Biron, S., Simard, S., Hould, F.S., Lebel, S., Marceau, S., and Marceau, P. (2006). Large maternal weight loss from obesity surgery prevents transmission of obesity to children who were followed for 2 to 18 years. Pediatrics *118*, e1644-1649.

l'Hereault, S., and Barden, N. (1991). Regulation of proopiomelanocortin messenger RNA concentrations by opioid peptides in primary cell cultures of rat hypothalamus. Brain Res Mol Brain Res *10*, 115-121.

Lein, E.S., Hawrylycz, M.J., Ao, N., Ayres, M., Bensinger, A., Bernard, A., Boe, A.F., Boguski, M.S., Brockway, K.S., Byrnes, E.J.*, et al.* (2007). Genome-wide atlas of gene expression in the adult mouse brain. Nature *445*, 168-176.

Lindqvist, N., Napankangas, U., Lindblom, J., and Hallbook, F. (2003). Proopiomelanocortin and melanocortin receptors in the adult rat retino-tectal system and their regulation after optic nerve transection. Eur J Pharmacol *482*, 85-94.

Markakis, E.A. (2002). Development of the neuroendocrine hypothalamus. Front Neuroendocrinol *23*, 257-291.

Ogden, C.L., Carroll, M.D., Curtin, L.R., Lamb, M.M., and Flegal, K.M. (2010). Prevalence of high body mass index in US children and adolescents, 2007-2008. Jama *303*, 242-249.

Padilla, S.L., Carmody, J.S., and Zeltser, L.M. (2010). Pomc-expressing progenitors give rise to antagonistic neuronal populations in hypothalamic feeding circuits. Nat Med *16*, 403-405.

Pelling, M., Anthwal, N., McNay, D., Gradwohl, G., Leiter, A.B., Guillemot, F., and Ang, S.L. (2010). Differential requirements for neurogenin 3 in the development of POMC and NPY neurons in the hypothalamus. Dev Biol.

Poulin, G., Turgeon, B., and Drouin, J. (1997). NeuroD1/beta2 contributes to cell-specific transcription of the proopiomelanocortin gene. Mol Cell Biol *17*, 6673-6682.

Rius, R.A., Barg, J., Bem, W.T., Coscia, C.J., and Loh, Y.P. (1991a). The prenatal development profile of expression of opioid peptides and receptors in the mouse brain. Brain Res Dev Brain Res *58*, 237-241.

Rius, R.A., Chikuma, T., and Loh, Y.P. (1991b). Prenatal processing of pro-opiomelanocortin in the brain and pituitary of mouse embryos. Brain Res Dev Brain Res *60*, 179-185.

Root, C.M., Velazquez-Ulloa, N.A., Monsalve, G.C., Minakova, E., and Spitzer, N.C. (2008). Embryonically expressed GABA and glutamate drive electrical activity regulating neurotransmitter specification. J Neurosci *28*, 4777-4784.

Rubinstein, M., Mogil, J.S., Japon, M., Chan, E.C., Allen, R.G., and Low, M.J. (1996). Absence of opioid stress-induced analgesia in mice lacking beta-endorphin by site-directed mutagenesis. Proc Natl Acad Sci U S A *93*, 3995-4000.

Satoh, M., and Ide, H. (1987). Melanocyte-stimulating hormone affects melanogenic differentiation of quail neural crest cells in vitro. Dev Biol *119*, 579-586.

Shimada, M., and Nakamura, T. (1973). Time of neuron origin in mouse hypothalamic nuclei. Exp Neurol *41*, 163-173.

Silverman, B.L., Rizzo, T.A., Cho, N.H., and Metzger, B.E. (1998). Long-term effects of the intrauterine environment. The Northwestern University Diabetes in Pregnancy Center. Diabetes Care *21 Suppl 2*, B142-149.

Tong, Y., Chabot, J.G., Shen, S.H., O'Dowd, B.F., George, S.R., and Quirion, R. (2000). Ontogenic profile of the expression of the mu opioid receptor gene in the rat telencephalon and diencephalon: an in situ hybridization study. J Chem Neuroanat *18*, 209-222.

Vernadakis, A., and Kentroti, S. (1990). Opioids influence neurotransmitter phenotypic expression in chick embryonic neuronal cultures. J Neurosci Res *26*, 342-348.

Wardlaw, S.L. (2011). Hypothalamic proopiomelanocortin processing and the regulation of energy balance. Eur J Pharmacol.

Yaswen, L., Diehl, N., Brennan, M.B., and Hochgeschwender, U. (1999). Obesity in the mouse model of pro-opiomelanocortin deficiency responds to peripheral melanocortin. Nat Med *5*, 1066-1070.

Chapter 5: Concluding Remarks

Neuronal determinants of body weight have largely been investigated in mature organisms with relatively little focus on the developmental establishment of the circuits and signals which mediate this output. While mounting evidence from epidemiological studies support that environmental factors present during development can influence the body weight outcome in individuals (reviewed in: (Grattan, 2008)), little is known regarding the differentiation of cells that mediate metabolic homeostasis. Our studies, focused on defining the ontogeny of two populations in the ARH – orexigenic NPY/AgRP and anorexigenic POMC neurons – that have been described to inversely modulate energy homeostasis. Unexpectedly, we found that *Pomc* was expressed in the majority of cells of the mediobasal hypothalamus during mid-gestation and was subsequently down-regulated during later stages of development. Using a genetic tracing technique (*Pomc-Cre;R26R-reporter*), we went on to show that in the ARH, along with other regions of the brain, *Pomc* is transiently expressed in many immature cells which ultimately differentiate into non-POMC terminal identities, some of which include NPY/AgRP neurons in the ARH.

These preliminary findings raise the possibility that developmental events can influence cell fate decisions in the hypothalamus. For example, if the immature *Pomc*-expressing population is homogeneous and gives rise to numerous cell fates based in extrinsic signaling factors, then it is possible that environmental factors present during gestation may influence the composition of many cell fates throughout the brain (cells derived from *Pomc*-expressing precursors). Because we find that both POMC and a subset of NPY/AgRP neurons contain the *Pomc*-Cre reporter signal, it is possible that both populations are derived from an immature *Pomc*-expressing precursor. In this case, it is intriguing to consider that this node of differentiation may be vulnerable to environmental factors during development, and as such, immature *Pomc*-expressing cells may provide a target to further investigate the mechanisms by which maternal

factors during gestation can influence cell fate decisions. While these preliminary findings are intriguing and have been at the forefront of discussion in the field, reviewed as a “must read” by the Faculty of 1000, this work is only the beginning of our lab’s efforts to define the differentiation of ARH populations. Important to the interpretation of our results thus far, is whether immature *Pomc*-expressing cells are homogeneous, or if *Pomc* is transiently expressed in many lineages (representative models presented in Figure 5.1)

Figure 5.1

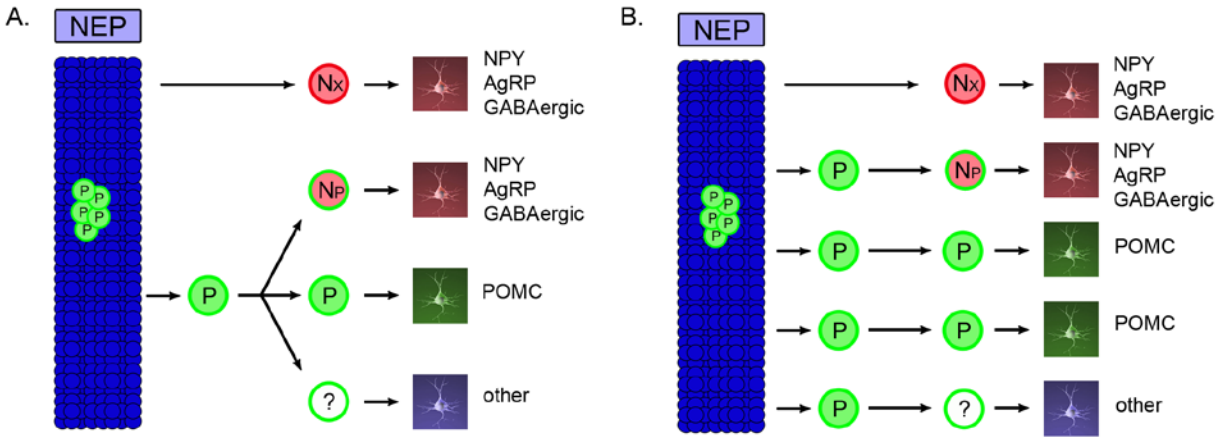

Fig. 5.1. Modeling *Pomc* progenitor Specification. Abbreviations: NEP, neural epithelial progenitor; N_P, NPY neurons derived from a *Pomc* progenitor; N_X, NPY neurons derived from a non-*Pomc* progenitor; P, POMC neurons; ?, yet undefined cell type.

ARH lineages: transcription factor screen

Our data in Appendix A support that POMC neurons in the ARH share a common lineage with other ARH cell types – potentially including NPY/AgRP. In this study, we performed a screen for lineage markers of NPY and POMC neurons in the ARH. Of 29 transcription factor candidates, none mapped exclusively to either *Pomc*- or *Npy*-expressing cells (Table A.1). Instead, the candidate lineage markers mapped to either all POMC/NPY cells plus other ARH cells, or were present in a subset of POMC/NPY cells plus other ARH cells. For instance, within POMC neurons, the transcription factors: *Tbx3*, *Peg3*, *Otp* and *Fto* were present in all POMC neurons along with other cell types in the ARH. These data are consistent with **model A**, a

scenario in which POMC neurons are derived from a multipotent immature precursor which differentiates into numerous terminal fates, including POMC.

In addition, we found that the candidate lineage markers: *Dlx6*, *Elk1*, *Er81*, *Lhx9*, *Lrrn3*, *Nhlh2* and *Tbx19* were co-expressed in a subset of POMC neurons along with other cell types in the ARH. Candidate markers present in subsets of POMC plus other ARH cells, raise the possibility that more than one progenitor cell type gives rise to a POMC terminal fate, as depicted in **model B**; however, this data also supports our findings above, that immature neurons of a POMC lineage are multipotent. Unlike the candidate lineage model discussed previously, in this model, a multipotent immature neuron differentiates into a limited subset of POMC neurons plus other cell types in the ARH.

Based on our lineage screen and *Pomc*-Cre reporter studies, we hypothesized that some NPY/AgRP neurons may be derived from a common progenitor as a subset of POMC neurons (Table A.1, Fig. 2.2). This concept of a common progenitor giving rise to numerous ARH cell types, some of which may be functionally opposing, lends to the potential that environmental factors during development can bias differentiation events and may influence the anorexigenic tone in the ARH. It is important to note that our candidate transcription factor screen was performed at P7 and validated in the mature ARH. We have yet to map our lineage candidates in the embryo, and therefore cannot conclude on how these markers relate to early *Pomc*- or *Npy*-expressing populations. To further elucidate the diagram of POMC lineages, our future studies will evaluate our candidate markers relative to *Pomc* and *Npy* across development.

Timing

In order to examine how cell fate decisions may influence the physiological outcomes in mature organisms, it is important to define the timing and signaling factors involved in these processes. As a first step, we performed stereological corrections on our previous analysis of

Pomc-expressing cells during embryogenesis to identify critical temporal periods of development in which *Pomc* is transcriptionally down-regulated.

Since the publication of our data in Chapter 2, we have investigated the stereology of the mediobasal hypothalamus during embryogenesis, finding that the area of the presumptive ARH undergoes a general expansion between E14.5 and E15.5, and subsequently remains constant through birth (stereologically corrected counts: Fig. 5.3). Upon correction, the largest decline in the number of *Pomc*-expressing cells occurs between E13.5 and E14.5, with another smaller decline in cell number between E17.5 and E18.5 (Fig. 5.2 A). These two time windows during embryogenesis represent changes in the differentiation of immature *Pomc*-expressing neurons; however, it is also important to consider that numerous lineages may contain an early transient *Pomc*-expressing state, and also that changes may occur independent to the dramatic changes in *Pomc* transcription.

Figure 5.2

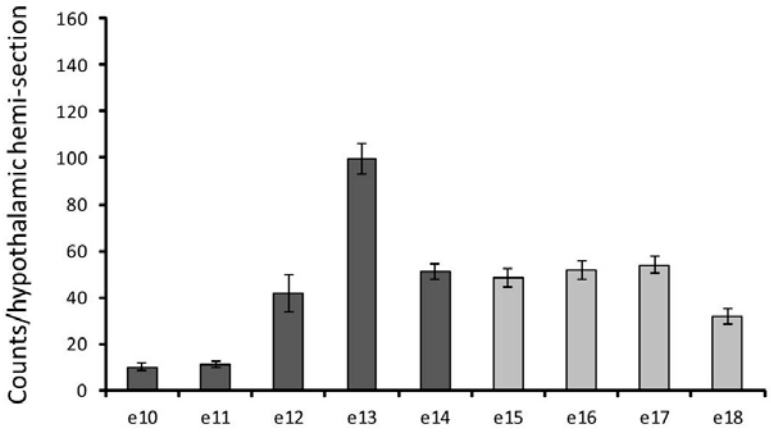

Fig. 5.2 *Pomc*-expressing cell count during embryogenesis with stereologic correction. The total area of the ARH undergoes a 22 percent expansion at E15. Cell numbers prior to this stage have been corrected, represented as 22 percent less than the original counts. *Pomc*-expressing cells detected by FISH were qualified by co-expression of the nuclear marker DAPI.

Terminal cell fates in the ARH

In Chapter 2 we demonstrated that the majority of both POMC and NPY/AgRP exit mitosis between E11-E12 (Fig. 2.1). We also determined that the number of *Npy*- and *Pomc*-

expressing cells at E18 was similar to that of the adult. This data may indicate that differentiation events of these cell types occur during the last week of gestation, however, it is important to consider that many terminal markers indicative of these terminal cell fates are not expressed until postnatal stages including: *Agrp*, *Cart* and letpin induced PSTAT3 (Ahima et al., 1998; Cottrell et al., 2009; Nilsson et al., 2005). Given this, differentiation of immature cells may also be susceptible to bias during the acquisition of a terminal fate in the postnatal period.

Numerous studies in the recent literature indicate that POMC neurons in the ARH are not homogenous. These studies determined heterogeneity among mature POMC neurons in an electorphysiologic response with respect to: leptin, insulin, glucose and also within expression of GABA and glutamate (Hentges et al., 2009; Ibrahim et al., 2003; Munzberg et al., 2003; Parton et al., 2007; Williams et al., 2010). In conjunction with this, we have determined that *Cart* is expressed in a subset of POMC neurons (Fig 5.2). These findings support that mature *Pomc*-expressing neurons are not homogeneous in function. In future studies we will map markers of these functional subsets to our lineage candidates to further elucidate terminal characteristics of each lineage within the ARH.

Figure 5.3

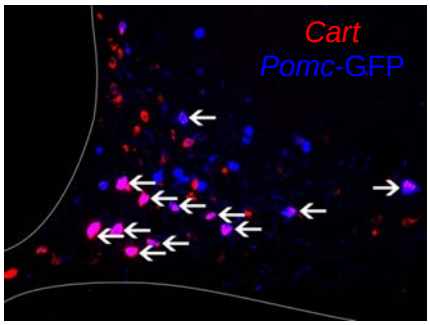

Fig. 5.3. *Cart* is expressed in a subset of POMC neurons. Representative ARH from *Pomc*-GFP reporter transgenic evaluated for *Cart* by FISH (red). Arrows indicate double positive GFP/Cart cells.

Progenitor fate: exogenous factors biasing orexigenic tone

Recent data in the literature demonstrate that the maternal environment can influence the differentiation of *Pomc* progenitors, a consequence that may impart body weight outcomes in exposed offspring. Below are three examples highlighting composition changes in the ARH at various stages of development when exposed to a particular maternal environment. These studies further allude to critical time windows and also implicate candidate signaling factors involved in the differentiation of ARH lineages, implicating candidate extrinsic signaling factors that may influence the developing: progenitor population, early differentiating cells and also the later stages of acquiring a terminal cell fate in the ARH.

Unpublished research from the Bouret lab has demonstrated that the maternal environment can influence progenitor proliferation in the mediobasal hypothalamus, a consequence which correlates to an alteration in the composition of cells in the mature ARH. Specifically, they determined that developing *ob/ob* animals, lacking intrinsic leptin, have increased cellular proliferation during embryogenesis and also found that these animals have statistically more NPY/AgRP and concomitantly less POMC neurons in the mature ARH (personal communication of unpublished data). Because *ob/ob* animals are largely infertile, these offspring were bred from pairs of heterozygous (*ob/*+) parents. Dams heterozygous at the leptin allele have: slightly more body fat, are hypoleptinemic relative to adiposity, are hyperglycemic and also hyperinsulimenic (Chung et al., 1998; Flatt and Bailey, 1981). Given this, it is possible that the altered nutrient and hormonal factors present in *ob/*+ dams during gestation and lactation influence the differentiation of hypothalamic progenitors.

In addition to this work, Pelling et al. (2010) investigated the fate of *Ngn3* descendent cell types in the ARH and found that the expression of this transcription factor can influence the composition of postmitotic cells during embryogenesis. They demonstrated that *Ngn3* null animals (*Ngn3*$^{-/-}$) had a reduced number of *Pomc*-expressing cells during embryogenesis (E10-

E17), accompanied by compensatory expansion of NPY and TH immunoreactive (IR) cells (Pelling et al., 2010). Because the number of NPY and TH IR cells was directly proportional to the loss of *Pomc*+ cells, it is possible that these cell types share a common *Ngn3*+ progenitor.

This study supports the idea that multiple progenitors give rise to postmitotic *Pomc*-expressing cell types of the hypothalamic parenchyma. Pelling et al. detect a reduction in only a subset of *Pomc*-expressing cells, suggesting that only a subset of the population is derived from an *Ngn3*+ progenitor. Furthermore, using an *Ngn3*-Cre reporter strategy, that determined that at E10 nearly all *Pomc*-expressing progenitor cells in the ventricular zone co-expressed the *Ngn3*-Cre reporter, while at E15 the reporter was only present in a subset of cells. This data supports the idea that non-*Pomc*-expressing progenitors can give rise to postmitotic cells which later obtain a *Pomc* transcriptional identity, further supporting the idea that *Pomc* is not a lineage marker, but rather, is transiently expressed in numerous hypothalamic lineages throughout development. The *Ngn3*-Cre reporter was also detected in a subset of *Npy*-expressing cells at E15. Given the proportional changes in Npy-expressing cell counts in the absence of *Ngn3*, and also given that we detected *Pomc*-Cre reporter in a subset of NPY/AgRP neurons, it is possible that some *Pomc*-expressing *Ngn3*+ cells in the ventricular zone at E10 differentiate into an *Npy*-expressing fate.

Due to perinatal lethality, the consequences of a loss of *Ngn3* on the ultimate composition of the ARH and its effects on energy homeostasis were not achieved. Unfortunately, this study was also terminated prior to the acquisition of terminal functional capacity (e.g. leptin sensing and/or *Cart* expression) and therefore does not specifically address the impact of *Ngn3* on mature POMC neurons. Considering the transient and likely multipotent nature of *Pomc* expressing cells during embryogenesis, it is possible that the early loss of *Pomc*+ cells in the absence of *Ngn3* will not predict the outcome of mature POMC neurons. In the future it would be interesting to conditionally target an *Ngn3* knock-out to the hypothalamus using *Nkx2.1*-Cre

(hypothalamic specific, (Xu et al., 2008)) crossed to *Ngn3*$^{fl/fl}$. Because the perinatal lethality due the global loss of *Ngn3* is likely due to misspecification of pancreatic progenitors (Apelqvist et al., 1999), this proposed hypothalamic specific deletion will likely result in viable animals, providing a means to evaluate the consequent composition of terminal fates in the ARH, along with evaluating the body composition phenotype in the absence of *Ngn3* in the hypothalamus.

Finally, in a model of maternal hyperinsulinemia, JS Carmody et al. (2010) investigated the ontogeny of hypothalamic cell fates and determined that the maternal environment can influence the acquisition of terminal cell fates in offspring. In this study, they identified more *Pomc*+ cells at P0, which reached statistical significance at P9. No changes were detected in the number of *Pomc* or *Npy*+ cells at E14 – a candidate phase of *Pomc* progenitor differentiation (Carmody et al., 2010). In conjunction with fewer *Pomc*+ cells in the postnatal period, there was a compensatory trend toward more *Npy*+ cells. This trend did not reach statistical significance in this study, however considering the possibility that that the increase in *Npy*+ cells occured in direct proportion to the decrease in *Pomc*+ counts, and that the number of *Npy*+ cells in the ARH is nearly double that of POMC neurons, this trend would not achieve significance within the number of animals tested in this study. This data supports the idea that maternal insulin may influence differentiation during later stages of gestation, but does not have an effect prior to E14. In conclusion, Carmody et al. argued that developmental alterations in the *Pomc*-expressing population during perinatal development provided adaptive response to the nutrient enriched environment, protecting the offspring from alterations in body weight, because unlike maternal obesity, isolated hyperinsulinemia did not confer a body weight phenotype in exposed offspring. This study did not consider the heterogeneity among POMC neurons, but it is also possible that composition of functional POMC subsets (introduced earlier in this discussion) is biased in exposed offspring.

POMC during development:

In the adult, POMC signaling is an integral component of circuits that mediate energy expenditure; however in the embryo, POMC signaling is thought to play a trophic role. During development, opioids, including β-endorphin (β-EP) and adrenocorticotropic hormone (ACTH) derived peptides, including α-melanocyte stimulating hormone (α-MSH), can influence the differentiation and specification of both neuronal and glial identity in aspects of the retina and spinal cord (Cossu et al., 1989; Eriksson et al., 1991; Hauser et al., 1996; Ilyinsky et al., 1987; Isayama et al., 1991; Lindqvist et al., 2003; Satoh and Ide, 1987; Vernadakis and Kentroti, 1990). Considering that most terminal cell fate decisions in the ARH are determined during embryogenesis, and also that high levels of *Pomc* transcript are present in the presumptive ARH during mid-gestation (Fig. 2.1 d,f), we hypothesized that POMC-derived protein was involved in the acquisition of terminal cell fates in the hypothalamus. In a preliminary data set we detected both β-EP and α-MSH in the MBH during embryogenesis (Table 4.1). Furthermore, using a genetic loss-of-function allele (*Pomc*$^{-/-}$) crossed to a transgenic reporter (*Pomc-GFP*), we determined first, that *Pomc* transcription was not necessary for the survival of this cell population, and second, that POMC-derived protein can dramatically influence differentiation amongst the *Pomc*-expressing lineage (Fig. 4.4). In the absence of POMC-derived protein, the *Pomc*-GFP population expanded 3-fold in cell count, a change that was not accompanied by a significant alteration in cell number or area of the ARH. We are currently working to further define the compensatory changes which account for the missing POMC neurons and also are working to determine the distinct POMC-derived processing products involved in these differentiation events. The details of these efforts are described in chapter 4: “Working Hypothesis and Future Studies.”

Future directions

Given the above arguments, it is likely that some NPY neurons are derived from a *Pomc* precursor and may also share a common lineage with some or all POMC neurons. We detected *Pomc*-Cre mediated reporter expression in a subset of ARH NPY neurons and have subsequently characterized that this *Pomc* derived NPY (NPY_P) subset also expresses markers involved in orexigenic signaling including: *Agrp* and *Gad65/67*. Distinctions within the NPY_P may involve projection patterns and/or the expression of alternative functional genes. In order to define molecular markers to distinguish NPY_P we will use a micro-array strategy of FACS purified fluorescent cells from: *Npy-GFP;Pomc-CRE;R26R-TOM* and Pomc-GFP. *Npy-GFP;Pomc-CRE;R26R-TOM* bisgenic tissue will provide a means to isolate NPY neurons [GFP+] from NPY_P [GFP+/TOM+]. Micro array analysis of extracted RNA from these isolates should indicate the intrinsic differences between NPY_P versus NPY_X providing markers to further investigate the physiologic contribution of these subsets. Within these studies we will also collect the TOM alone fraction, representing non-NPY cells derived from a *Pomc* lineage in the MBH. We expect this fraction to contain both POMC neurons and also the 'other' yet undefined X-POMC populations. To obtain molecular distinction of X-POMCs from POMC neurons, we will compare the isolated TOM+ population to GFP+ cells collected from *Pomc*-GFP transgenic animals at the same age. Efforts are currently underway to collect these FACS isolates for the prospective comparative microarrays. It is important to note that neurite outgrowth from the soma prevents successful dissociation of live cells in primary culture. To avoid this, the studies mentioned above are performed at P9, a developmental state which is indicative of the mature neuronal profile, yet prior to axonal outgrowth. Our data from these arrays should help to determine: molecular markers for the subset NPY_P neurons, distinguish functional markers and neurotransmitter profile in the yet undefined X-POMC population and

also to determine the degree to which NPY_P and NPY_X are related along with the relationship between *Pomc*-GFP and X-POMC neurons.

Conclusion

In this discussion POMC signaling has been demonstrated to play a distinct functional role depending on maturation state of the cell. In the mature ARH POMC neurons produce the anorexigenic neuropeptide αMSH, which when transmitted to downstream MC circuits regulate appetite and energy expenditure. During development however, POMC processing products have been demonstrated to act as trophic factors. Our preliminary studies are consistent with the model that there is heterogeneity among progenitors that give rise to *Pomc*-expressing cells in the embryo and in the adult. While our data support that a common multipotent immature cell likely gives rise to numerous cell types in the ARH, some of which may be functionally opposing, we believe that it is unlikely that *Pomc* expression during embryogenesis is restricted to one specific lineage. In this case, *Pomc* expression in immature neurons likely acts as a differentiation signal to certain regions of the brain (Table 3.1), and not as a bona fide lineage marker for POMC neurons.

Ongoing studies in the lab are aimed at developing new tools to investigate lineages in the ARH, and to characterize critical time windows for differentiation events. We have mapped both candidate lineage markers and also functional markers relative to POMC and NPY in the ARH (Table A.1 and 4.2). Sorting studies outlined above will likely identify additional markers. Each candidate marker will need to be validated based on expression pattern of the transcript of interest in both the embryo and in the mature ARH. Co-expression analysis will then be performed relative to POMC, NPY/AgRP and leptin-sensing neurons in the adult.

Consistent with previously published reports, we find that following a fast challenge and IP leptin bolus, PSTAT3 (an indicator of leptin signal transduction) immunoreactivity is co-expressed in subsets of NPY/AgRP and POMC neurons, along with marking other cell in the

ARH (Fig. 5.4 A) (Cowley et al., 2001; Hill et al., 2010). Many of our candidate lineage marker expression profiles demonstrate a similar distribution; namely: *Dlx6*, *Elk1*, *Lhx9*, *Nhlh2* and *Tbx19*. While we have not yet evaluated these markers relative to the PSTAT3 population, there is a possibility that the leptin sensing ARH terminal cell fate arises from a common lineage. Given that the profile of PSTAT3 matches many of our lineage candidates, is possible that the leptin sensing terminal fate in the ARH is derived from a common lineage; fitting the model that subsets of POMC and NPY/AgRP have a common progenitor (Fig 5.4 B).

There is evidence in the literature to support that the maternal nutrient environment can influence the ontogeny of leptin-sensing cells in the ARH. Polygenetic DIO animals are predisposed to obesity when exposed to a HFD (Levin et al., 1997). Offspring of obese DIO dams reared on a HFD, develop obesity when fed a chow diet (Levin and Govek, 1998). Using this model, Simerly and Bouret have shown that such obesity-prone offspring have fewer leptin-sensing neurons in the ARH compared to controls (Bouret et al., 2008). Because AgRP and a subset of POMC neurons are leptin-sensing, we anticipate that the composition of these two populations may be biased in this model and thus the lineage giving rise to the leptin-sensing terminal identity may be of critical importance to the composition of ARH neurons.

In conclusion, it is likely that *Pomc* expression in the embryo plays a functional role in the proliferation and differentiation of ARH cell types. We are pursuing these possibilities as noted in Chapter 4 using a *Pomc*$^{-/-}$ model. Along with this, data has shown that POMC neurons in the ARH differ in many physiologic properties; it is likely that some of these subsets are derived from unique progenitor pools. Findings in the recent literature support to idea that subsets of POMC and NPY/AgRP neurons are derived from a common lineage, and also that the maternal nutrient environment can influence this common progenitor to bias the establishment of orexigenic tone in the ARH ((Carmody et al., 2010; Pelling et al., 2010), and Bouret unpublished). Utilizing reagents and techniques to map various functional and lineage markers

to *Pomc* and *Npy*-expressing populations in the mature ARH, should provide useful to resolve a conclusive model depicting the ontogeny of cell types in the ARH. These studies provide a critical foundation for efforts to understand how the maternal environment can influence hypothalamic development and program offspring toward phenotypes related to body weight.

Figure 5.4

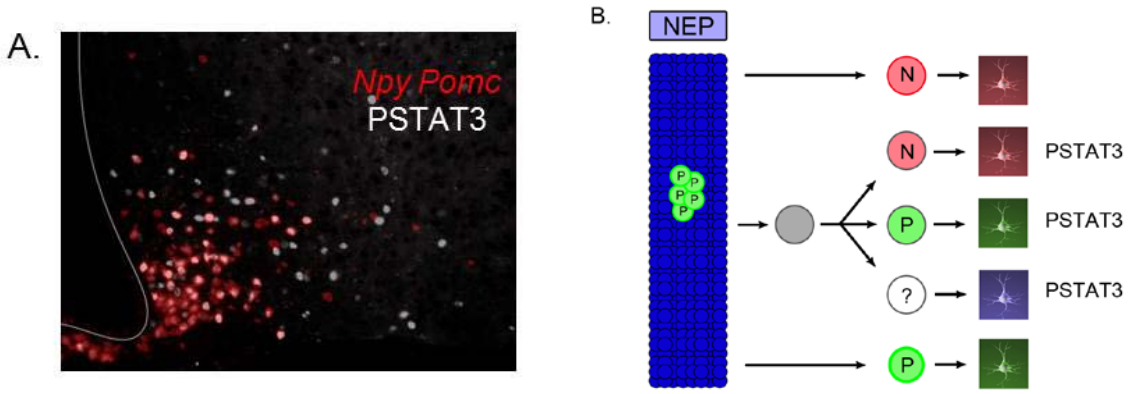

Fig. 5.4. Candidate lineage of a leptin-sensing ARH terminal fate. (A) Double FISH/IHC against *Pomc/Npy* (red) and PSTAT3 (white); note independent populations of both red and white exist in the ARH. (B) Theoretical model. Abbreviations: N, NPY neurons; P, POMC neurons; ?, yet undefined cell type.

References

Ahima, R.S., Prabakaran, D., and Flier, J.S. (1998). Postnatal leptin surge and regulation of circadian rhythm of leptin by feeding. Implications for energy homeostasis and neuroendocrine function. The Journal of clinical investigation *101*, 1020-1027.

Apelqvist, A., Li, H., Sommer, L., Beatus, P., Anderson, D.J., Honjo, T., Hrabe de Angelis, M., Lendahl, U., and Edlund, H. (1999). Notch signalling controls pancreatic cell differentiation. Nature *400*, 877-881.

Bouret, S.G., Gorski, J.N., Patterson, C.M., Chen, S., Levin, B.E., and Simerly, R.B. (2008). Hypothalamic neural projections are permanently disrupted in diet-induced obese rats. Cell Metab *7*, 179-185.

Carmody, J.S., Wan, P., Accili, D., Zeltser, L.M., and Leibel, R.L. (2010). Respective Contributions of Maternal Insulin Resistance and Diet to Metabolic and Hypothalamic Phenotypes of Progeny. Obesity (Silver Spring).

Chung, W.K., Belfi, K., Chua, M., Wiley, J., Mackintosh, R., Nicolson, M., Boozer, C.N., and Leibel, R.L. (1998). Heterozygosity for Lep(ob) or Lep(rdb) affects body composition and leptin homeostasis in adult mice. Am J Physiol *274*, R985-990.

Cossu, G., Cusella-De Angelis, M.G., Senni, M.I., De Angelis, L., Vivarelli, E., Vella, S., Bouche, M., Boitani, C., and Molinaro, M. (1989). Adrenocorticotropin is a specific mitogen for mammalian myogenic cells. Dev Biol *131*, 331-336.

Cottrell, E.C., Cripps, R.L., Duncan, J.S., Barrett, P., Mercer, J.G., Herwig, A., and Ozanne, S.E. (2009). Developmental changes in hypothalamic leptin receptor: relationship with the postnatal leptin surge and energy balance neuropeptides in the postnatal rat. Am J Physiol Regul Integr Comp Physiol *296*, R631-639.

Cowley, M.A., Smart, J.L., Rubinstein, M., Cerdan, M.G., Diano, S., Horvath, T.L., Cone, R.D., and Low, M.J. (2001). Leptin activates anorexigenic POMC neurons through a neural network in the arcuate nucleus. Nature *411*, 480-484.

Eriksson, P.S., Hansson, E., and Ronnback, L. (1991). Mu and delta opiate receptors in neuronal and astroglial primary cultures from various regions of the brain--coupling with adenylate cyclase, localisation on the same neurones and association with dopamine (D1) receptor adenylate cyclase. Neuropharmacology *30*, 1233-1239.

Flatt, P.R., and Bailey, C.J. (1981). Abnormal plasma glucose and insulin responses in heterozygous lean (ob/+) mice. Diabetologia *20*, 573-577.
Grattan, D.R. (2008). Fetal programming from maternal obesity: eating too much for two? Endocrinology *149*, 5345-5347.

Hauser, K.F., Stiene-Martin, A., Mattson, M.P., Elde, R.P., Ryan, S.E., and Godleske, C.C. (1996). mu-Opioid receptor-induced Ca2+ mobilization and astroglial development: morphine inhibits DNA synthesis and stimulates cellular hypertrophy through a Ca(2+)-dependent mechanism. Brain Res *720*, 191-203.

Hentges, S.T., Otero-Corchon, V., Pennock, R.L., King, C.M., and Low, M.J. (2009). Proopiomelanocortin expression in both GABA and glutamate neurons. J Neurosci *29*, 13684-13690.

Hill, J.W., Elias, C.F., Fukuda, M., Williams, K.W., Berglund, E.D., Holland, W.L., Cho, Y., Chuang, J., Xu, Y., Choi, M.*, et al.* (2010). Direct insulin and leptin action in pro-opiomelanocortin neurons is required for normal glucose homeostasis and fertility. Cell Metabolism *In Press*.

Ibrahim, N., Bosch, M.A., Smart, J.L., Qiu, J., Rubinstein, M., Ronnekleiv, O.K., Low, M.J., and Kelly, M.J. (2003). Hypothalamic proopiomelanocortin neurons are glucose responsive and express K(ATP) channels. Endocrinology *144*, 1331-1340.

Ilyinsky, O.B., Kozlova, M.V., Kondrikova, E.S., Kalentchuk, V.U., Titov, M.I., and Bespalova, Z.D. (1987). Effects of opioid peptides and naloxone on nervous tissue in culture. Neuroscience *22*, 719-735.

Isayama, T., McLaughlin, P.J., and Zagon, I.S. (1991). Endogenous opioids regulate cell proliferation in the retina of developing rat. Brain Res *544*, 79-85.

Levin, B.E., Dunn-Meynell, A.A., Balkan, B., and Keesey, R.E. (1997). Selective breeding for diet-induced obesity and resistance in Sprague-Dawley rats. Am J Physiol *273*, R725-730.
Levin, B.E., and Govek, E. (1998). Gestational obesity accentuates obesity in obesity-prone progeny. Am J Physiol *275*, R1374-1379.

Lindqvist, N., Napankangas, U., Lindblom, J., and Hallbook, F. (2003). Proopiomelanocortin and melanocortin receptors in the adult rat retino-tectal system and their regulation after optic nerve transection. Eur J Pharmacol *482*, 85-94.

Munzberg, H., Huo, L., Nillni, E.A., Hollenberg, A.N., and Bjorbaek, C. (2003). Role of signal transducer and activator of transcription 3 in regulation of hypothalamic proopiomelanocortin gene expression by leptin. Endocrinology *144*, 2121-2131.

Nilsson, I., Johansen, J.E., Schalling, M., Hokfelt, T., and Fetissov, S.O. (2005). Maturation of the hypothalamic arcuate agouti-related protein system during postnatal development in the mouse. Brain Res Dev Brain Res *155*, 147-154.

Parton, L.E., Ye, C.P., Coppari, R., Enriori, P.J., Choi, B., Zhang, C.Y., Xu, C., Vianna, C.R., Balthasar, N., Lee, C.E.*, et al.* (2007). Glucose sensing by POMC neurons regulates glucose homeostasis and is impaired in obesity. Nature *449*, 228-232.

Pelling, M., Anthwal, N., McNay, D., Gradwohl, G., Leiter, A.B., Guillemot, F., and Ang, S.L. (2010). Differential requirements for neurogenin 3 in the development of POMC and NPY neurons in the hypothalamus. Dev Biol.

Satoh, M., and Ide, H. (1987). Melanocyte-stimulating hormone affects melanogenic differentiation of quail neural crest cells in vitro. Dev Biol *119*, 579-586.

Vernadakis, A., and Kentroti, S. (1990). Opioids influence neurotransmitter phenotypic expression in chick embryonic neuronal cultures. J Neurosci Res *26*, 342-348.

Williams, K.W., Margatho, L.O., Lee, C.E., Choi, M., Lee, S., Scott, M.M., Elias, C.F., and Elmquist, J.K. (2010). Segregation of acute leptin and insulin effects in distinct populations of arcuate proopiomelanocortin neurons. J Neurosci *30*, 2472-2479.

Xu, Q., Tam, M., and Anderson, S.A. (2008). Fate mapping Nkx2.1-lineage cells in the mouse telencephalon. J Comp Neurol *506*, 16-29.

APPENDIX A: Screen for Lineage Markers of the Arcuate Nucleus of the Hypothalamus

Overview

A growing body of evidence supports that POMC and AgRP neurons in the ARH are not homogenous. Both electrophysiological recordings and histological expression analysis reveal discrete subpopulations of both POMC and AgRP neurons (de Souza et al., 2011; Fioramonti et al., 2007; Hentges et al., 2004; Hentges et al., 2009; Murphy et al., 2009; Parton et al., 2007; Williams et al., 2010). The elucidation of genetic reagents for distinct POMC and AgRP homogenous subpopulations will be paramount to defining the physiologic relevance of these subsets and may.

In this study we sought to define molecular markers of NPY/AgrP and POMC subsets, which can be used as tools to target and investigate the physiologic contribution of each homogenous subset. It is known that specification of cellular identity relies on intrinsic activation of genetic programs by unique combinations of transcription factors and therefore select transcription factors can act as signatures (lineage markers) for distinct populations (Edlund and Jessell, 1999). Using public expression databases and the literature searches we identified 295 transcription factors present in the ARH (Gong et al., 2003; Jing et al., 2004; Lein et al., 2007; Su et al., 2004; Visel et al., 2004). To narrow this pool down to lineage marker candidates, we then segregated our selection based on two main criteria: 1) expression patterns relatively restricted to the ARH, and 2) expression that was consistent across a broad range of developmental stages, leaving us with 65 candidate transcription factor lineage markers.

To describe the regional specificity of all 65 transcription factors, we developed ribo-probes and mapped each on cryo-sections of the ARH (note: probes were designed in consideration of known splice variants). For each probe, we initially performed an *in-situ* hybridization (ISH) alkaline phosphatase (AP) stain on sections from both adult and P7 brains. From this, we determined that 29 transcription factors of the 65 candidates were expressed at sufficient levels

to define distinct cellular expression and also presented a similar pattern of expression at both P7 and adult stages (Table A.1). The expression of these 29 candidates with respect to *Npy*- and *Pomc*-expressing populations was performed using two-color FISH and shown in Table A1. We did not find any markers to exclusively reside in subsets of either Npy or Pomc cells in the ARH, which may reflect that the lineage of these populations is not restricted to an NPY or POMC terminal cell fate.

Table A.1

	NPY		POMC		Other
Markers	Pan	Subset	Pan	Subset	ARH
BarH1					x
BarX2					x
Bsx	x				
Dlx1					x
Dlx5		x			x
Dlx6		x		x	x
Elk1		x		x	x
Ets1					x
Etv1/ER81				x	x
Fatso	x		x		x
Fhl2	x				x
Lhx2					vz+other
Lhx5					x
Lhx9		x		x	x
Lim1					x
Lrrn3				x	x
Nhlh2		x		x	x
Nkx2.4					vz, x
Nr3c1		x			x
Otp	x		x		x
Peg3	x		x		x
Six1					x
Six3					vz, x
Six4	x				x
Six6					x
Sox9	x				vz, x
Tbx3			x		x
Tbx19		x		x	x
Tcf7L2					x

Methods

Animals

Animals were housed in temperature controlled rooms at 21 °C and subject to a 12 h light-dark cycle. Mice had *ad libitum* access to standard chow diet (Lab Diet: PicoLab Rodent Diet 5053) and water. C57BL/6 mice were obtained from the Jackson Laboratory and bred at the Russ Berrie Animal Facility. All procedures were performed in accordance with the guidelines of the Institutional Animal Care and Use Committee at the Columbia University Health Sciences Division.

Fluorescent *In Situ* Hybridization

Tissue Processing: FISH: Adult mice were anesthetized and perfused transcardially with 0.9% NaCl followed by 4% paraformaldehyde (PFA) in phosphate buffer (PB). Brains were post-fixed at 4°C overnight and cryoprotected with 30% sucrose for 48 h. For embryonic tissue, dams were anesthetized with Avertin and embryos were dissected in cold PBS and fixed at 4 °C overnight and cryoprotected with 30% sucrose for 24 h. Tissue was embedded in O.C.T (Tissue Tek) and frozen at –80°C. 10 µm-thick coronal sections were collected across the rostral–caudal extent of the ARH on Superfrost Plus slides (Fisher).

FISH: Frozen sections were processed as described in the TSA Plus Cy3 System manual (Perkin Elmer). Antisense digoxigenin- and fluorescence-labeled riboprobes were generated using the following primers sets:

Npy-F 5'-TGCTAGGTAACAAGCGAATGG-3'

Npy-R 5'-CAACAACAACAAGGGAAATGG-3

Pomc-F 5'-GTTAAGAGCAGTGACTAAGAGAGGC-3'

Pomc-R 5'-CCTAACACAGGTAACTCTAAGAGGC-3'

BarH1-F 5'-AGATGGCAGTCCAGAGCCGAGTCCACGCGAGGGCAA

BarH1-R-5'-AGTCCGTGGATGAGGATGCGGG

BarX2-F 5’-AGACAGAACAGCCCACGC

BarX2-R 5’-GGAGGGAGAAGAGCAGCC

Bsx-F 5’-CCGCTGGGGCAAGCCGGTGGGCAAGAAACGG

Bsx-R 5’-CTGGAACCACGTTTTCACCT

Dlx1-F 5’-TACGTCAACTCGGTCAGCAGCC

Dlx1-R 5’-GGAAAAAGTGGTCCAGGACTCGG

Dlx5-F 5’-CAGGTGAAAATCTGGTTTCAGAAC

Dlx5-R 5’-CACCATTGATAGTGTCCACAGTTG

Dlx6-F 5’-TAGTAACCCACACGAGAGTGAC

Dlx6-R 5’-CCATGTTTGCGCAGATTCTTCTG

Elk1-F 5’-AGCGGCCAGAAGTTTGTCTA

Elk1-R 5’-AAGGTATGTGTGGGGAGCAG

Ets1-F 5’-TAGGGTTGCGCTCTGTCC

Ets1-R 5’-ATGACTGGCTGCTCCAGG

Etv1/Er81-F 5’-GTGCCTCTGTCTCACTTTGATG

Etv1/Er81-R 5’-CTACTGGCCTGTGACTCAGTTG

Fto-F 5’-TGTTTTGGCTGGCTCACA

Fto-R 5’-ATGGCCAGGCCTACTTCC

Fhl2-F 5’-GGACACAAGGATCGCCAC

Fhl2-R 5’-TGGCGTTCCTCGAAAGAG

Lhx2-F 5’-GGGCGAGCTGATGACCTCTAGCCTCTTAGAGTTACC

Lhx2-R 5’-ATTGTCCGAAGCTGGTGGTGC

Lhx5-F 5’-CCCATCCTCGACCGCTTTCTGC

Lhx5-R 5’-GTAGACCCCAACGCGTGTCTCC

Lhx9-F 5’-GGAGGAGATGGAGCGCAGATCC

Lhx9-R 5’-CAAGCTGTTTGAGGTCCTTGGC

Lim1-F 5’-GCACAAGAAGGGCCAGTGAGGGTGCAGGGG

Lim1-R 5’-CGCTGACATGGAGTGGAGAGG

Lrrn3-F 5’-CAGTCTCGCTGTGGATAACTTG

Lrrn3-R 5’-CAACACAGGCCACAAATACTGT

Nhlh2-F 5’-CAAACTCGACCTCTCGCTGGAGACGCCCGTGTT

Nhlh2-R 5’-CAGGGCATCTCATTCTAGGTGC

Nkx2.4-F 5’-CAGAACCATCGCTACAAGATGA

Nkx2.4-R 5’-TTCTGCCATAGAGCAGGTTG

Nr3c1-F 5’-ACAGACTTTCGGCTTCTGGA

Nr3c1-R 5’-TACAGCTTCCACACGTCAGC

Otp-F 5’-AGGCGGTGAAGTGTAGGCTGGG

Otp-R 5’-TTGGACAAGCCCATGGAGTTGG

Peg3-F 5’-TTGCTTGCAGGTCACCGTAGGG

Peg3-R 5’-TGAGATCAGTAAAGCCCAGCC

Six1-F 5’- CTCGGTCCTTCTGCTCCA

Six1-R 5’-TCGCTGCTACCCTAACCG

Six3-F 5’-GGAGGAGACGGGCGACATCGA

Six3-R 5’-GAGGATCGAAGTGCCGGTGTCC

Six4-F 5’-CCTTTATGCTGTTAGTCCAGGG

Six4-R 5’-CCGCCTTATAGAACGTTTTGAC

Six6-F 5’-ACGTGAGAAAGGGCTGATGTAT

Six6-R 5’-GTAGCCAAGGTTGGTCTGAAAC

Tbx19-F 5’-CCAGCATGTGACCTACTCTCAC

Tbx19-R 5’-GGCACTTAGACCAAGCTGACTT

Tcf7l2-F 5’-GTCCTCGCTGGTCAATGAAT

Tcf7l2-R 5’-TGAATGCATTAAGGGGCTTC

References

de Souza, F.S., Nasif, S., Lopez-Leal, R., Levi, D.H., Low, M.J., and Rubinsten, M. (2011). The estrogen receptor alpha colocalizes with proopiomelanocortin in hypothalamic neurons and binds to a conserved motif present in the neuron-specific enhancer nPE2. Eur J Pharmacol.

Edlund, T., and Jessell, T.M. (1999). Progression from extrinsic to intrinsic signaling in cell fate specification: a view from the nervous system. Cell *96*, 211-224.

Fioramonti, X., Contie, S., Song, Z., Routh, V.H., Lorsignol, A., and Penicaud, L. (2007). Characterization of glucosensing neuron subpopulations in the arcuate nucleus: integration in neuropeptide Y and pro-opio melanocortin networks? Diabetes *56*, 1219-1227.

Gong, S., Zheng, C., Doughty, M.L., Losos, K., Didkovsky, N., Schambra, U.B., Nowak, N.J., Joyner, A., Leblanc, G., Hatten, M.E.*, et al.* (2003). A gene expression atlas of the central nervous system based on bacterial artificial chromosomes. Nature *425*, 917-925.

Hentges, S.T., Nishiyama, M., Overstreet, L.S., Stenzel-Poore, M., Williams, J.T., and Low, M.J. (2004). GABA release from proopiomelanocortin neurons. J Neurosci *24*, 1578-1583.

Hentges, S.T., Otero-Corchon, V., Pennock, R.L., King, C.M., and Low, M.J. (2009). Proopiomelanocortin expression in both GABA and glutamate neurons. J Neurosci *29*, 13684-13690.

Jing, E., Nillni, E.A., Sanchez, V.C., Stuart, R.C., and Good, D.J. (2004). Deletion of the Nhlh2 transcription factor decreases the levels of the anorexigenic peptides alpha melanocyte-stimulating hormone and thyrotropin-releasing hormone and implicates prohormone convertases I and II in obesity. Endocrinology *145*, 1503-1513.

Lein, E.S., Hawrylycz, M.J., Ao, N., Ayres, M., Bensinger, A., Bernard, A., Boe, A.F., Boguski, M.S., Brockway, K.S., Byrnes, E.J.*, et al.* (2007). Genome-wide atlas of gene expression in the adult mouse brain. Nature *445*, 168-176.

Murphy, B.A., Fioramonti, X., Jochnowitz, N., Fakira, K., Gagen, K., Contie, S., Lorsignol, A., Penicaud, L., Martin, W.J., and Routh, V.H. (2009). Fasting enhances the response of arcuate neuropeptide Y-glucose-inhibited neurons to decreased extracellular glucose. Am J Physiol Cell Physiol *296*, C746-756.

Parton, L.E., Ye, C.P., Coppari, R., Enriori, P.J., Choi, B., Zhang, C.Y., Xu, C., Vianna, C.R., Balthasar, N., Lee, C.E.*, et al.* (2007). Glucose sensing by POMC neurons regulates glucose homeostasis and is impaired in obesity. Nature *449*, 228-232.

Su, A.I., Wiltshire, T., Batalov, S., Lapp, H., Ching, K.A., Block, D., Zhang, J., Soden, R., Hayakawa, M., Kreiman, G.*, et al.* (2004). A gene atlas of the mouse and human protein-encoding transcriptomes. Proc Natl Acad Sci U S A *101*, 6062-6067.

Visel, A., Thaller, C., and Eichele, G. (2004). GenePaint.org: an atlas of gene expression patterns in the mouse embryo. Nucleic Acids Res *32*, D552-556.

Williams, K.W., Margatho, L.O., Lee, C.E., Choi, M., Lee, S., Scott, M.M., Elias, C.F., and Elmquist, J.K. (2010). Segregation of acute leptin and insulin effects in distinct populations of arcuate proopiomelanocortin neurons. J Neurosci *30*, 2472-2479.